DEMOCRATIC AND PEOPLE'S REPUBLIC OF ALGERIA

MINISTRY OF HIGHER EDUCATION AND SCIENTIFIC RESEARCH

MOHAMED BOUDIAF UNIVERSITY - M'SILA

FACULTY OF TECHNOLOGY

DEPARTMENT OF ELECTRICAL ENGINEERING

Nº: ……..

DOMAIN: SCIENCES AND TECHNOLOGY

SECTOR: ELECTRICAL ENGINEERING

OPTION: ELECTRICAL CONTOL

Memory submitted for obtaining the Academic Master

Presented by:

- BOUSSAG Mohammed Eddora
- BAKRI Abdelkader

Title

Direct Power Control of three-phase PWM Rectifier based on Neuro-Fuzzy controller.

- **Supervised by** : **Dr.** BEDBOUDI Mohamed
- **Defended before the jury composed of:**

BELHAMDI Saad	Mohammed Boudiaf University - M'sila	**President**
BOUGUERRA Abderrahmen	Mohammed Boudiaf University - M'sila	**Examiner**
BEDBOUDI Mohamed	Mohammed Boudiaf University - M'sila	**Rapporteur**

Academic year : 2022/2023

THANKS

بسم الله الرحمن الرحيم

الحمد لله وكفى والصلاة والسلام على النبي المصطفى وعلى آله وصحبه ومن سار على نهجه واقتفى

عن أبي هريرة رضي الله عنه أن النبي صلى الله عليه وسلم قال : «لا يَشْكُرُ اللَّهَ مَنْ لا يَشْكُرُ النَّاسَ»

وعلى أثر قول رسولنا الكريم

We would like to thank Allah the Almighty for giving us knowledge, health and will to accomplish this study. We would like to express our great gratitude to our supervisor: Dr. BEDBOUDI Mohamed for his guidance, help and support throughout the project and always being there for us whenever we needed him. We could not have done it without him. We also wish to thank the President of jury and jury members for accepting to take part of the examining committee. We are thankful that in the midst of all their activities, they dedicated time and effort to read and evaluate our project. Finally yet importantly, we are grateful to our parents for their encouragement, guidance and unconditional support, both psychologically and financially during our years of education; May Allah bless them.

DEDICATION

We dedicate this modest work to:

Our parents.

Our brothers and sisters.

To the entire BOUSSAG and BAKRI family.

To all our friends and colleagues from our personal life and from the University of M’SILA

In addition, all those who carry Algeria in their hearts.

ABSTRACT: This memory initiation research is in the field of power electronics to study and eliminate harmonic pollution of the distribution network. This power and current pollution creates a major problem, especially in industrial and high-voltage services, which is a product of nonlinear loads from non-sinusoidal current networks. Stationary converters such as rectifier based on thyristors are nonlinear and are a major source of harmonic current injection into the network. Therefore, they require special attention to reduce the levels of harmonics in their operation. In this case, the modern preventive solutions employed, in addition to active filtering, which represent a therapeutic solution, consist in replacing traditional rectifiers with new structures of non-polluting AC /DC converters, which have resistance to the behavior of the network. This work makes it possible to control the nominal PWM voltage during the absorption of sinusoidal current. Indeed, different control strategies have been developed, simulated with the common aim of obtaining an effective modulation of DC vector voltages and a sampling of sinusoidal currents. We study three strategies of control, Direct Power Control based on switching table, Direct Power Control with Fuzzy Controller and Direct Power Control based on ANFIS. These techniques make it possible to reduce the cost of the installation and to improve the behaviors dynamics and permanent.

KEY WORDS: PWM Rectifier, THD, Rule table, Direct Power Control. ANFIS.

RÉSUMÉ : Cette mémoire est une initiation à la recherche dans le domaine de l'électronique de puissance visant à étudier et éliminer la pollution harmonique du réseau de distribution. Cette pollution de puissance et de courant crée un problème majeur, notamment dans les services industriels et à haute tension, et est le résultat de charges non linéaires des réseaux de courant non sinusoïdal. Les convertisseurs statiques tels que les redresseurs à thyristors sont non linéaires et constituent une source majeure d'injection de courant harmonique dans le réseau. Par conséquent, ils nécessitent une attention particulière pour réduire les niveaux d'harmoniques lors de leur fonctionnement. Dans ce cas, les solutions préventives modernes utilisées, en plus du filtrage actif qui représente une solution thérapeutique, consistent à remplacer les redresseurs traditionnels par de nouvelles structures de convertisseurs AC/DC non polluantes, qui résistent au comportement du réseau. Ce travail permet de contrôler la tension PWM nominale lors de l'absorption de courant sinusoïdal. En effet, différentes stratégies de contrôle ont été développées, simulées avec pour objectif commun d'obtenir une modulation efficace des tensions vectorielles DC et un échantillonnage des courants sinusoïdaux. Nous étudions trois stratégies de contrôle : le Contrôle Direct de Puissance basé sur la table de commutation, le Contrôle Direct de Puissance avec Contrôleur Flou et le Contrôle Direct de Puissance basé sur l'ANFIS. Ces techniques permettent de réduire le coût de l'installation et d'améliorer les comportements dynamiques et permanents.

MOTS CLÉS : Redresseur MLI, THD, Tableau de règles, Contrôle direct de la puissance, ANFIS.

الملخص :هذه المذكرة تمثل انطلاقة بحثية في مجال إلكترونيات الطاقة لحل مشكلة التلوث التوافقي لشبكة التوزيع الكهربائي هذه الطاقة والتلوث الحالي يخلق مشكلة كبيرة، وخاصة في الخدمات الصناعية وعالية الجهد، وهو نتاج الأحمال الغير خطية من الشبكات الحالية الغير جيبيه. المحولات الثابتة مثل الثنائيات المتحكمة غير خطية وهي مصدر رئيسي لحقن التيار التوافقي في الشبكة. ولذلك، فإنها تتطلب اهتماما خاصا للحد من مستويات التوافقيات في عملها. في هذه الحالة، تتمثل الحلول الوقائية الحديثة المستخدمة، بالإضافة إلى التصفية النشطة، والتي تمثل حال علاجيا، في استبدال المقومات التقليدية بهياكل جديدة لمحولات التيار المتردد /التيار المستمر نقي، والتي لها مقاومة لسلوك الشبكة. هذا العمل يجعل من الممكن السيطرة على الجهد خلال امتصاص التيار الجيبي. في الواقع، تم تطوير استراتيجيات تحكم مختلفة ومحاكاتها بهدف الحصول على تعديل فعال لجهد ناقل التيار المستمر وأخذ عينات

من التيارات الجيبة. نقوم بدراسة ثلاثة استراتيجيات للتحكم، التحكم المباشر في القدرة بناءً على جدول التبديل، التحكم المباشر في القدرة بواسطة المراقب الضبابي، والتحكم المباشر في القدرة بناءً على .ANFIS تلك التقنيات تمكن من تقليل تكلفة التركيب وتحسين سلوكيات النظام بشكل ديناميكي ودائم.

الكلمات المفتاحية :محول النبض العرضي، معامل التشويه، جدول القواعد، التحكم المباشر في الطاقة، متحكم عصبي ضبابي.

Table of Contents

Table of Contents

CHAPTER II: Mathematical model and hysteresis control of PWM Rectifier.

CHAPITRE III : Direct Power Control of three-phase PWM Rectifier.

Table of Contents

Table of Contents

List of Figures

CHAPTER I

CHAPTER II

CHAPTER III

List of Figures

CHAPTER IV

List of Figures

List of Tables

CHAPTER II

CHAPTER III

CHAPTER IV

List of Symbols

Symbol	Meaning	Unit
e_a, e_b, e_c	The phase voltages of the electrical network	**Volt [V]**
i_a, i_b, i_c	Network currents	**Ampere [A]**
v_a, v_b, v_c	Simple voltages at the input of the rectifier bridge	**[V]**
V_{dc}, I_{dc}	DC voltage of the bus and DC current of the bus	**[V], [A]**
V_1, V_h	RMS value of the fundamental voltage and RMS value of the h-th harmonic voltage	**[V]**
I_1, I_h	RMS value of the fundamental current and RMS value of the h-th harmonic current	**[A]**
C	Output capacitance for filtering the DC output voltage.	**Farad [F]**
L	Inductance of the coupling coil	**Henrys(H)**
r	resistance of the coupling coil	**Ohms [Ω]**
R_d	DC-side pure resistive load	**[Ω]**
w	Fundamental frequency of the electrical network	**[rad/s]**
S_a, S_b, S_c	Control signals for power switches	/
S	Apparent power	**[VA]**
P	Active power	**[W]**
Q	Reactive power	**[VAR]**
α-β	stationary reference frame	/
d-q	rotating synchronous reference frame	/
$\mathbf{e_d}, \mathbf{e_q}$	Line voltages in the d, q synchronous reference frame	**[V]**
e_α, e_β	Line voltages in the α, β reference frame	**[V]**
i_α, i_β	Line currents in the α, β reference frame	**[A]**
θ	Position of the voltage vector in the stationary reference frame	**[rad]**
θ_n	Sector number n	/
S_d, S_q	Digital output of the hysteresis comparators for power P and Q	/
P_{ref}, Q_{ref}	Reference for active and reactive power	**[W] [VAR]**
H_p, H_q	Hysteresis band for active and reactive power	**[W] [VAR]**
ΔI	Hysteresis bandwidth	/
$\mu_{Ai}(x)$	Degree of membership of x in the subset Ai	/
V_{dc}^*	DC voltage reference of the bus	**[V]**
D	**P**ower Distortion	**[W]**

Acronyms

Acronyms	Meaning
RMS	**R**oot **M**ean **S**quare
THD	**T**otal **H**armonic **D**istortion
PF	**P**ower **F**actor
HVDC	**H**igh-**V**oltage **D**irect **C**urrent
AC/DC	**C**onverting **A**lternating current to **D**irect current
IGBT	**I**nsulated **G**ate **B**ipolar **T**ransistor
FACTS	**F**lexible **A**lternating **C**urrent **T**ransmission **S**ystems
PWM	**P**ulse **W**idth **M**odulation
PI	**I**ntegral **P**roportional **R**egulator
EMF	**E**lectromotive **F**orce
UPF	**U**nit **P**ower **F**actor
CC	**C**urrent **C**ontrol
HCC	**H**ysteresis **C**urrent **C**ontrol
PLL	**P**hase **L**ocked **L**oop
DPC	**D**irect Power **C**ontrol
FLC	**F**uzzy **L**ogic **C**ontroller
FDPC	**F**uzzy **D**irect **P**ower **C**ontrol
FFT	**F**ast **F**ourier **T**ransform
VOC	**V**oltage **O**riented **C**ontrol
DTC	**D**irect **T**orque **C**ontrol
ANN	**A**rtificial **N**eural **N**etworks
ANFIS	**A**daptive **N**euro-**F**uzzy **I**nference **S**ystem
FIS	**F**uzzy **I**nference **S**ystem
MF	**M**embership **F**unction
VSI	**V**oltage **S**ource **I**nverter

General Introduction

The main objective of operation planning in the distribution system is to consistently satisfy the electricity load with acceptable quality of energy supply that meet the needs of their customers. This has become a complicated task owing to the significant growth in both the industrial sector and population, which increases the demand for electrical energy, additionally, the significant progress in both the unit and power of power electronic equipment on the electric grid has made this task even more challenging. These devices are considered as sources of pollution by energy distributors and pose serious problems for them. **[Uli 10],** if not carefully managed the disturbances caused by these converters may result in such as a degradation of power factor and generation of non-sinusoidal alternating currents rich in harmonics. These incidents result in voltage distortion, reduced transport capacity, and increased losses.

Classical static converters are the primary source of harmonic current injection into the grid, reducing that voltage and current waveform distortion of the classical converters to acceptable levels has been a problem in power system design from the early days of alternating current.

Many solutions have been discussed in the literature to avoid the power quality problems in distribution systems. The best preventive modern solutions adopted consist of replacing classical rectifiers with new non-polluting AC/DC converter structures, which is three phase Pulse Width Modulation (PWM) Rectifiers, as it has several significant advantages:

- Power is bidirectional (reversible).
- Low harmonic distortion of the grid current.
- Almost Unit Power Factor.
- Control of the direct current bus voltage.
- Reduction of the size of the direct current bus capacitor **[Jam 18][Bou 07]**.

With advances in power electronics, power electronics technology has widely used for many applications. Nowadays, AC/DC converters, which are also known as rectifiers, are used in adjustable speed drives, uninterruptible power supply systems, photovoltaic systems, battery energy storage systems, DC motor drives and communication systems**[Aci 16]**, that's what made research in this field considers several aspects, including converter topologies, power switch structures and performance, and control techniques. There are different control techniques for this type of converter. The main goal of these control techniques is to eliminate the current harmonics and to regulate the DC bus voltage. The hysteresis control technique is widely used in the field of

power electronics. It involves developing the Pulse Width Modulation (PWM) signal directly from the controlled variable, using binary decisions. Another type of control technique is Direct Power Control (DPC) **[Bou 07],** which involves adjusting the output based on the difference between the desired and actual output power and a switching table, the main goal of these control techniques is to eliminate the current harmonics and to regulate the DC bus voltage. The PI controller is a crucial component of the DPC control technique, to improve on the drawbacks of these control techniques, replacing classical PI controllers with artificial fuzzy logic or neuro-fuzzy controllers can improve control performance and provide more accurate and stable control.

The various theoretical developments and results obtained during this work are organized into four chapters:

• ***Chapter 1:*** discusses the increasing concern of electric utilities regarding power system harmonics and voltage and current distortion caused by power electronic devices and understanding the origin of disturbances and finding solutions to mitigate their effects is important to enhance the quality of energy supplied to customers.

• ***Chapter 2:*** This chapter covers PWM Rectifiers, including their model and operating principle. It also discusses their characteristics, such as high efficiency and low harmonic distortion that make them ideal for power electronics applications. The control strategy for PWM voltage rectifiers using hysteresis is also explained.

• ***Chapter 3:*** This chapter presents a study and simulation of the DPC control technique for PWM Rectifiers (DPC with a pre-defined switching table and a new table).

• ***Chapter 4:*** We will present an overview of fuzzy logic and Adaptive Neural Fuzzy Inference System (ANFIS), and an improvement DPC of three-phase PWM rectifier technique based on changing the classical PI controller with a fuzzy and ANFIS controller.

Finally, the memory concludes with a conclusion and future perspectives.

CHAPTER I Electrical disturbances, origin and solutions to ensure optimal power quality.

I.1. Introduction

The fundamental objective of electrical networks is to provide customers with electrical energy with perfect continuity, in the form of a sinusoidal voltage, with anticipated amplitude and frequency values. However, Electric utilities are becoming more concerned about power system harmonics and voltage distortion. This increased concern is due to the increase in application of power electronic type devices such as rectifiers and inverters, The result is increased injection of power system harmonics, Also the increase application of shunt capacitor banks for power factor correction resulting in increase potential for resonant conditions which can magnify the existing harmonic levels are of concern. The increase of power system harmonics in the power system not only threatens the quality of the electricity supplied to the consumers but also raises concerns about the degradation of power quality and the potential malfunction or destruction of the components of the electrical network our final receivers, it is essential to understand the origin of disturbances and to seek appropriate solutions to eliminate them, For this reason the chapter will focus on understanding the origin of disturbances and harmonics, and presenting effective solutions to mitigate their effects, thereby enhancing the quality of energy supplied **[Ben 13] [Bei 91].**

I.2. Quality of electrical energy

Power quality is related to magnitude, frequency, and waveform of voltage and current. For good power quality level, supply voltages and line currents should be within their rated magnitudes, the frequency close to the prescribed supply frequency and sinusoidal waveform. There are many events disturbing power quality performance such as over-undervoltages, harmonic distortion, flickers, unbalance, sags, swells, transients, interruptions and frequency deviations. In addition, harmonic distortion is recognized as one of the most important power quality events in the literature since it has many adverse effects on operation and control of power system equipment [**Zob 18**].

CHAPTER I

The quality of electrical power supply or waveform quality refers to the measurement of the degree of conformity of an electrical power source to a certain number of quantitative and absolute criteria or standards. Electrical energy is delivered in the form of a three-phase system of sinusoidal voltages:

- The frequency.
- The amplitude.
- The waveform, which must be sinusoidal.
- The symmetry of the three-phase system, characterized by the equality of the magnitudes of the three voltages and their relative phase shifts **[Bou 10].**

I.3. The issue of harmonics

Any change in Voltage waveform and frequency waveform are called harmonics. Harmonics are the main issue on a power network. Power issue occurs on a voltage, current or frequency deviations and result in failure or improper operation of user equipment. The growing use of automatic equipment's produces many harmonics in sharing network because non-sinusoidal current spent by non-linear loads. Along to increasing demand for better power quality i.e. generally defined any change to the voltage, current, or frequency they affects with the regular operation of electrical equipment. Harmonics cause distortion on current and voltage waveforms resultant in the fall to the power network, the first step to do is to new the harmonic sources, which has much importance [**Maz 18**].

I.3.1. Origin of harmonic

Harmonics are created when non-linear loads, draw current from the power system. These loads create power system harmonics which are defined as sinusoidal voltage and currents at frequencies that are integer multiples of the main generated (or fundamental) frequency. They constitute the major distorting components of the mains voltage and load current waveforms. Harmonics are particularly distinguished by their order [**Arr 03**].

Even harmonics: are the even multiples of the fundamental frequency ($2f$, $4f$, $6f$, … , $2nf$) which are frequently negligible in an industrial environment since they cancel out due to the symmetry of the signal.

Odd harmonics: are odd multiples of the fundamental frequency ($3f$, $5f$, $7f$, … , $(2n+1)f$) this order is often encountered in an electrical network.

Here, n is a natural number **[Ham 16].**

However, the increasing content of power system inter-harmonics, i.e. Distorting components at frequencies that are not integer multiples of the fundamental, has prompted a need to give them greater attention **[Arr 03]**.The Figure I.1 illustrate, when harmonics are added to the fundamental, its waveform will be distorted and it becomes a non-perfect condition for an electrical grid or a power supply **[Ros 06]**.

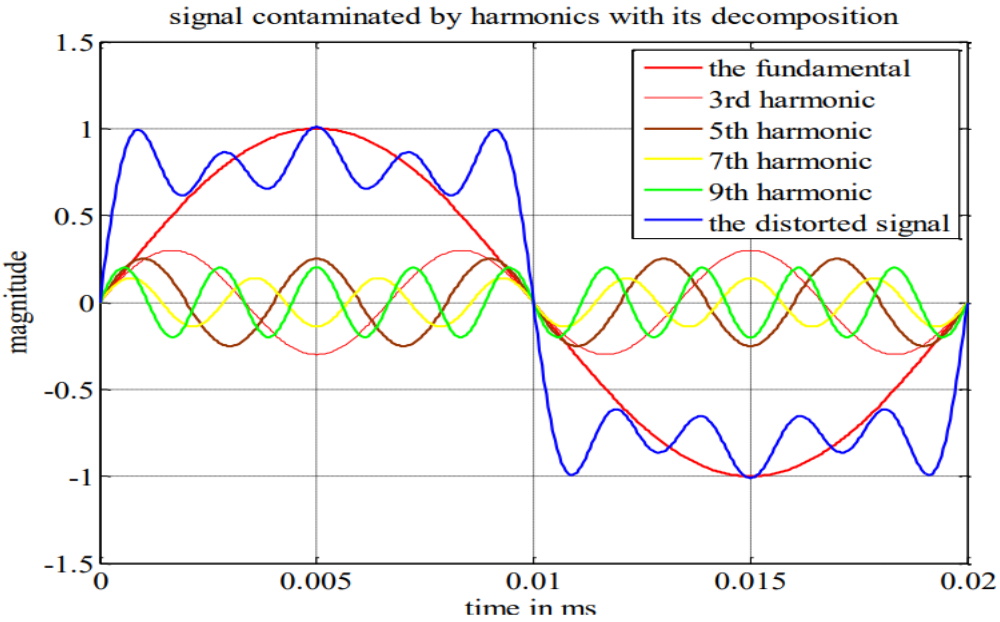

Figure I.1 Harmonic distortion illustration.

I.3.2. Harmonic sources.

The nonlinear loads, such as (computers, laser printers, converters, refrigerators, and TVs etc.), are widely used in energy production and are the main source of harmonics in power networks. These loads are the main sources that generate harmonic currents, leading to injecting of non-sinusoidal currents into the network, causing the existence of voltage harmonics, which can affect both the equipment present on the distribution side and load connected to it [**Maz 18**].

I.3.2.1. Identifiable harmonic sources

Equipment equipped with power electronics devices, such as rectifiers and cycloconverters of significant power, installed on high and medium voltage networks are typically identifiable harmonic sources. With this type of non-linear load, the energy distributor is able to identify the point of harmonic injection and quantify the disturbance caused. In this case, it is the user who must obtain the necessary means to reduce this disturbance below the threshold required by the energy distributor, under penalty of being penalized.

I.3.2.2. Non-identifiable harmonic sources

This type of harmonic current generator is mainly represented by devices used in household or tertiary sectors such as televisions and microcomputers. Given their wide distribution, these devices, often equipped with a single-phase diode rectifier with a smoothing capacitor, draw non-negligible harmonic currents. In this case, it is the responsibility of the electric energy distributor to prevent the propagation of the harmonic disturbance on the network since each user individually generates a low level of harmonics [**Ben 98].**

I.3.3. Characteristics of harmonics

Harmonic distortion is usually characterized by the Total Harmonic Distortion (THD) rate defined for voltage or current. This criterion is most often used to quantify the harmonic content of a distorted signal. It also measures the degree of deformation of the signal caused by harmonics compared to a sinusoidal wave. It goes without saying that the complete spectral distribution generally supplements the information on THD by indicating the order of dominant harmonics. The Power Factor (PF) is generally used to quantify the consumption of reactive power **[Bou 10].**

I.3.3.1. Total Harmonic Distortion

Total Harmonic Distortion (THD) is an important index widely used to describe power quality issues in transmission and distribution systems. It considers the contribution of every individual harmonic component on the signal. THD is defined for voltage and current signals, respectively, as follows:

$$THD_V = \frac{\sqrt{\sum_{h=2}^{\infty} V_h^2}}{V_1} \quad \text{(I.1)}$$

$$\mathrm{THD_I} = \frac{\sqrt{\sum_{h=2}^{\infty} I_h^2}}{I_1} \quad \text{(I.2)}$$

This means that the ratio between Root Mean Square (RMS) values of signals including harmonics and signals considering only the fundamental frequency define the total harmonic distortion **[Ros 06]**.

I.3.3.2. Power factor

Power factor is a measure of how efficiently a load utilizes the current from AC power system. There are some utility rate schedules that offer incentives to large customers to improve power factor near 1 as it will improve overall efficiency. The largest contributors to low (PF). Are reactive loads. However, harmonics can also have an adverse impact on (PF). True power factor is the ratio of active power (P) and apparent power (S) [**God 13**]. In the case of harmonics in three-phase systems, an additional power called the distortion power D, given by the relation (I.3), appears as shown in the Fresnel diagram of powers in Figure I.2.

$$D = 3 * V_1 \sqrt{\sum_h^{\infty} i_h^2} \quad \text{(I.3)}$$

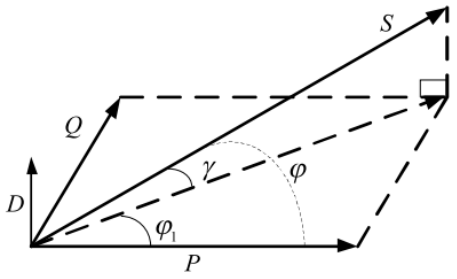

Figure I.2 Fresnel diagram of powers.

The power factor (PF) becomes:

$$PF = \frac{P}{\sqrt{P^2+Q^2+D^2}} = \cos\varphi \cos\gamma \quad \text{(I.4)}$$

It can be noted that in sinusoidal regime, the distortion power is zero. The power factor is then simply expressed as:

$$PF = \cos\varphi \quad \text{(I.5)}$$

I.3.4. Harmful consequences of harmonics

Once the harmonic sources are clearly defined, they must be interpreted in terms of their effects on the rest of the system and on personnel and equipment external to the power system. Each element of the power system must be examined for its sensitivity to harmonics as a basis for recommendations on the allowable levels. The main effects of voltage and current harmonics within the power system are **[Arr 03]:**

I.3.4.1. Heating

The total Joule losses are the sum of the fundamental and harmonic losses:

$$Ri^2 = \sum_{h=2}^{\infty} i_h^2 R \quad \text{(I.6)}$$

Where i is the total current, i_h is the h-th order harmonic current which represents the fundamental for h=1, and R is the resistance traversed by the current i **[Mas 22]**.

I.3.4.2 Malfunction of certain equipment

In the presence of harmonics, the voltage (or current) can change sign multiple times within one half-cycle; therefore, any device whose operation is based on the zero-crossing of electrical quantities (devices using voltage as a reference) can be disturbed **[Mas 22].**

I.3.4.3 Telephone interference

The common construction of telephone lines built underneath power conductors on electric utility distribution poles makes them prone to the electromagnetic coupling that can take place between a power and a telephone line, it can induce significant noise in the latter **[Ros 06]**.

I.3.4.4 Resonance

The presence of capacitors connected to the grid, such as those used for power factor correction, can result in local system resonances which become quite low and thus coincide with those of harmonics generated by static converters, which lead in to phenomena of harmonic amplification **[Arr 03].**

I.4 Disturbances produced by natural commutation

Rectifiers Before the emergence of static power converters in power electronics, magnetization currents of transformers, electrical machines, and ballasts constituted the majority of nonlinear loads present on the electrical grid. However, today, with the development of power electronics, static converters have become the most widespread source of harmonics on the grid. Uncontrolled diode rectifiers and thyristor-controlled rectifiers operating in natural commutation represent the most commonly used nonlinear load. These converters are present in many industrial and domestic equipment as well as in electric energy conversion devices. The most common applications include:

- Variable speed drives for AC and DC motors.
- Excitation circuits for alternators.
- Battery chargers.
- High-Voltage Direct Current (HVDC) links.
- Power supply for information technology and audiovisual systems.
- Next-generation lighting devices.

We distinguish two rectifier structures:

1. **Diode bridges**: They constitute the AC/DC energy conversion stage (supply of the DC bus of inverters for AC machine variable speed drives, for example).
2. **Thyristor bridges**: Same role as the diode bridge with the possibility of controlling the DC voltage level at the output and adding energy flow reversibility **[bou 10].**

Figure I.3 shows the three-phase thyristor rectifier bridge configuration. The diode bridge configuration is obtained by substituting the diodes with thyristors.

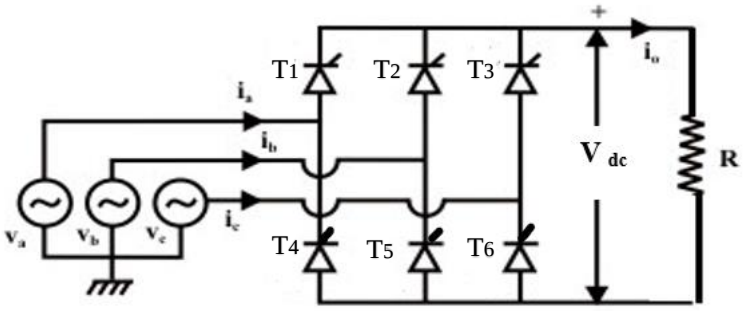

Figure I.3 Three-phase thyristor rectifier bridge.

Figure I.4.(a) illustrates the waveforms of non-sinusoidal currents i_a multiplied by 20 absorbed by the three-phase thyristor rectifier bridge compared to waveforms of sinusoidal source voltage, obtained through simulation, Figure I.4.(b) shows the associated spectrum where the predominance of the 5th, 7th, 11th, and 13th order harmonics appears, as well as the importance of the current harmonic distortion (THDi=34.65%).

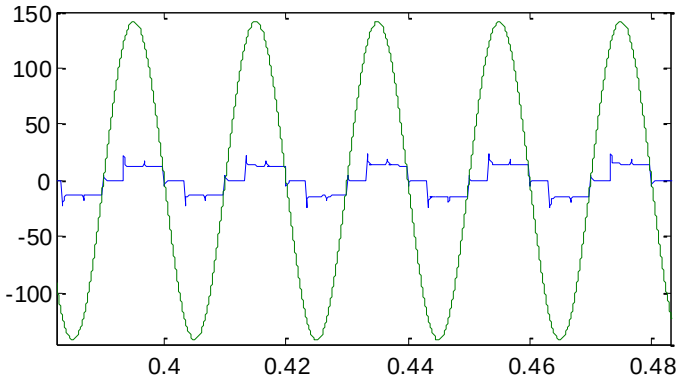

(a)

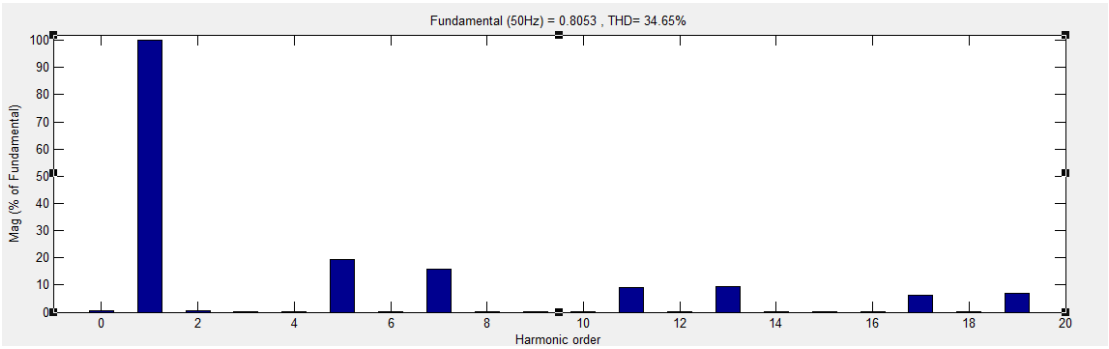

Figure I.4 Currents absorbed by the thyristor rectifier bridge compared to voltage and associated spectrum: **(a)** Grid voltage and current, **(b)** FFT analysis for current THD.

I.5 Harmonic pollution solutions for the electrical network

Several solutions for reducing harmonics exist, these methods based on passive or active components can be divided into two categories **[Fek 18]:**

- Traditional solutions.
- Modern solutions based on power electronics.

I.5.1 Traditional solutions

All electricians should know these techniques. They provide an easy and quick solution for certain cases of well-localized disturbances and use passive components (inductors, capacitors, transformers) and/or connections that modify the installation diagram. Several solutions exist to limit the propagation and effect of harmonics in electrical networks **[Kas 19].**

I.5.1.1 Inductors (AC line, or DC link)

Harmonics currents pollution of non-linear loads can be minimized by placing series inductor (reactor), either to the AC line, this solution is used for adjustable speed drives (variable frequency drives) and three-phase rectifiers, or to the DC link circuit, or both, with the ability of filtering upstream harmonic current, and also decoupling the line voltage distortion from that at the non-linear load side. Either of these added elements can limit also current peaks **[Pin 15].**

I.5.1.2 Reactive power compensation

Many devices consume reactive energy to create electromagnetic fields (such as motors, transformers, and more recently by power electronics devices.). Compensating reactive energy involves providing this energy instead of the distribution network by installing a battery of capacitors in parallel with the network, near the loads that have a poor power factor, which serves as a source of reactive power **[Een 11].**

I.5.1.3 Passive filters

Passive filters are inductance, capacitance, and resistance elements configured and tuned to control harmonics. In general, harmonic passive filters are combination of capacitive and inductive elements connected in parallel with loads that inject harmonic currents (diode or thyristor rectifiers, etc), this allows for a series resonant tuning on the harmonic orders to be eliminated. They are commonly used and are relatively inexpensive compared with other means for eliminating harmonic distortion. However, they have the disadvantage of potentially interacting adversely with the power system, and it is important to check all possible system interactions when

they are designed. They are employed either to shunt the harmonic currents of the line or to block their flow between parts of the system by tuning the elements to create a resonance at a selected frequency **[Dug 02].**

The following can be found under this category:

- Single-tuned filters.
- High- (or band-) pass filters (first, second, and third order).

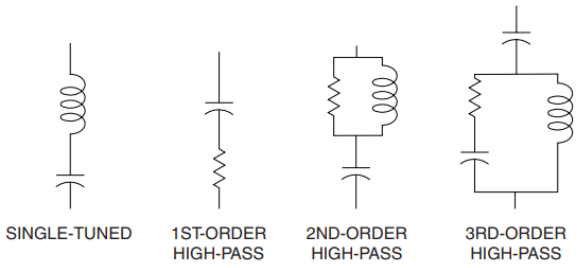

Figure I.5 Electric diagrams of passive filters.

In addition, with this, we can classify them into:

I.5.1.3.1 Parallel passive filter

A very low impedance tuned to the harmonic frequency to be trapped is placed in parallel with the power supply network.

I.5.1.3.2. Series passive filter

The principle is the same as the previous one, but instead of trapping the harmonics, they are prevented from returning to the source **[Mas 22].**

I.5.2 Modern solutions

The remarkable progress made, on the one hand, in the field of semiconductor components, such as IGBTs, IGCTs, GTOs, and MOSFETs, as well as the mastery of their implementation, and on the other hand, the existence of new analog and digital signal processing methods, have led to the emergence of modern and efficient means to deal with various disturbances (harmonics, reactive power, fluctuations, voltage dips) affecting electrical systems. Among these modern means, we can mention **[Fek 18]:**

- Active filters: parallel, series, hybrids, and combinations of structures.

- Uninterruptible power supplies.
- FACTS devices.
- Sinusoidal sampling converters.

I.5.2.1 Active filters

Active filters are relatively new types of devices for eliminating harmonics. They are based on sophisticated power electronics composed of an inverter connected to the grid through a passive filter. And they are much more expensive than passive filters. However, they have the distinct advantage that they do not resonate with the system. Active filters can work independently of the system impedance characteristics. They can be used in very difficult circumstances where passive filters cannot operate successfully because of parallel resonance problems. They can also address more than one harmonic at a time and combat other power quality problems such as flicker. They are particularly useful for large, distorting loads fed from relatively weak points on the power system **[Dug 02].**

I.5.2.1.1 Parallel active filter

The parallel active filter, also known as a shunt compensator, can, with appropriate control, neutralize the harmonic currents of polluting loads and compensate for imbalances and reactive currents. Generally, a preliminary analysis of the load is performed to identify disturbances and compensate for them at the network level through the parallel active filter. The resulting current on the network side is sinusoidal in shape and may be in phase with the voltage at the connection point in the case of harmonic compensation and reactive fundamental compensation.

I.5.2.1.2 Series active filter

This filter is used to filter disturbances coming from the network, and acts as a voltage source that opposes harmonic voltage disturbances coming from the network, protecting the load from network voltage imperfections. It prevents harmonic currents consumed by the non-linear load from flowing back to the source. Therefore, the voltage at the terminals of the protected load is purely sinusoidal. The energy storage element of a series active filter is designed to meet the most severe compensation requirements, particularly in the case of long-lasting voltage dips **[Fek 18].**

I.6 Conclusion

We have presented in this chapter a general overview concerning one of the most important problem affecting power systems, which is harmonics and disturbances affecting the voltage of the grid and degrading the quality of electrical energy. Defining these problems origins and precising their sources and their impacts in all parts of the power systems, and one of the sources that we focused on is the harmonics generated by static converters**,** we have then presented the different traditional and modern means of reducing harmonics. In this context, we have highlighted the contribution of power electronics in the fight against harmonics and the improvement of the quality of electrical energy.

CHAPTER II Mathematical model and hysteresis control of PWM Rectifier.

II.1 Introduction

The PWM Rectifiers by theirs capabilities are going to replace conventional diode. These changes are forced also because of the results in a high distortion rate in the network, which causes distortions in the voltage waveform and leads to a malfunction of the power factor in the network.

The main task of the control system in PWM Rectifiers can be summarized as:

- Precise regulation of output DC voltage,
- Low harmonic distortion of line currents,
- Near sinusoidal current waveforms,
- Regulation of input power factor to unity and bi-directional power flow **[Mar 02].**

Furthermore, the control system in PWM Rectifiers is responsible for efficient energy conversion and management. It optimizes the power transfer between the rectifier and the load, ensuring maximum power utilization and minimizing energy losses. Additionally, PWM Rectifiers contribute to sustainable energy usage and help mitigate environmental impact.

Within this chapter, our exploration is going to be around PWM Rectifiers. Covering their general overview, model, operating principle, and important characteristics. Specifically, our focus will be on the control strategy of the voltage rectifier bridge using Hysteresis-based PWM, incorporating classical PI adjustment.

II.2 PWM Rectifier

The PWM converter consists of three legs with two active switches and two anti-parallel diodes. It performs energy conversion between an AC voltage source and a DC current load. It is also called an active front-end rectifier because it allows power to flow in both directions. All desirable current and voltage waveforms can be achieved by using different PWM methods to control the six switches. By controlling the voltage and current waveforms, it is possible to control

the power factor as well as the amount and direction of power **[Fer 11]**. There are two types of PWM converters:

- **PWM current source rectifier**, also called a buck rectifier (reduces the voltage) which operates with fixed DC current. The switches are unidirectional in current but bidirectional in voltage the use of PWM techniques results in an AC side current with controlled harmonic pollution. This structure is often equipped with a second-order LC filter on the AC side.

- **PWM voltage source rectifier**: also called a boost rectifier (increases the voltage) which works with fixed DC voltage. The switches are unidirectional in voltage and bidirectional in current. Therefore, this converter, due to its structure, is reversible in current. It can instantly control the waveform of the currents drawn from the grid. It supplies a continuous load (active or passive) from an AC grid, with the absorbed current being sinusoidal and potentially in phase with the corresponding grid voltage **[Ben 13] [Dja 20]**.The structure of the two type of PWM converter is shown in Figure II.1. In addition to harmonic elimination and power factor correction, PWM rectifiers provide DC bus voltage stabilization and can also operate properly under line voltage distortion, notching, and line voltage frequency variations. On the other hand, they are expensive, have a complex control structure and a lower efficiency due to extra switching losses **[Dja 20]**.

Nevertheless, PWM Rectifiers are the most promising harmonic mitigation technique among all the ones listed above especially that the speed and performance of power switching devices and digital signal processors are being enhanced and their cost is generally decreasing **[Dja 20]**.

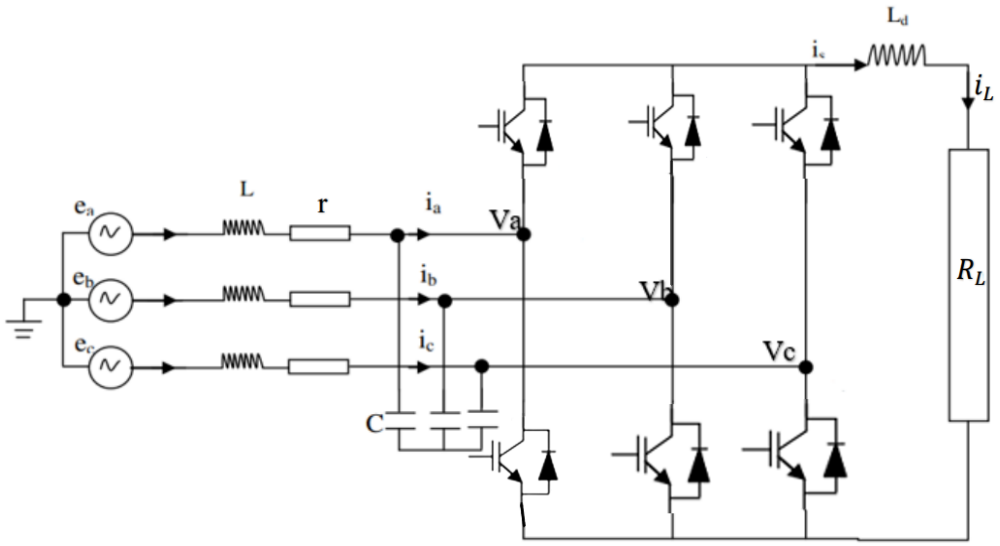

(a)

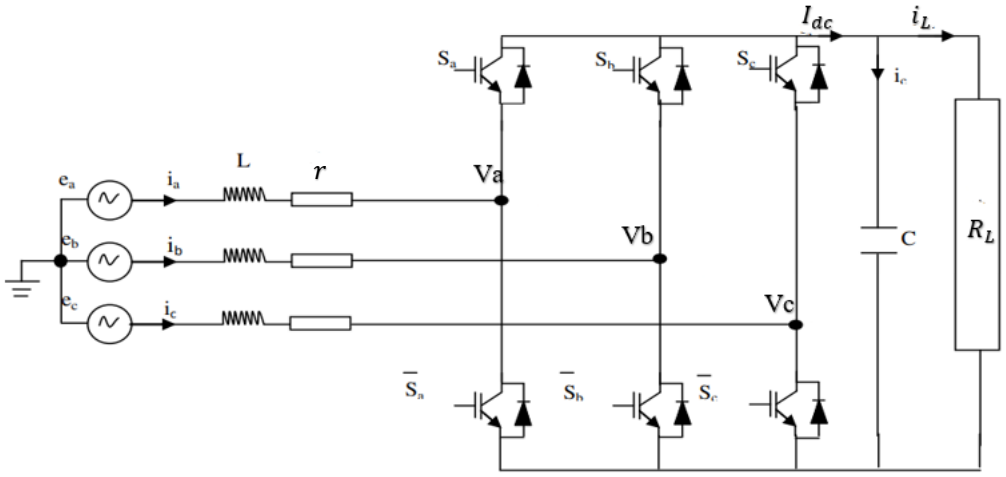

(b)

Figure II.1 PWM Rectifier circuit : **(a**) Current source rectifier, **(b)** Voltage source rectifier.

II.3 The structure and modeling of a three-phase PWM Rectifier

II.3.1 The structure of the Voltage PWM Rectifier

The circuit topology diagram of three-phase PWM Rectifier with pure resistance when it operates independently. In the Figure II.2.(a), e_a, e_b and e_c represent the ideal three-phase balanced grid voltage; RL represents the filter on the AC side of the three-phase PWM Rectifier which function as low-pass filters, restricting the current ripple to the switching frequency. i_a , i_b and i_c represent the grid current; the three-phase full bridge PWM circuit is composed of six switch S_a,S_b,S_c,$\overline{S_a}$, $\overline{S_b}$and $\overline{S_c}$. Each switch consists of an IGBT (Insulated Gate Bipolar Transistor) and an anti-parallel diode that allows current conduction in the opposite direction. V_a, V_b and V_c represent the voltage of the three-phase PMW Rectifier after modulation; C in the DC side is capacitor who act as an equivalent voltage source.

V_{dc} and I_{dc} is the output voltage and current of three-phase PWM Rectifier DC side respectively; R_L is the DC-side pure resistive load **[Bie 21].**

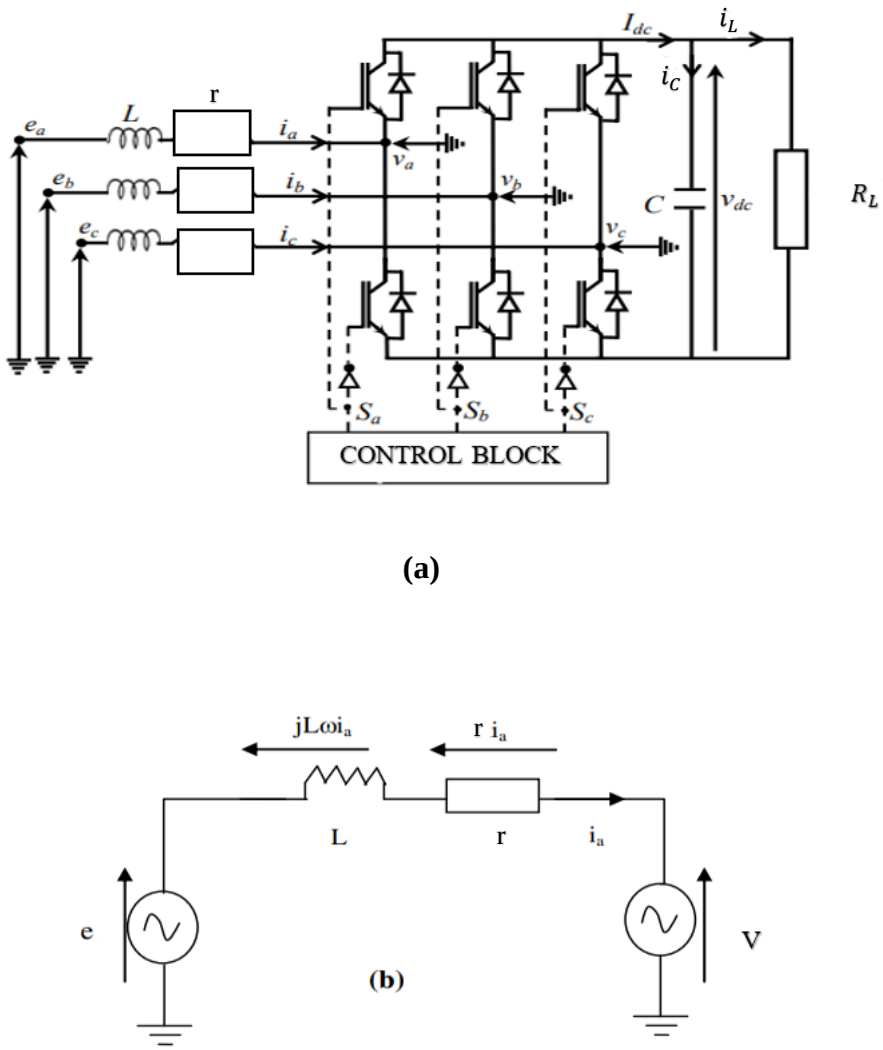

Figure II.2 (a) Three-phase voltage PWM Rectifier structure, **(b)** Equivalent circuit of a single phase **(a)**.

Figure II.2. (b) Shows the equivalent circuit of the grid-side PWM Rectifier. By manipulating the control signals (S_a, $S_b$and S_c), the voltage drop across the input filter (r, L) can be controlled, there by regulating the current i. Achieving unity power factor operation (zero reactive power) is achieved by synchronizing the grid voltage vector with the current vector in both rectifier and inverter modes of operation, as depicted in Figure II.3 **[Rah 17]**.

The structure of PWM Rectifier can be divided into an AC-side and a DC-side. Power can flow from and into either side, it flows from AC-side to DC-side in rectification mode and in reverse direction in regenerative mode. In rectification mode, when the load connected to the DC bus

consumes active power, the converter extracts active power from the grid. In this case, the voltages and currents on the grid side are in phase Figure II.3. (a). In regeneration mode, when the load produces active power, the converter feeds active power back to the grid. In this case, the voltages and currents on the grid side are in phase opposition Figure II.3. (b) **[Rah 17] [Lis 01] [Dja 20]**.

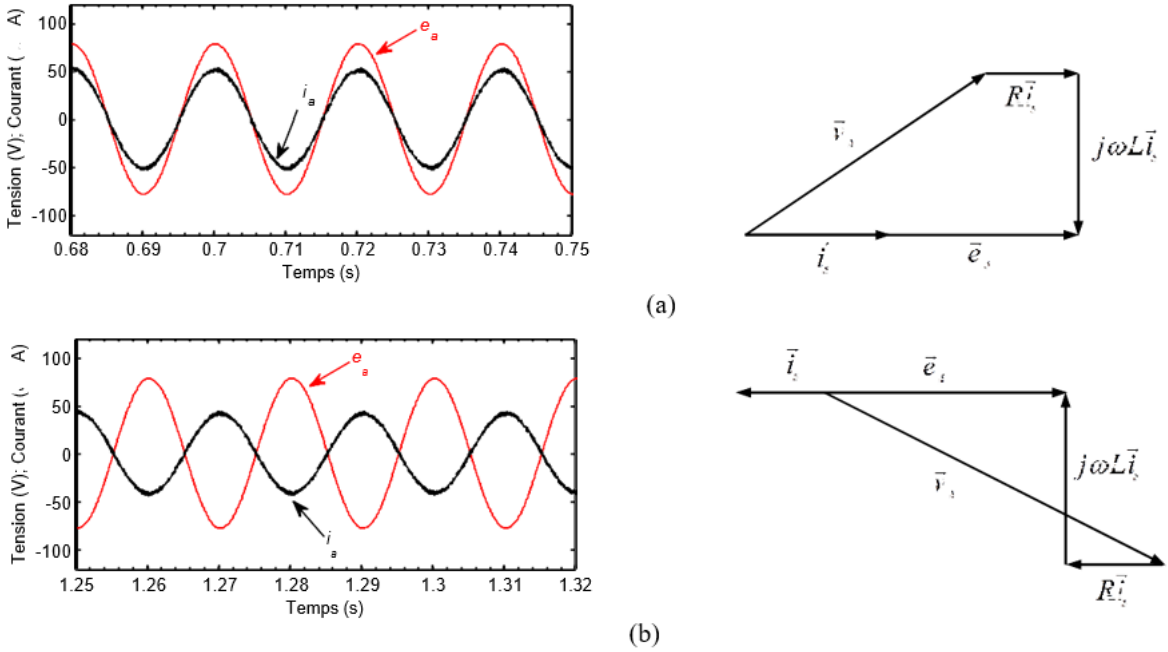

Figure II.3 Vector diagram of operation: **(a)** in rectifier mode and, **(b)** in inverter mode.

II.3.2 Modeling of the three PWM Rectifier

Constructing the mathematical model of the PWM Rectifier is the first step towards designing and implementing its control. In this section, we will present the mathematical model of the PWM Rectifier, Source and load Figure II.4 **[Rah 17]**.

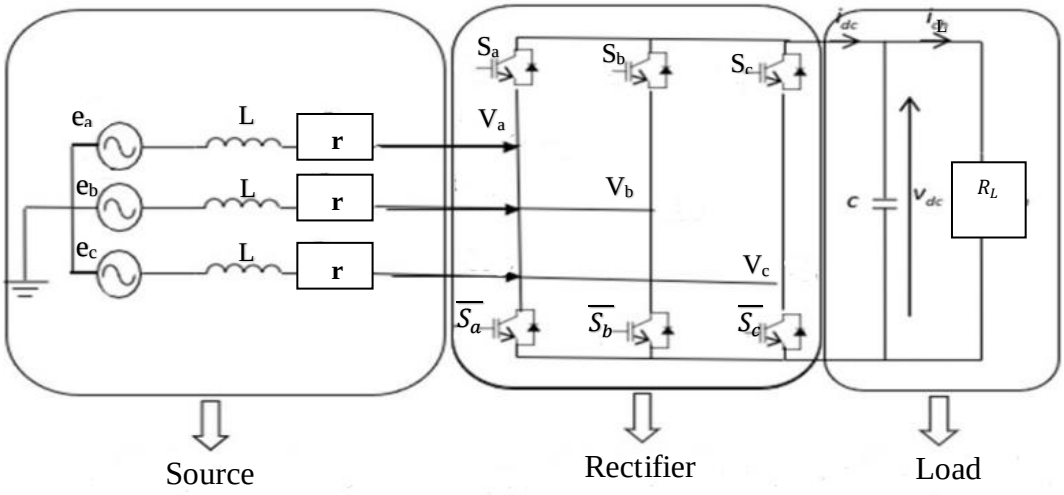

Figure II.4 Diagram of the overall system source-rectifier-load.

II.3.2.1 Power supply

The source is modeled by a three-phase sinusoidal electromotive force (EMF) in series with an inductance (L) and a resistance (r), which represent the total impedance of the line.

$$\begin{cases} e_a = r.i_a + L.\frac{di_a}{dt} + V_a \\ e_b = r.i_b + L.\frac{di_b}{dt} + V_b \\ e_c = r.i_c + L.\frac{di_c}{dt} + V_c \end{cases} \quad \text{(II.1)}$$

We assume a balanced network with the same impedances in all three phases. The line voltages can be expressed as follows **[Ben 14]**:

$$\frac{d}{dt}\begin{bmatrix} i_a \\ i_b \\ i_c \end{bmatrix} = \begin{bmatrix} \frac{-r}{L} & 0 & 0 \\ 0 & \frac{-r}{L} & 0 \\ 0 & 0 & \frac{-r}{L} \end{bmatrix}\begin{bmatrix} i_a \\ i_b \\ i_a \end{bmatrix} + \frac{1}{L}\begin{bmatrix} e_a - V_a \\ e_b - V_b \\ e_c - V_c \end{bmatrix} \quad \text{(II.2)}$$

II.3.2.2 PWM rectifier

It is represented in the diagram in Figure II.4. The IGBTs and diodes constituting the bridge are assumed to ideal, neglecting the switching phenomena.

It is modeled by associating a logical function to each arm **[Ben 14]**:

$$\begin{cases} \text{if Si} = 1 \quad \text{than} \quad \text{Si is closed and } \overline{Si} \text{ is open.} \\ \text{if Si} = 0 \quad \text{than} \quad \text{Si is open and } \overline{Si} \text{ is closed.} \end{cases} \quad \text{I=a, b, c.}$$

The individual phase voltages at the input of the rectifier can be expressed in terms of the control commands by the following relationship **[Rah 17]**:

$$\begin{bmatrix} V_a(t) \\ V_b(t) \\ V_c(t) \end{bmatrix} = \frac{V_{dc}(t)}{3} \begin{bmatrix} 2 & -1 & -1 \\ -1 & 2 & -1 \\ -1 & -1 & 2 \end{bmatrix} \begin{bmatrix} S_a \\ S_b \\ S_c \end{bmatrix} \quad \text{(II.3)}$$

The current drawn by the rectifier can be expressed in terms of the currents taken from the grid by the following expression:

$$I_{dc}(t) = [S_a \quad S_b \quad S_c] \begin{bmatrix} i_a(t) \\ i_b(t) \\ i_c(t) \end{bmatrix} \quad \text{(II.4)}$$

II.3.2.3 Load Block

This stage consists of a capacitance C (to reduce the ripples of the rectified voltage) placed in parallel with a resistance R_L, representing the continuous load. The DC voltage across the load is given by the following equation **[Mas 22]**:

$$\begin{cases} \frac{dV_{dc}}{dt} = \frac{1}{c}(I_{dc} - i_L) \\ V_{dc} = R_L i_L \end{cases} \quad \text{(II.5)}$$

Based on the relationships (II.1), (II.2), (II.3), (II.4) (II.5), we can establish the overall functional diagram of the PWM rectifier Figure II.5, with the trigger command of the upper switches (S_a, S_b and S_c) as input and the rectified voltage V_{dc} as output.

II.3.2.4 Calculation of instantaneous powers in the abc reference frame

Instantaneous active power is defined as the dot product between line currents and voltages, while instantaneous reactive power is defined as their cross product **[Fek 18].**

$$\mathrm{P} = \mathrm{e_a i_a} + \mathrm{e_b i_b} + \mathrm{e_c i_c} \quad \text{(II.6)}$$

$$Q = \frac{1}{\sqrt{3}}[(e_b - e_c)i_a + (e_c - e_a)i_b + (e_a - e_b)i_c] \quad \text{(II.7)}$$

The complex apparent power S can be expressed by the following expression:

$$\begin{cases} \overline{S} = P + jQ \\ \overline{S} = \mathrm{e_a i_a} + \mathrm{e_b i_b} + \mathrm{e_c i_c} + j\frac{1}{\sqrt{3}}[(e_b - e_c)i_a + (e_c - e_a)i_b + (e_a - e_b)i_c] \end{cases} \quad \text{(II.8)}$$

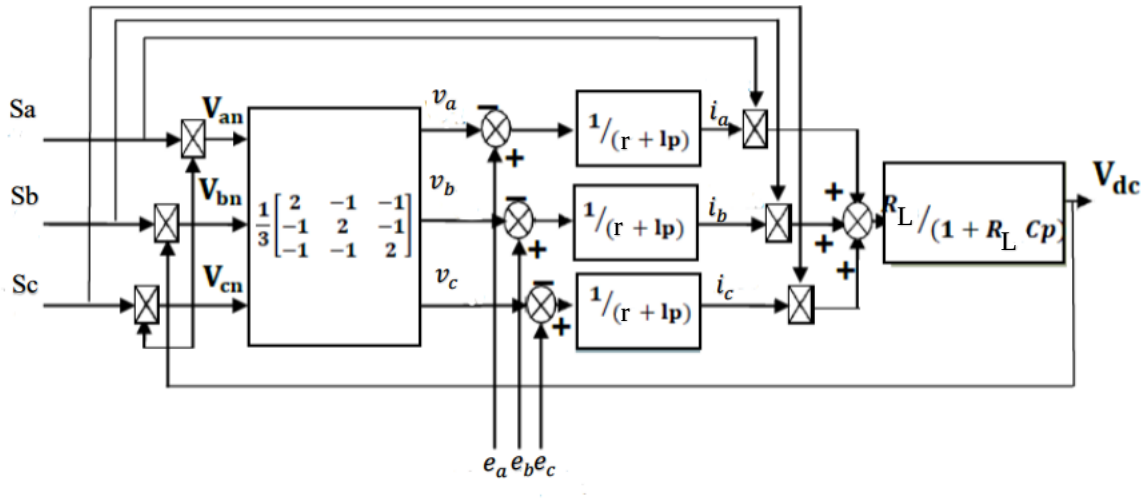

Figure II.5 Functional diagram of the PWM Rectifier.

II.3.3 Modeling of IGBT Bridge

Semiconductor switches, controllable for opening and closing, allow for efficient control of power converters connected to the grid. These switches act as an interface in executing control algorithms. It is possible to replicate the reference voltages generated by the control by varying the opening-closing duration of these switches. This ensures precise control of power flow.

Different construction topologies have been developed. Among these topologies, the two-level PWM Rectifier is widely used as a high-performance interface. It is possible to control the input voltage as well as optimize the shape of the currents absorbed by the rectifier by controlling the switch commutations**.** Figure II.2 represents the simplified diagram of the voltage PWM Rectifier. The symbols S_a, S_b, and S_c denote the control signals or switching states of each switch, with a value of either 0 or 1. Note that the two switches in each leg are complementary ($S_a + \overline{S_a}$ = 1, $S_b + \overline{S_b}$ = 1, $S_c + \overline{S_c}$ = 1), meaning that only one switch is closed for each leg at any given time. Table 2.1 represents the eight possible configurations of the rectifier based on the control signals (S_a, S_b and S_c) **[Rah 17]**.

N°	S_a	S_b	S_c	V_a	V_b	V_c
0	0	0	0	0	0	0
1	1	0	0	$2V_{dc}/3$	$-V_{dc}/3$	$-V_{dc}/3$
2	1	1	0	$V_{dc}/3$	$V_{dc}/3$	$-2V_{dc}/3$
3	0	1	0	$-V_{dc}/3$	$2V_{dc}/3$	$-V_{dc}/3$
4	0	1	1	$-2V_{dc}/3$	$V_{dc}/3$	$V_{dc}/3$
5	0	0	1	$-V_{dc}/3$	$-V_{dc}/3$	$2V_{dc}/3$
6	1	0	1	$V_{dc}/3$	$-2V_{dc}/3$	$V_{dc}/3$
7	1	1	1	0	0	0

Table II.1 Truth table of the Voltage Source Inverter (VSI) rectifier.

II.4 Control strategies for the grid-connected PWM rectifier

For the type of PWM Rectifiers, research interest in three-phase Pulse Width modulated (PWM) Rectifiers (AC/DC converters) has grown rapidly over the past few years due to some of their important advantages, such as power regeneration capabilities, control of dc-bus voltage, low harmonic distortion of input currents, and high power factor (usually, near unity). Various control strategies have been proposed in recent work on this type of PWM converter. Although these control strategies can achieve the same main goals, such as the high power factor and near-sinusoidal current waveforms, their principles different and one of thus techniques are **[Mal 01]:**

II.4.1 Current Control Techniques for Three-Phase Voltage-Source PWM Converters

Most applications of three-phase voltage-source pulse width modulated (Voltage-Source PWM) converters have a control structure comprising an internal current feedback loop. Consequently, the performance of the converter system largely depends on the quality of the applied current control strategy. Therefore, current control of PWM converters is one of the most important subjects of modern power electronics**.**

II.4.1.1 Basic Scheme of Current Control-PWM

The main task of the control scheme in a CC-PWM converter Figure II.6 is to force the currents in a three-phase ac load to follow the reference signals. By comparing the command (i_{Ac},$i_{Bc}$and i_{Cc}) and measured (i_A,$i_B$and i_C)instantaneous values of the phase currents, the CC generates the switching states (S_A ,S_B and S_C) for the converter power devices which decrease the current errors Hence, in general, the CC implements two tasks: error compensation (decreasing ε_A,ε_B and ε_C) and modulation (determination of switching states S_A ,S_B and S_C) [**Kaz 98].**

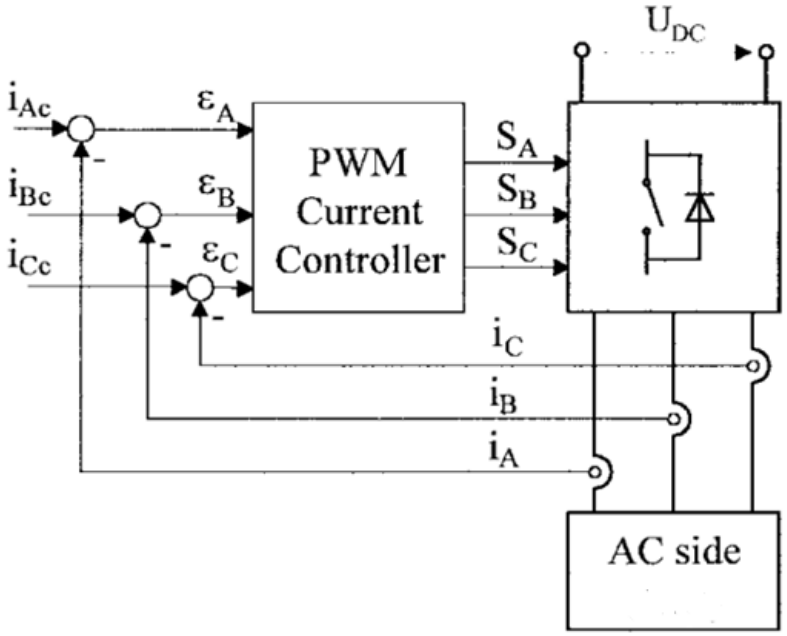

Figure II.6 Block diagram of Current Control-PWM converter.

II.4.1.2 Basic Requirements and Performance Criteria

The accuracy of the CC can be evaluated with reference to basic requirements, valid in general, and to specific requirements, typical of some applications. Basic requirements of a Current Control are the following [**Kaz 98]**:

1) No phase and amplitude errors (ideal tracking) over a wide output frequency range.
2) To provide high dynamic response of the system.
3) Limited or constant switching frequency to guarantee safe operation of converter semiconductor power devices.
4) Low harmonic content.
5) Good dc-link voltage utilization.

II.4.2 Fundamental concepts hysteresis current control

The Hysteresis Current Control is well-known method and offers significant advantages in terms of robustness and simplicity of implementation, reveals very fast transient effect and is appropriate for easily applications. In HCC method as proven in Figure II.7, i_{mes}(real line current) is compared with i_{ref} (reference current). The preferred shape and magnitude of i_{ref} are derived from the voltage controller output. Hysteresis based (ΔI) is output of the hysteresis comparator. It is difference of i_{mes}actual and i_{ref} reference.

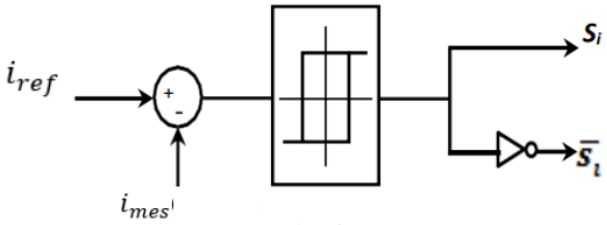

Figure II.7 Principle of Hysteresis Current Control.

For control converter, switches are turned ON/OFF using the end result of comparator output signal shows switching signal variation, which made this control technique is considered a non-linear control. Therefore, the operations of switches of converter were forced to observe the preferred reference interior hysteresis band. However, the disadvantage is that there is no limit to the switching frequency. On the other hand, additional circuitry can be used to limit the maximum switching frequency. The principle of the hysteresis control method is implemented by presenting the upper and lower tolerance limits, which need to be compared to the extraction error signal. The maximum error is the difference between the upper and lower limit, and this hysteresis tolerance bandwidth is mostly equal to two times of the error. If the error signal is within the tolerance band, there will be no switching action for the filter. However, when the error leaves the tolerance band, switching pulses will be generated Figure II.8 illustrates the ramping of the current between the two limits **[Dwi 17] [Blo 11]**.

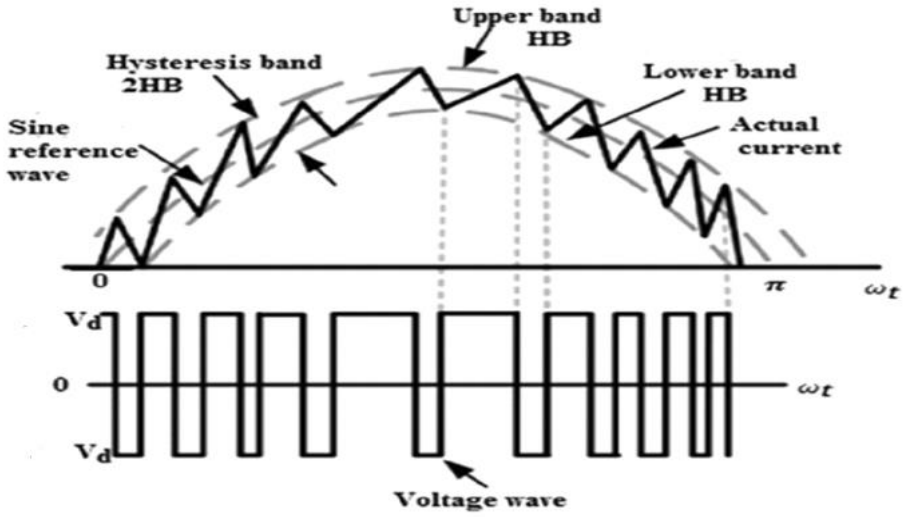

Figure II.8 Hysteresis Current Control (HCC) operation waveform.

Several other studies have been proposed to improved the main drawback of this modulation technique which lies in the irregular and uncontrollable switching frequency of the switches, which generates an extended and highly distorted harmonic spectrum that is difficult to filter, this studies allow for controlling the minimum duration between successive switchings or working at a constant switching frequency. However, these modifications significantly limit the advantages of this control technique (loss of simplicity and robustness) and require a good understanding of the system parameters, which considerably reduces the overall performance **[Bou 10].**

II.4.2.1 Basic scheme of hysteresis current control strategy in the application of converter

The overall structure of hysteresis current control for the currents drawn from the grid by a three-phase PWM voltage-source rectifier is depicted in Figure II.9. The three currents at the input of the rectifier are controlled using three fixed hysteresis comparators Figure II.7. The combination of the three-comparator outputs determines the control commands for the switches of the rectifier. The determination of the switching instants follows the following logic **[Mas 22]:**

$$i_{i\,ref} - i_i = \frac{\Delta I}{2} \rightarrow S_i = 1 \qquad i = a, b, c \tag{II.9}$$

$$i_{i\,ref} - i_i = -\frac{\Delta I}{2} \rightarrow S_i = 0 \qquad i = a, b, c \tag{II.10}$$

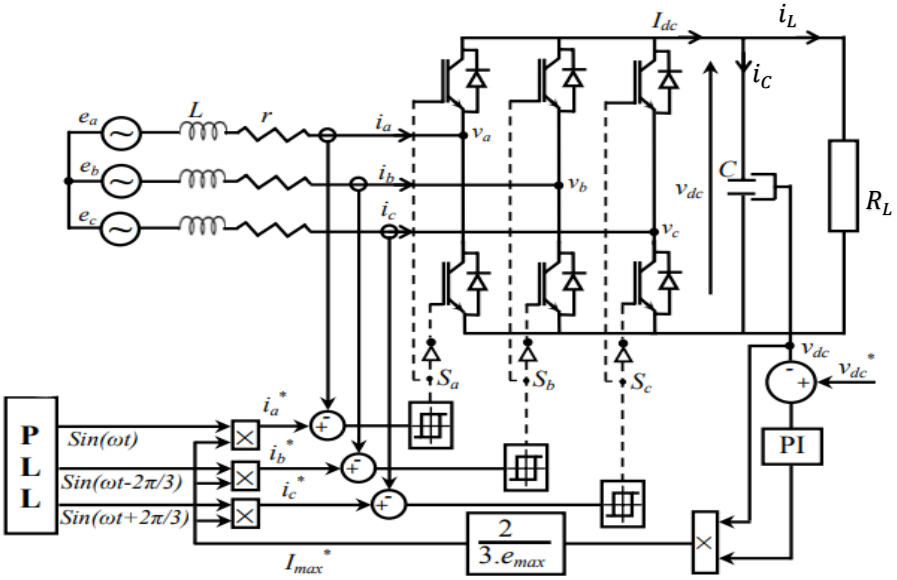

Figure II.9 Structure of Hysteresis Current Control absorbed by the PWM Rectifier.

II.4.2.2 PLL for the synchronization of the PWM Rectifier with the electrical grid

In order to ensure Unity Power Factor operation and controlled exchange of active and reactive power, the PWM Rectifier must always be synchronized with the grid. A Phase-Locked Loop (PLL) is commonly used for synchronization the basic configuration of the PLL system is shown in Figure II.10. This technique allows obtaining the instantaneous angle of the grid voltages by exploiting a fundamental property of the Park transformation, which states that if the instantaneous angle involved in the transformation θ is equal to the instantaneous angle θ_{est} of the balanced three-phase voltage system, then the components along the d-q axes will be constant **[Rah 17]**.

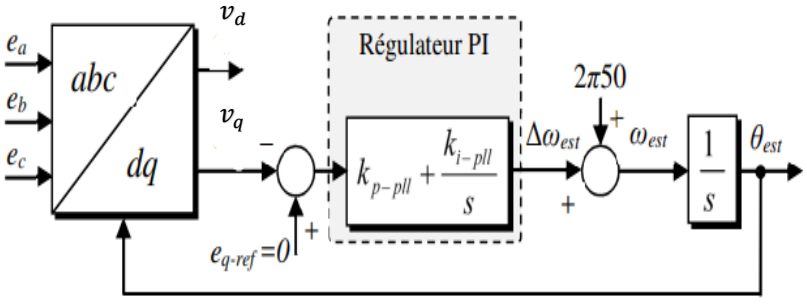

Figure II.10 Three phase PLL algorithm block diagram.

The three-phase voltage system (e_a, e_b, e_c), when expressed in the synchronous reference frame, yields the d-axis and q-axis voltages v_d and v_q, respectively. The PLL presented here achieves the tracking of the instantaneous angle of the grid voltages through a control loop. Assuming balanced three-phase voltages, a model can be developed for the PLL control loop. Thus, by applying the Park-Clark transformation, given by the equation (II.12), to the three-phase voltages, we have:

$$e_a = E_m sin(\theta t)$$

$$e_b = E_m sin(\theta t - 2\pi/3) \quad \text{(II.11)}$$

$$e_c = E_m sin(\theta t + 2\pi/3)$$

$$\begin{bmatrix} v_d \\ v_q \end{bmatrix} = \begin{bmatrix} \cos(\theta) & \cos(\theta - 2\pi/3) & \cos(\theta + 2\pi/3) \\ -\sin(\theta) & -\sin(\theta - 2\pi/3) & -\sin(\theta + 2\pi/3) \end{bmatrix} \begin{bmatrix} e_a \\ e_b \\ e_c \end{bmatrix} \quad \text{(II.12)}$$

If the error $\Delta\theta$ between the angle θ and the estimated angle by the PLL θ_{est} is zero, $V_{Si} = E_m$ and $v_q = 0$. It is then possible to track the instantaneous angle of the grid voltages.

The linearized model that allows for easy synthesis of the PLL regulator. We have chosen a PI-type regulator. The control loop obtained is given in the transfer function module **[Rah 17]**.

$$G_c(s) = \frac{k_{p-PLL}s + k_{i-PLL}}{s} \quad \text{(II.13)}$$

The output of the controller is the actuation signal and it is added to the center frequency ω_c.=*2.pi.f* , the generated result of the sum block is the frequency in radian and is integrated to obtain the angle θ. After obtaining the angle θ we take it and the constant 2π and passed to a modulo operation. The output of the mod block properly wraps the angle θ and maintains it between 0 and 2π.

The transfer function is given as follows

$$G_{open\ loop} = E_m \frac{k_{p-PLL}s + k_{i-PLL}}{s} \frac{1}{s} \quad \text{(II.14)}$$

$$G_{closd\ loop} = \frac{E_m(k_{p-PLL}s + k_{i-PLL})}{s^2 + E_m k_{p-PLL}s + E_m k_{i-PLL}} \quad \text{(II.15)}$$

There are different methods to choose the $k_{p-PLL}$and k_{i-PLL} parameters of the PI regulator. The most appropriate method depends on the performance criteria to be imposed on the regulator. In this case, we have a second-order system. Therefore, we have used the pole-placement method. By matching it to a second-order system, we obtain:

$$\begin{cases} \mathrm{k_{p-PLL}} = -\frac{\omega_{\mathrm{C-PLL}}^2}{\mathrm{E_m}} \\ \mathrm{k_{i-PLL}} = -\frac{2\xi\omega_{\mathrm{c-PLL}}}{\mathrm{E_m}} \end{cases} \quad \text{(II.16)}$$

Since the closed-loop system acts as a low-pass filter, choosing a cutoff frequency ω_{c-PLL} close to the grid frequency ω is the best solution to attenuate the effect of harmonics on the angle θest without the need for an external filter. Therefore, the cutoff frequency ωc-pll is chosen for a damping factor ξ = 0.7. We then obtain $\mathrm{k_{p-PLL}} = 6.337$ and $\mathrm{k_{i-PLL}} = 1422.13$ **[Rah 17]**.

II.4.2.3 DC voltage regulation loop

The role of the regulation loop for the DC bus voltage is to maintain a constant reference value by controlling the charging and discharging of the capacitor. Voltage variations are primarily caused by losses in converter switches (conduction and switching), coupling inductance losses, and variations in the connected load. The regulation of DC voltage is achieved by adjusting the amplitude of the current references to control the active power flow between the grid and the DC bus, compensating for disturbances from the converter and load sides. The loop takes reference voltage (V_{dc}*) and measured voltage (V_{dc}) as inputs. A PI controller is commonly used to regulate the voltage. By neglecting losses due to switching and conduction in the IGBT switches, as well as losses from Joule effects in the input filter, the power conservation principle establishes a relationship between the input and output powers of the rectifier **[Bou 10]**. This relationship can be expressed as follows:

$$P = V_{dc}I_{dc} = \frac{1}{2}C\frac{{V_{dc}}^2}{dt} + \frac{V_{dc}^2}{R_L} \quad \text{(II.15)}$$

From this equation, we deduce the following first-order transfer function.

$$\frac{V_{dc}^2(s)}{p(s)} = \frac{R_L}{1+\frac{R_L.C}{2}s} \quad \text{(II.16)}$$

On the other hand, the active power supplied by the grid is defined by the following relationship:

$$P = \frac{3}{2} e_{max} . I_{max} \tag{II.17}$$

Assuming a constant amplitude of the grid voltage. In this case, the previous transfer function transforms into the following form.

$$\frac{V_{dc}^2(s)}{I_{max}(s)} = \frac{3}{2} e_{max} . \frac{R_L}{1+\frac{R_L.C}{2}s} \tag{II.18}$$

The block diagram of the regulation loop of the DC bus voltage is represented in Figure (II.11). In this structure, the current loop is considered ideal (unity) assuming that it is much faster than the voltage loop and that the actual current is approximated to its reference value.The regulator is chosen to provide the value of the DC bus current I_{dc} necessary to maintain capacitor charge and meet the load requirements. The amplitude of the reference currents is then calculated based on the following relation:

$$\frac{3}{2} e_{max} . I_{max} = V_{dc} . I_{dc} \tag{II.19}$$

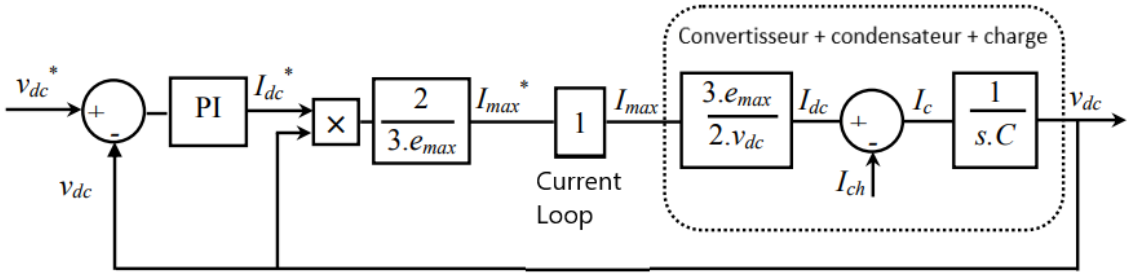

Figure II.11 Block diagram of the regulation loop for the DC bus voltage.

In this work, we used the regulation loop for the V_{dc} voltage, and the parameters of the PI controller are calculated based on the dominant pole compensation principle. They are given by the following expressions:

$$\begin{cases} T_i = \frac{3.R_L.e_{max}}{4.\pi.f_c} \\ K_p = \frac{C.R_L}{2.T_i} \end{cases} \qquad with\ f_c\ being\ the\ cutoff\ \ frequency \tag{II.20}$$

II.5 Simulation results and discussion

This section show cases the performance evaluation of hysteresis current control implemented in a Pulse Width Modulation (PWM) voltage source rectifier in hysteresis bandwidth $\mathbf{\Delta I = 0.1}$. The evaluation was conducted through simulation, considering both steady-state and transient scenarios, while incorporating a closed-loop configuration with DC bus voltage regulation. A series of tests were carried out in the closed-loop system, exploring both transient and steady-state operating conditions. The circuit and control parameters are indicated in Table II.2.

Coupling inductance resistance *r*	**0.56 Ω**
Coupling inductance self-inductance *L*	**19.5 mH**
DC bus capacitance *C*	**1100 µF**
Load resistance	**68.6 Ω**
Effective composite grid voltage *E*	**85 V**
Grid frequency *f*	**50Hz**
Output DC voltage reference v_{dc}	**180 V**

Table II.2 Electrical circuit parameters and control data.

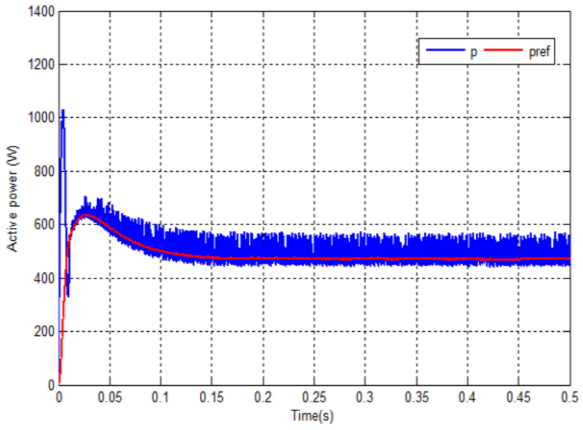

(a)

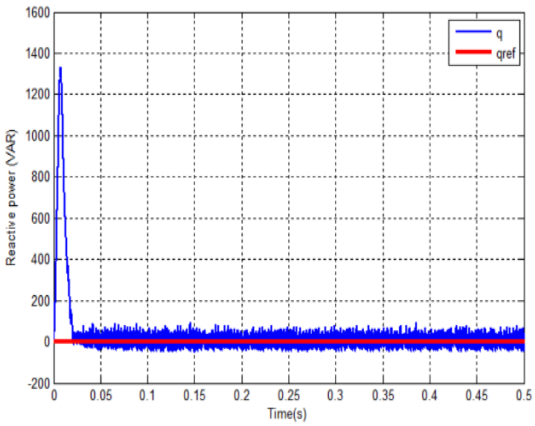

(b)

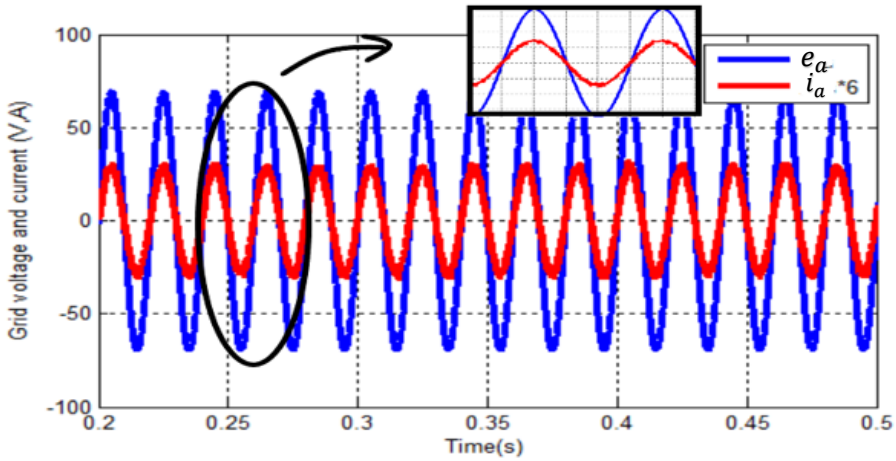

(c)

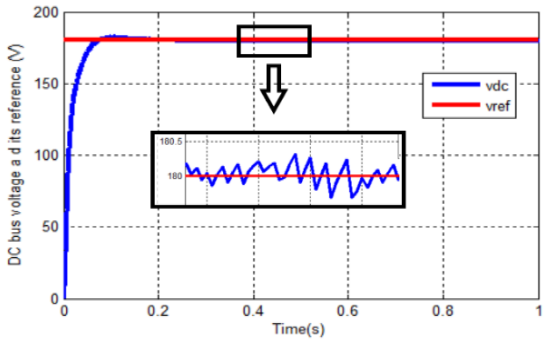

(d)

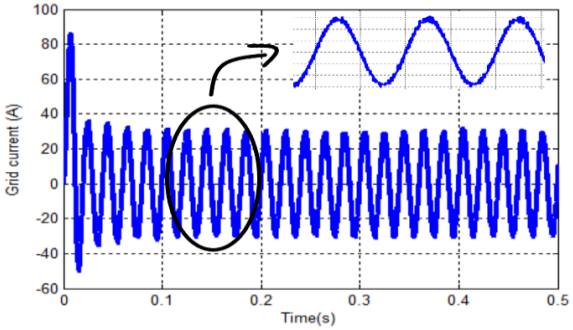

(e)

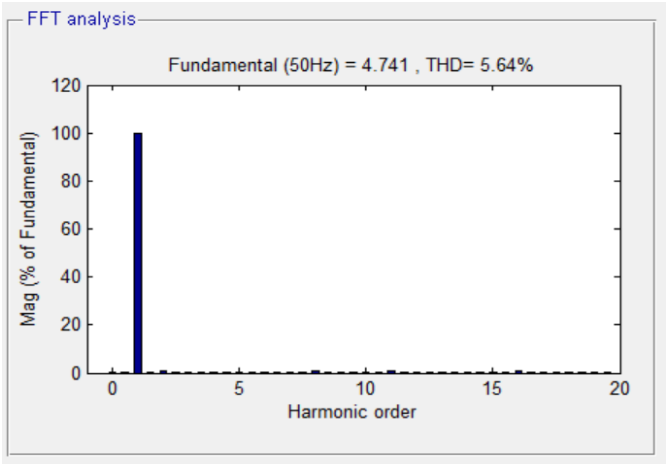

(f)

Figure II.12 Performance of the hysteresis-controlled PWM Rectifier for V_{dc}^{*}=180V: **(a)** The active power P and its reference, **(b)**The reactive power Q and it's reference, **(c)** Grid voltage and current, **(d)** The DC bus voltage and it's reference**, (e)** Grid current.

(f) FFT analysis for current THD**.**

- Here, in this test a step of the reference DC voltage is applied at t = 0.3s from 180 V to 220 V, so that we can observe the changes that will occur in the current, voltage, and THD. Thus, we obtain the following results :

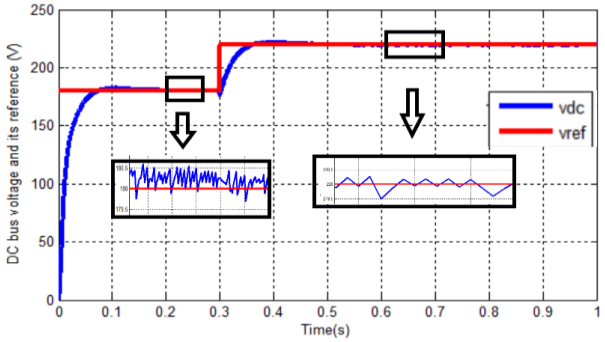

(a)

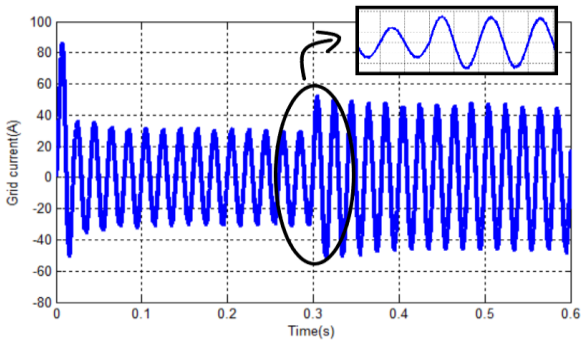

(b)

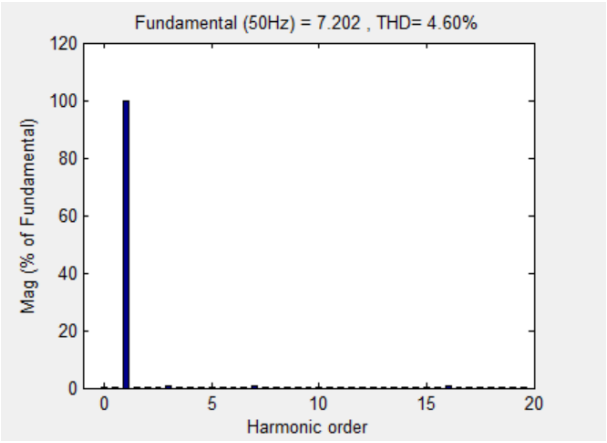

(c)

Figure II.13 Performance of the hysteresis-controlled PWM Rectifier for a variable reference voltage V_{dc}^{*}: **(a)**The DC bus voltage and it's reference, **(b)** Grid current , **(c)** FFT analysis for current THD .

- Here, in this test a step of the load R_L is applied at t = 0.3s from 68.6 Ω to 120 Ω , so as to observe the same changes in the system and obtain the following results :

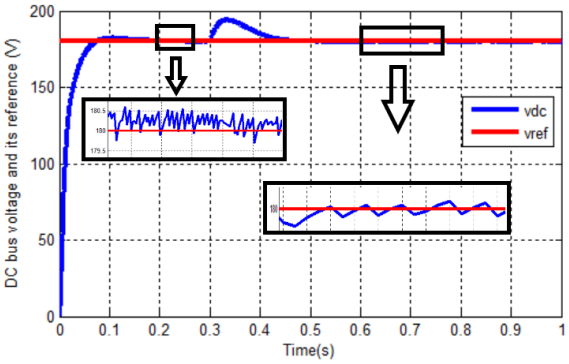

(a)

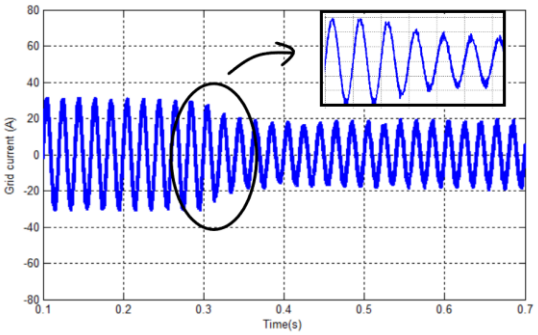

(b)

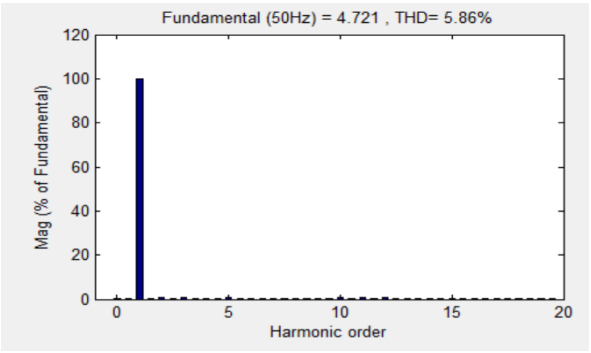

(c)

Figure II.14 Performance of the hysteresis-controlled PWM Rectifier for variable load R_L: **(a)**The DC bus voltage and its reference, **(b)** Grid current, **(c)** FFT analysis for current THD **.**

II.6 Interpretation of simulation results

- **The Figure II.12** represents the simulation results for a constant output reference voltage V_{dc}^{*} , we can clearly observed that :
  - The current harmonic distortion rate is low (5.64 %).
  - The grid voltage and current are synchronized.
  - Reactive power is almost constant at 70 VAR, and the active power remains consistently high at 500 watts.
  - The DC bus voltage reaches the reference voltage.

- **The Figure II.13** represents the results for a variable output voltage reference

V_{dc}^{*} with a constant load (R_L= 68,6 Ω) , we can notice that :

- The grid current increases with the increase of the reference.
- The current harmonic distortion rate is (THD=4.60 %).
- The DC bus voltage reaches the reference value (after 0.1 s).

- **The Figure II.14** represents the results for the case of a variable load R_L , while the reference voltage remains constant (V_{dc} = 180v) , we notice that :
  - The grid current value shows an inverse relationship with the variable load.
  - The current harmonic distortion rate is (THD=5.68 %).
  - The DC bus voltage reaches the reference value.

II.7 Conclusion

In this chapter, the study on Hysteresis Current Control (HCC) technique for rectifiers has shed light on its significant impact on the rectifier, grid, and load. Through this chapter, we have explored the various aspects of HCC and its implications. The HCC technique offers several advantages in rectifier operation. Firstly, it provides a simple and straightforward control strategy that is relatively easy to implement. This simplicity allows for efficient control of the rectifier, resulting in improved overall performance. Secondly, HCC ensures a unity power factor, leading to enhanced power quality and reduced reactive power demand from the grid. This not only benefits the utility company but also contributes to a more stable and reliable power supply. Moreover, the HCC technique exhibits a remarkable ability to minimize harmonic distortion. The major disadvantage of hysteresis control is the variable switching frequency that depends on the bandwidth.

CHAPITRE III Direct Power Control of three-phase PWM Rectifier.

III.1. Introduction

In recent years, several control strategies for three-phase PWM Rectifiers have been developed thanks to the advanced development of semiconductor devices and to digital methods **[Mal 04].** These control techniques have the same goal with a different operating principle, it can be divided into two categories, according to their use of the control loops of the powers and the currents of a three-phase PWM Rectifier. In particular, the DPC is based on the direct use of the instantaneous active and reactive power as control variables, by changing the variables of current served in embedded systems **[Mar 14]**. However, it ensured of better dynamic performance as well as a regulation of active and reactive power. We find their application in the control of active filters **[Cha 08]** and the PWM rectifier **[Vaz 08]** . The first DPC was presented in 1991 **[Ohn 91]** as a simple means of controlling a three-phase grid-connected rectifier. This algorithm was based on a switching table that provided an adequate inverter state by taking into account only the signs of the desired active and reactive power changes and the grid-voltage phase angle. Later, in 1998, a similar algorithm was presented **[Nou 98]** that had a greater impact in the scientific community and that still nowadays is regarded as a benchmark to which new DPC implementations are compared.

- This chapter is subdivided as follows :
    - Classic DPC with pre-defined switching table.
    - Classic DPC with a new switching table.

We will present the simulation results that highlight the performance of these methods, develop the operating principle, and discover the advantages and disadvantages of each method.

III.2 Direct Power Control (DPC)

III.2.1 Principle of Direct Power Control (DPC)

The main idea of the Direct Power Control (DPC), initially proposed by Ohnishi in 1991 and later developed by Noguchi and Takahashi in 1998, is similar to the Direct Torque Control (DTC) of induction machines. Instead of flux and torque, the instantaneous active (P) and reactive (Q) powers are chosen as the two variables to be controlled Figure III.1 **[Bel 17] [Sad 17].**

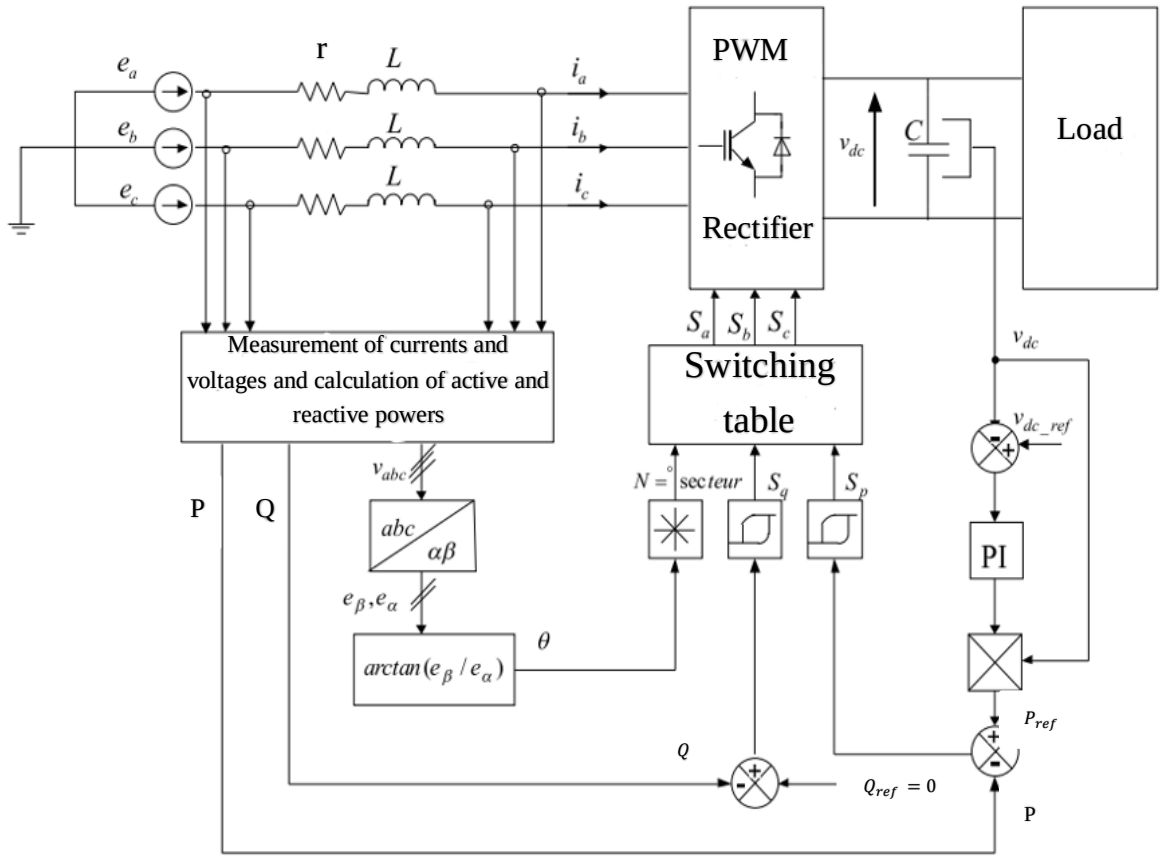

Figure III.1 Configuration of the DPC for three-phase PWM Rectifier with predefined switching table.

The Figure III.1 shows the overall configuration of the sensorless Direct Power Control for a three-phase PWM Rectifier. The DPC consists of selecting a control vector from a switching table. This table is based on the digitized errors S_p and S_q of the instantaneous active and reactive powers (errors between the estimated active and reactive powers and the reference values) provided by the two-level hysteresis controllers, as well as on the estimated voltage vector's angular position.

Depending on the value of this position, the (α-β) plane is divided into twelve sectors of 30°. Each control sequence (S_a, S_b, S_c) corresponds to a voltage vector at the input of the rectifier **[Bou 10]**

[Ben 13]. The reference of the active power P_{ref} is obtained by regulating the dc-bus voltage V_{dc}, while the reference of the reactive power Q_{ref} is set to zero to ensure a Unity Power Factor operation**.**

III.3 DPC with a predefined switching table

The switching table referred to in this work is made by the DTC initiator, first proposed in **[Nog 98]** and later in **[Mal 01]**. The voltage vector v at the input of the PWM Rectifier depends on the switching states (S_a, S_b and S_c) of the semiconductors. Depending on the different possible combinations of these three states, the eight input voltage vectors that can be applied to the rectifier are two empty vectors named (v_0 and v_7) and six non-empty vectors (v_1, v_2, v_3, v_4, v_5, v_6). These vectors are represented in the stationary (α-β) reference frame as shown, with six non-zero vectors dividing the alpha-beta plane into six sectors, each of which is then divided into two equal sectors.

III.3.1. Instantaneous power estimation

III.3.1.1 Calculation of instantaneous injected powers

Based on the measurement of injected voltages and currents, instantaneous active and reactive powers can be calculated using these expressions:

- **For Active power :**

$$P = i^T * e = [i_a \quad i_b \quad i_c] . \begin{bmatrix} e_a \\ e_b \\ e_c \end{bmatrix} = i_a e_a + i_b e_b + i_c e_c \qquad \text{(III.1)}$$

- **For Reactive power :**

$$Q = \frac{1}{\sqrt{3}} [(e_b - e_c) . i_a + (e_c - e_a) . i_b + (e_a - e_b) . i_c] \qquad \text{(III.2)}$$

However, the number of required sensors increases the cost and reduces the reliability of the system. Therefore, in order to accurately estimate power while reducing the number of voltage sensors, noguchi proposes the use of a voltage vector estimator **[Tak 86].**

III.3.1.2 Regulation of DC voltage (the active power reference)

Comparing the instantaneous active power with a reference power, this latter is obtained by the DC voltage control block at the capacitor terminals, where we use a PI controller (Proportional, integrator) to control the error between the sensed voltage (continuous) and reference as shown in Figure III.2 .Whilst to achieve a unity power factor, reactive power reference is directly imposed zero.

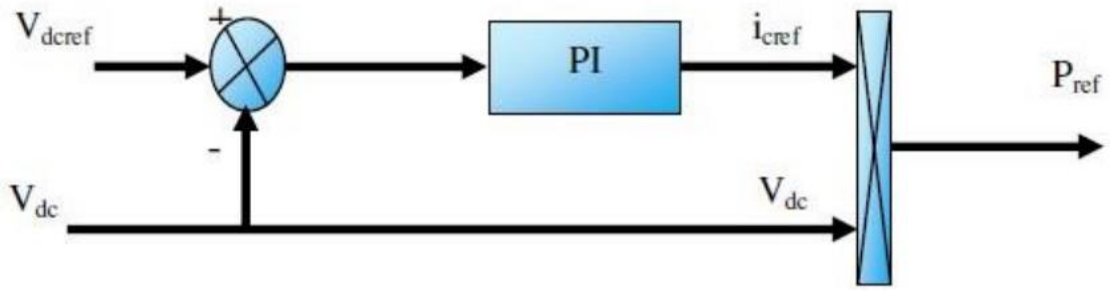

Figure III.2 Control of direct voltage V_{dc}.

III.3.2 Estimation of the network voltage

The working area of the line voltage is required to determine the commands. Moreover, it is important to estimate the line voltage correctly, even with the existence of harmonics, in order to obtain a high-power factor. The voltage drop across the inductor can be calculated by deriving the current. Thus, the voltage can be calculated by summing the reference voltage at the input of the converter with the voltage drop already calculated **[Fek 16] [Den 17]**. On the other hand, this approach has a disadvantage, which is the derivative of the current, where the noise is amplified. To avoid this drawback, a voltage estimate based on the power calculation can be applied The following expression (III.3) gives the line currents i_a , i_b , i_c in the stationary coordinates α, β :

$$\begin{bmatrix} i_\alpha \\ i_\beta \end{bmatrix} = \sqrt{\frac{2}{3}} \begin{bmatrix} 1 & -\frac{1}{2} & -\frac{1}{2} \\ 0 & \frac{\sqrt{3}}{2} & -\frac{\sqrt{3}}{2} \end{bmatrix} \begin{bmatrix} i_a \\ i_b \\ i_c \end{bmatrix} \quad \text{(III.3)}$$

The expressions of the active and reactive powers can be written as follows:

$$P = e_\alpha i_\alpha + e_\alpha i_\beta \quad \text{(III.4)}$$

$$Q = e_\alpha i_\beta - e_\beta i_\alpha \quad \text{(III.5)}$$

III.3.3 Determination of the sector

The DPC technique makes the position of the voltage vector of the grid, for this, the plane (α–β) is divided inside twelve sectors, as shown in Figure III.3. This relation can make the sectors explicit numerically:

$$(n-2)\,\frac{\pi}{6} \leq \theta n \leq \frac{\pi}{6}\,(n-1) \qquad avec: n = 1, 2, 3, \ldots, 12 \quad \text{(III.6)}$$

Here *n* is the sector number. It is instantly set by the position of the grid voltage vector and is calculated by:

$$\theta = arctg\,(\frac{e_\beta}{e_\alpha}) \quad \text{(III.7)}$$

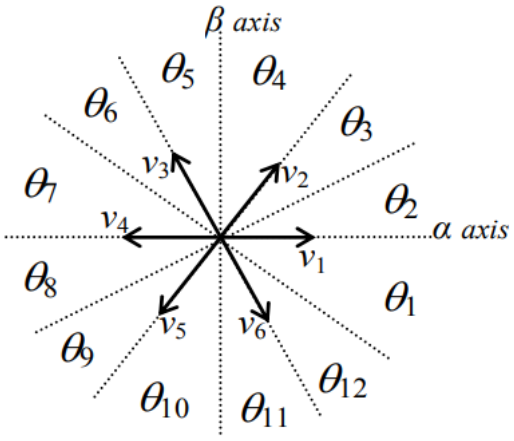

Figure III.3 Sectors and vectors of the rectifier voltages.

Sectors are used to optimize the switching of converters by choosing adjacent vectors. The plane is divided into 12 sectors for greater accuracy and to avoid problems that arise at the borders of each control vector.Meanwhile, the required voltage vector V_i is determined from the commutation table Table III.1 based on the sign of the derivatives of active and reactive power in each sector.

III.3.4 Hysteresis regulator

The instantaneous errors of active and reactive powers are converted into logic outputs S_p and S_q using two two-level hysteresis comparators as shown as in Figure III.4 , if the error increases or decreases beyond a limited band , the output of the hysteresis will take the states 1 or 0 respectively, if the errors are within the permissible error range, the output will remain the same. So, for hysteresis bands H_P and H_Q of active and reactive powers respectively, the outputs of the hysteresis comparators are **[Dja 21]**:

$$\begin{cases} S_p = 1 & if \;\; P < P_{ref} - H_P \\ S_p = 0 & if \; P > P_{ref} + H_P \\ S_q = 1 & if \;\; Q < Q_{ref} - H_Q \\ S_q = 0 & if \;\; Q > Q_{ref} + H_Q \end{cases} \tag{III.8}$$

H_P and H_Q represent the deviations of hysteresis regulators

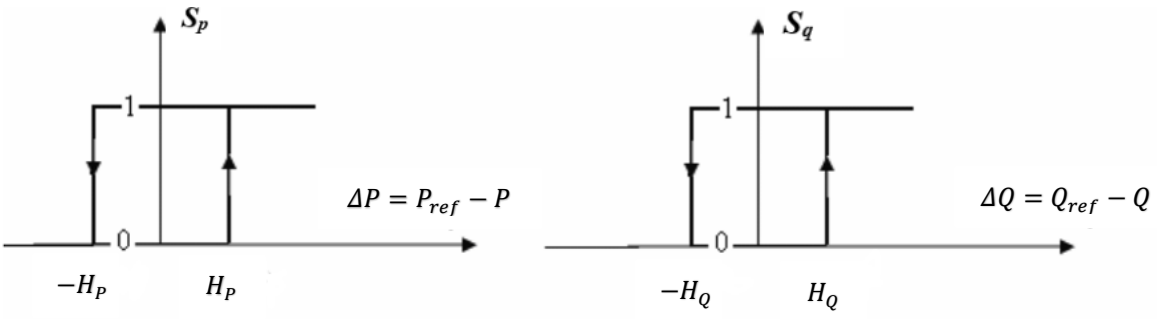

Figure III.4 Characteristics of two-level hysteresis regulators.

III.3.5 The switching table

The selection of switching sequences (S_a, S_b, S_c) of the PWM rectifier depends on the digitized errors S_p and S_q, as well as the angular position of the line voltage vector in the $\alpha\beta$ reference frame. The 12 sectors on stationary coordinate and the rectifier voltage vectors are presented in Figure III.3. **[Dja 21].** When the digitized values S_p, S_q, and the sector of work θn are well determined. The switching states of the three-phase PWM rectifier for all sectors are given by the switching table represented in Table III.1: **[Jam 17]**

S_P	S_q	θ_1	θ_2	θ_3	θ_4	θ_5	θ_6	θ_7	θ_8	θ_9	θ_{10}	θ_{11}	θ_{12}
1	0	v_6	v_7	v_1	v_0	v_2	v_7	v_3	v_0	v_4	v_7	v_5	v_0
	1	v_7	v_7	v_0	v_0	v_7	v_7	v_0	v_0	v_7	v_7	v_0	v_0
0	0	v_6	v_1	v_1	v_2	v_2	v_3	v_3	v_4	v_4	v_5	v_5	v_6
	1	v_1	v_2	v_2	v_3	v_3	v_4	v_4	v_5	v_5	v_6	v_6	v_1

$v_1(100), v_2(110), v_3(010), v_4(011), v_5(001), v_6(101), v_0(000), v_7(111).$

Table III.1 Switching table for classical DPC.

III.4. Simulation of DPC control (with predefined commutation table)

III.4.1 Simulation Results

To study the operation of the classical direct power control of the PWM Rectifier, it is implemented in MATLAB/SIMULINK environment. The simulation results obtained for different conditions show in the following Figures III.5, Figures III.6 and Figures III.7.The simulations have been carried out using the main electrical parameters of power circuit and control data showed in Table III.2.

Coupling inductance resistance *r*	**0.56 Ω**
Coupling inductance self-inductance *L*	**19.5 Mh**
DC bus capacitance *C*	**1100 µF**
Load resistance R_L	**68.6 Ω**
Effective composite grid voltage *E*	**85 V**
Grid frequency *f*	**50Hz**
Output DC voltage reference V_{dc}^*	**180 V**

Table III.2 Electrical circuit parameters and control data.

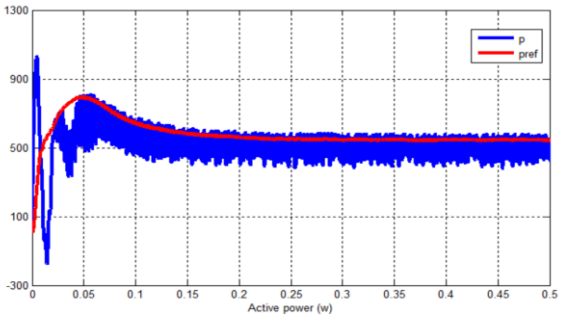
p
pref
Active power (w)

(a)

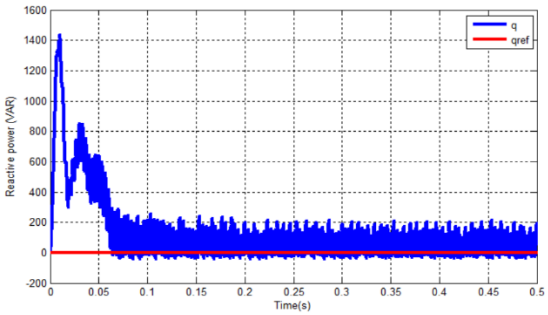
q
qref
Reactive power (VAR)
Time(s)

(b)

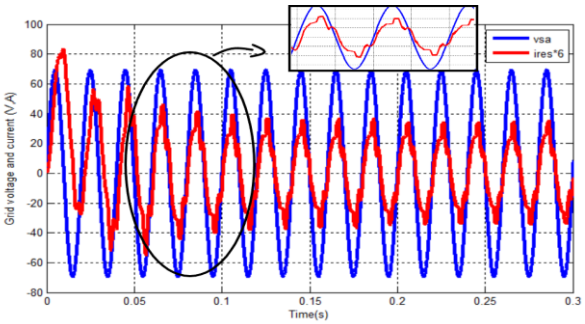
vsa
ires*6
Grid voltage and current (V,A)
Time(s)

(c)

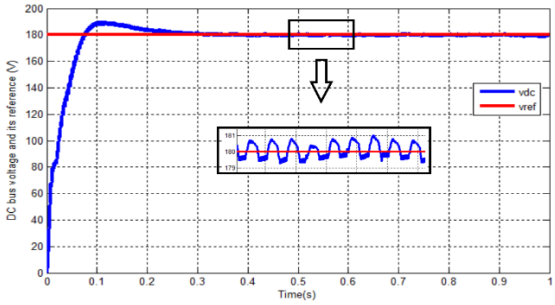
vdc
vref
DC bus voltage and its reference (V)
Time(s)

(d)

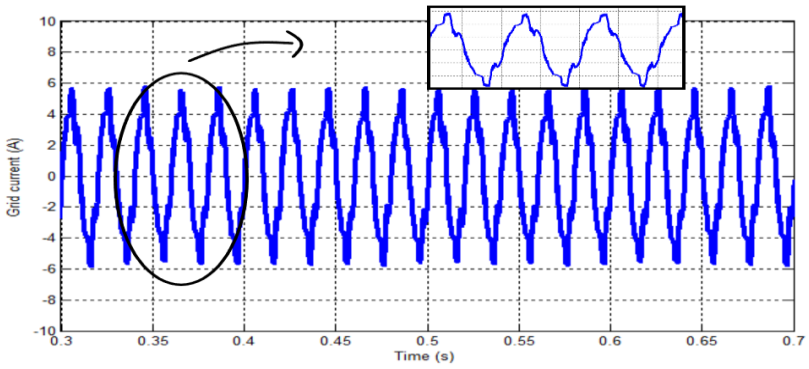
Grid current (A)
Time (s)

(e)

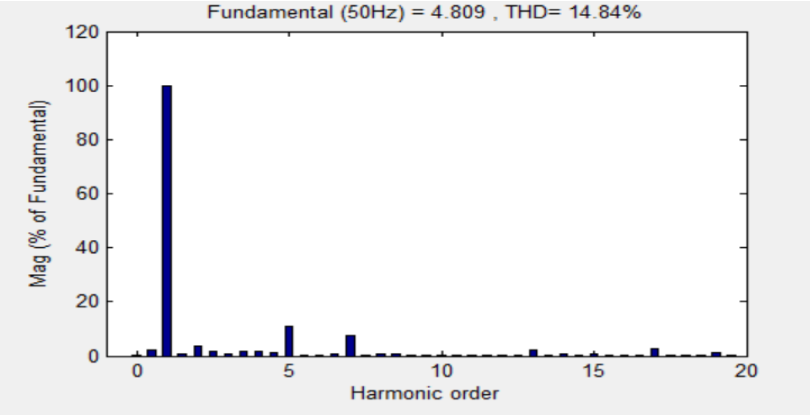

(f)

Figure III.5 Performance of the DPC-controlled PWM Rectifier with predefined table for V_{dc}^{*}=180V : **(a)** The active power P and its reference, **(b)** The reactive power Q and its reference,**(c)** Grid voltage and current, **(d)** The DC bus voltage and it's reference**, (e)** Grid current, **(f)** FFT analysis for current THD**.**

- Here , in this test a step of the reference DC voltage is applied at t = 0.3s from 180 V to 220 V , so that we can observe the changes that will occur in the current, voltage, and THD. Thus, we obtain the following results :

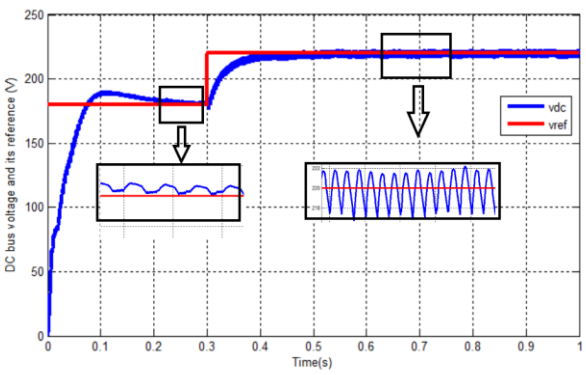

(a)

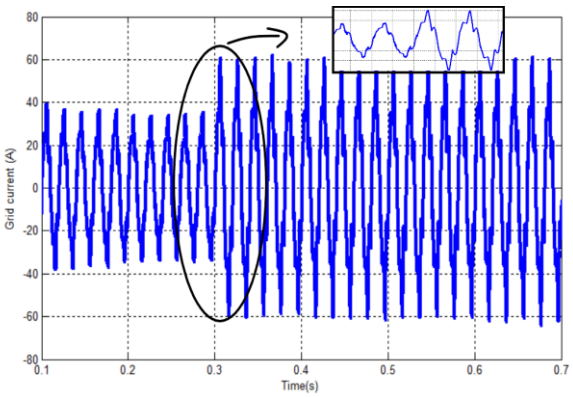

(b)

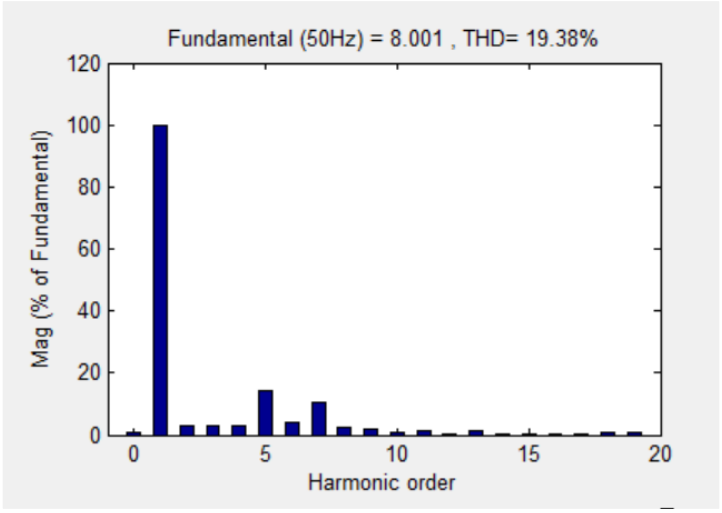

(c)

Figure III.6 Performance of the DPC-controlled PWM Rectifier with predefined table for a variable reference voltage V_{dc}^{*}:**(a)** The DC bus voltage and its reference, **(b)** Grid current, **(c)** FFT analysis for current THD.

- Here , in this test a step of the load R_L is applied at t = 0.3s from 68.6 Ω to 120 Ω , so as to observe the same changes in the system and obtain the following results :

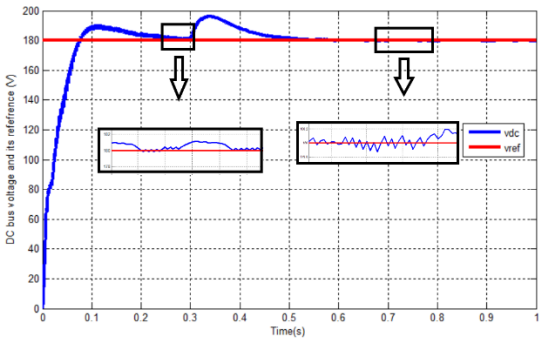

(a)

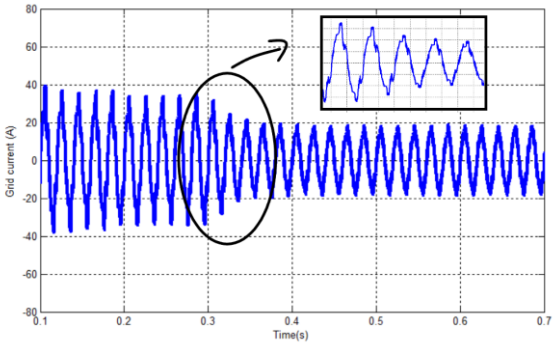

(b)

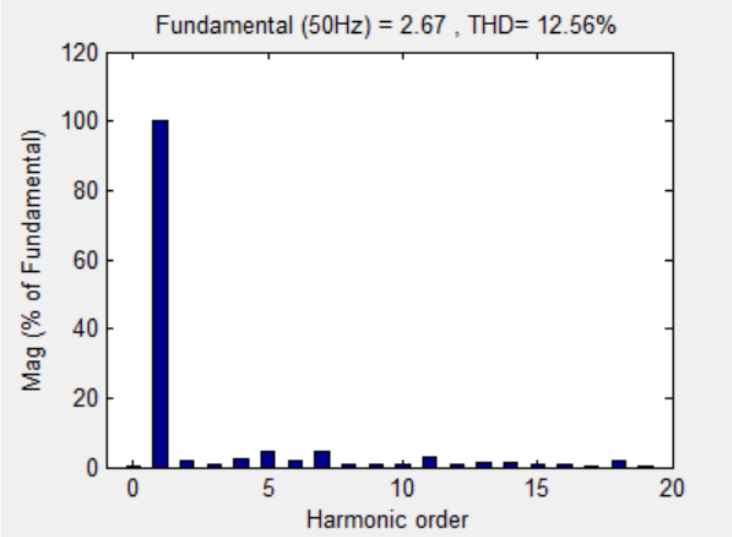

(c)

Figure III.7 Performance of the DPC-controlled PWM Rectifier with predefined table for a variable load R_L: **(a)** The DC bus voltage and its reference, **(b)** Grid current, **(c)** FFT analysis for current THD.

III.4.2 Interpretation of simulation results

- **The Figure III.5** represents the simulation results for a constant output reference voltage V_{dc}^{*}, we can clearly observed that :
  - The current harmonic distortion rate is high (14.84 %).
  - A phase shift between the grid voltage and current.
  - Reactive power is almost constant between two values 100VAR and 200VAR. and the active power is almost constant on 500 watts.
  - The DC bus voltage reaches the reference voltage.

- **The Figure III.6** represents the results for a variable output voltage reference V_{dc}^{*} with a constant load (R_L = 68,6 Ω) , we can notice that :
  - The grid current increases with the increase of the reference.
  - The current harmonic distortion rate is (THD=19.38 %).
  - The DC bus voltage reaches the reference value (after 0.15 s).

- **The Figure III.7** represents the results for the case of a variable load R_L, while the reference voltage remains constant (V_{dc} = 180v) , we notice that :

- The grid current value shows an inverse relationship with the variable load.
- The current harmonic distortion rate is (THD =12 .56%).
- The DC bus voltage reaches the reference.

III.5. DPC with a new switching table

III.5.1 Synthesis of the new switching table for DPC control

The synthesis of a new switching table for DPC (Direct Power Control) control refers to the process of designing a new set of switching patterns or rules for the DPC technique used in power electronic systems. We will study the variation of instantaneous powers to obtain a new switching table because in the states, the previous method reached the non-control zone **[Fek 19].**

In the stationary reference frame (α-β) and for a balanced three-phase system, the line currents equation can be represented as follows:

$$\begin{cases} \frac{di_\alpha}{dt} = \frac{1}{L}\left(e_\alpha - v_\alpha - R * i_\alpha\right) \\ \frac{di_\beta}{dt} = \frac{1}{L}\left(e_\beta - v_\beta - R * i_\beta\right) \end{cases} \quad \text{(III.9)}$$

From (III.9)**,** line current vector $\left[i_\alpha\ i_\beta\right]^T$ can be controlled by selecting the proper rectifier voltage vector. The change in line current depends on the actual supply voltage vector $e_{\alpha\beta}$, on the selected rectifier voltage vector $v_{\alpha\beta}$, and in less measure on the actual line current. The parameter R can be practically neglected and a discrete first order approximation of (III.9) can be adopted. So the change in line current vector for the next control period is given by:

$$\begin{cases} \Delta i_\alpha = i_\alpha(k+1) - i_\alpha(k) = \frac{T_s}{L}\left(e_\alpha(k) - v_\alpha(k)\right) \\ \Delta i_\beta = i_\beta(k+1) - i_\beta(k) = \frac{T_s}{L}\left(e_\beta(k) - v_\beta(k)\right) \end{cases} \quad \text{(III.10)}$$

The instantaneous active and reactive power can be represented as follows:

$$\begin{bmatrix} P \\ Q \end{bmatrix} = \begin{bmatrix} e_\alpha & e_\beta \\ e_\beta & -e_\alpha \end{bmatrix} \begin{bmatrix} i_\alpha \\ i_\beta \end{bmatrix} \quad \text{(III.11)}$$

As first approximation, and if the switching frequency is high enough, the change in power-source voltage can be neglected. The change in the active and reactive power can be estimated for the next control cycle as follows:

$$\begin{cases} \Delta P = e_\alpha(k).\Delta i_\alpha + e_\beta(k).\Delta i_\beta \\ \Delta Q = e_\beta(k).\Delta i_\alpha - e_\alpha(k).\Delta i_\beta \end{cases} \quad \text{(III.12)}$$

By replacing (III.10) in (III.12) we obtain:

$$\begin{cases} \Delta P = \frac{T_S}{L}\left({e_\alpha}^2(k) + {e_\beta}^2(k) \right) - \frac{T_S}{L}\left(e_\alpha(k).v_\alpha(k) + e_\beta(k).v_\beta(k) \right) \\ \Delta Q = \frac{T_S}{L}\left(e_\alpha(k).v_\beta(k) - e_\beta(k).v_\alpha(k) \right) \end{cases} \quad \text{(III.13)}$$

The equation (III.13) reveals that the changes in active and reactive powers are influenced by both the rectifier voltage vector applied (control vector) applied during the switching period and the grid voltage vector. As a result, there are different ways of selecting the corresponding switching state that controls the evolution in active and reactive power. For i = 0, 1, 2,…,6 change in the active and reactive power are given by the following expressions:

$$\begin{cases} \Delta P_i = \frac{T_S}{L}\left({e_\alpha}^2(k) + {e_\beta}^2(k) \right) - \frac{T_S}{L}\left(e_\alpha(k).v_{\alpha i} + e_\beta(k).v_{\beta i} \right) \\ \Delta Q_i = \frac{T_S}{L}\left(e_\alpha(k).v_{\beta i} - e_\beta(k).v_{\alpha i} \right) \qquad i = 0,1,2,\ldots..,6 \end{cases} \quad \text{(III.14)}$$

In the (α-β) plane, the vector $e_{\alpha\beta}$ can be represented as:

$$\begin{cases} e_\alpha = E\cos(\theta) \\ e_\beta = E\sin(\theta) \end{cases} \quad \text{With} \quad E = \left\| e_{\alpha\beta} \right\| \quad \text{(III.15)}$$

Where:

E: RMS (Root Mean Square) value of the composite grid voltage.

θ = Angular position of the grid voltage vector defined by: $-\frac{\pi}{6} \leq \theta \leq \frac{11\pi}{6}$

By using (III.15) in (III.14) we obtain:

$$\begin{cases} \Delta P_i = \frac{T_S}{L}\left\| e_{\alpha\beta} \right\|^2 - \frac{T_S}{L}\left\| e_{\alpha\beta} \right\|.\left(\cos(\theta).v_{\alpha i} + \sin(\theta).v_{\beta i} \right) \\ \Delta Q_i = \frac{T_S}{L}\left\| e_{\alpha\beta} \right\|.\left(\cos(\theta).v_{\beta i} - \sin(\theta).v_{\alpha i} \right) \qquad i = 0,1,2,\ldots..,6 \end{cases} \quad \text{(III.16)}$$

For the rectifier voltage vector, v, the typical space vector representation, for each converter switching state and its corresponding, $v_{\alpha i}$ and $v_{\beta i}$ components values are shown in the following Table III.3:

v_i	v_a	v_b	v_c	$v_{\alpha i}$	$v_{\beta i}$
0	0	0	0	0	0
1	$2/3v_{dc}$	$-1/3v_{dc}$	$-1/3v_{dc}$	$\sqrt{2/3}\ v_{dc}$	0
2	$1/3\ v_{dc}$	$1/3v_{dc}$	$-2/3v_{dc}$	$1/\sqrt{6}\ v_{dc}$	$1/\sqrt{2}\ v_{dc}$
3	$-1/3v_{dc}$	$2/3v_{dc}$	$-1/3v_{dc}$	$-1/\sqrt{6}\ v_{dc}$	$1/\sqrt{2}\ v_{dc}$
4	$-2/3v_{dc}$	$1/3v_{dc}$	$1/3v_{dc}$	$-\sqrt{2/3}\ v_{dc}$	0
5	$-1/3v_{dc}$	$-1/3v_{dc}$	$2/3v_{dc}$	$-1/\sqrt{6}\ v_{dc}$	$-1/\sqrt{2}\ v_{dc}$
6	$1/3\ v_{dc}$	$-2/3v_{dc}$	$1/3v_{dc}$	$1/\sqrt{6}\ v_{dc}$	$-1/\sqrt{2}\ v_{dc}$

Table III.3 Rectifier voltage space vectors.

The rectifier voltage vector in (α-β) plane is given by:

$$\overline{v_{\alpha i}} = \frac{v_{\alpha i}}{\|v_{\alpha\beta i}\|},\ \overline{v_{\beta i}} = \frac{v_{\beta i}}{\|v_{\alpha\beta i}\|},\ \text{with}\ \ \|v_{\alpha\beta i}\| = \frac{\sqrt{3}}{2}\ v_{dc} \tag{III.17}$$

These two quantities can be expressed as follows:

$$\begin{cases} \overline{v_{\alpha i}} = \cos((i-1).\frac{\pi}{3})) \quad , \quad \overline{v_{\alpha 0}} = 0 \\ \overline{v_{\beta i}} = \sin((i-1).\frac{\pi}{3})) \quad , \quad \overline{v_{\beta 0}} = 0 \qquad i = 0,1,2,\ldots..,6 \end{cases} \tag{III.18}$$

The normalized value of the change in active power and reactive power can be expressed as follows:

$$\begin{cases} \overline{\Delta P_i} = \frac{\Delta p_i}{\left(\frac{T_S}{L}\right).\|e_{\alpha\beta}\|.\|v_{\alpha\beta}\|} = \frac{\|e_{\alpha\beta}\|}{\|v_{\alpha\beta}\|} - (\cos(\theta).\overline{v_{\alpha i}} + \sin(\theta).\overline{v_{\beta i}}) \\ \overline{\Delta Q_i} = \frac{\Delta q_i}{\left(\frac{T_S}{L}\right).\|e_{\alpha\beta}\|.\|v_{\alpha\beta}\|} = \cos(\theta).\overline{v_{\beta i}} - \sin(\theta).\overline{v_{\alpha i}} \quad for \quad i = 0,1,2,\ldots..,6 \end{cases} \tag{III.19}$$

By using (III.18) on (III.19) we obtain:

$$\begin{cases} \overline{\Delta P_i} = \frac{\|e_{\alpha\beta}\|}{\|v_{\alpha\beta}\|} - \cos(\theta - (i-1).\frac{\pi}{3}) \\ \overline{\Delta Q_i} = -sin\,(\theta - (i-1).\frac{\pi}{3}) \end{cases} for\ i = 0,1,2,\ldots..,6 \quad \begin{cases} \overline{\Delta P_0} = \frac{\|e_{\alpha\beta}\|}{\|v_{\alpha\beta}\|} \\ \overline{\Delta Q_0} = 0 \end{cases}$$

(III.20)

It can be seen from (III.20) that the change in reactive power during all sectors has a sinusoidal waveform for all rectifier voltage vectors v_i. The change in active power has a shifted sinusoidal waveform as shown in Figure.III.8 and Figure.III.9 respectively.

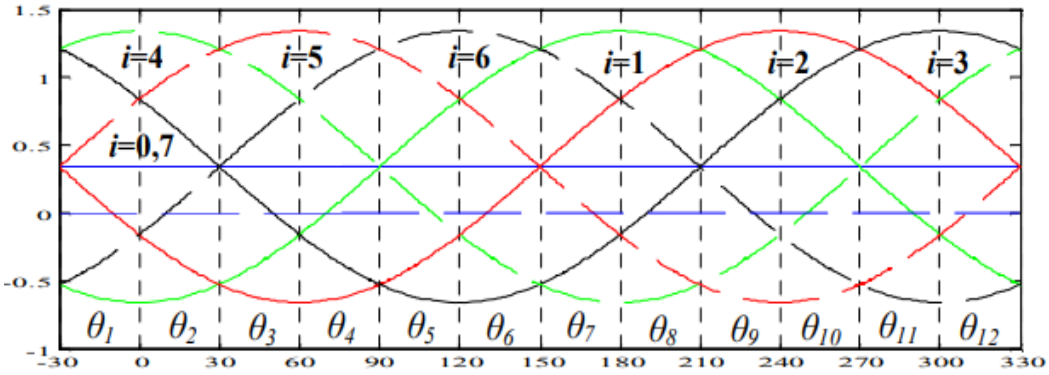

Figure III.8 Change in instantaneous active power $\overline{\Delta P_i}$.

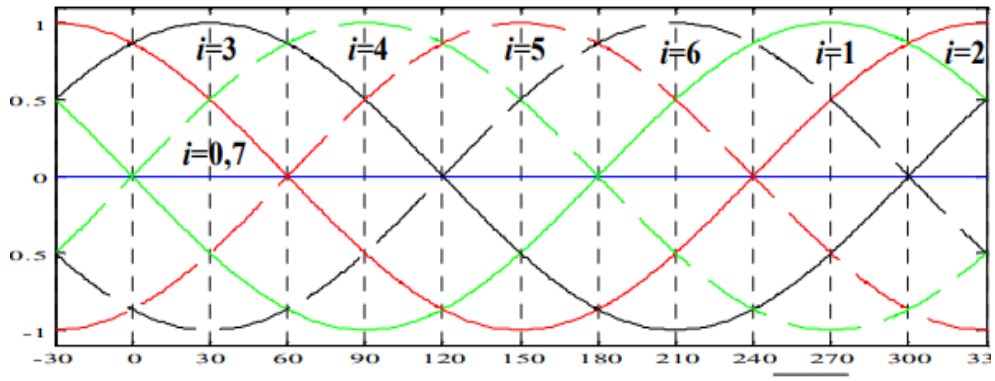

Figure III.9 Change in instantaneous reactive power $\overline{\Delta Q_i}$.

III.5.2. Development of the new switching table

The basic idea of the proposed DPC was to choose the best rectifier voltage vector among the seven possible vectors in order to ensure smooth control of instantaneous active and reactive power during each sector. To maintain the dc-bus voltage close to the reference value, and to keep the unity power factor, active power is controlled to be constant and equal to its reference value, the reactive power should be maintained zero for all sectors. For this reason, the new switching table synthesis is based on the sign and magnitude of the change in active and reactive power for each sector, as shown in Figure III.8 and Figure III.9. For example, for sector one the sign of the change in active and reactive power are shown in Table III.4 **[Bou 08]:**

$\overline{\Delta P_i}$		$\overline{\Delta Q_i}$		
>0	**<0**	**>0**	**=0**	**<0**
v_4, v_3, v_5, v_0, v_7	v_1, v_6	v_1, v_2, v_3	v_0, v_7	v_5, v_6, v_7

Table III.4 Sign of change in active and reactive power for sector 1.

For each combination of hysteresis output signals, S_p and S_q, rectifier voltage vectors are selected for sector one as shown in Table III. 1.

Secteur 1		$\overline{\Delta Q_i}$	
		$> 0 \leftrightarrow S_q = 1$	$< 0 \leftrightarrow S_q = 0$
$\overline{\Delta P_i}$	$> 0 \leftrightarrow S_p = 1$	V_3, V_2	V_4, V_5
	$< 0 \leftrightarrow S_p = 0$	V_1	V_6

Table III.5 Selected rectifier voltage vectors for sector 1.

For all sectors, the proposed new switching table [**Bou 10]** is represented in the following Table **(see Appendix):**

S_p	S_q	θ_1	θ_2	θ_3	θ_4	θ_5	θ_6	θ_7	θ_8	θ_9	θ_{10}	θ_{11}	θ_{12}
1	0	V_5	V_6	V_6	V_1	V_1	V_2	V_2	V_3	V_3	V_4	V_4	V_5
1	1	V_3	V_4	V_4	V_5	V_5	V_6	V_6	V_1	V_1	V_2	V_2	V_3
0	0	V_6	V_1	V_1	V_2	V_2	V_3	V_3	V_4	V_4	V_5	V_5	V_6
0	1	V_1	V_2	V_2	V_3	V_3	V_4	V_4	V_5	V_5	V_6	V_6	V_1

Table III.6 The new switching table for DPC.

$v_1(100)$, $v_2(110)$, $v_3(010)$, $v_4(011)$, $v_5(001)$, $v_6(101)$, $v_0(000)$, $v_7(111)$.

III.6. DPC Control Simulation (with a new switching table)

III.6.1 Simulation Results

The simulations have been carried out using the same electrical parameters of power circuit and control data used in DPC control simulation with predefined switching table.

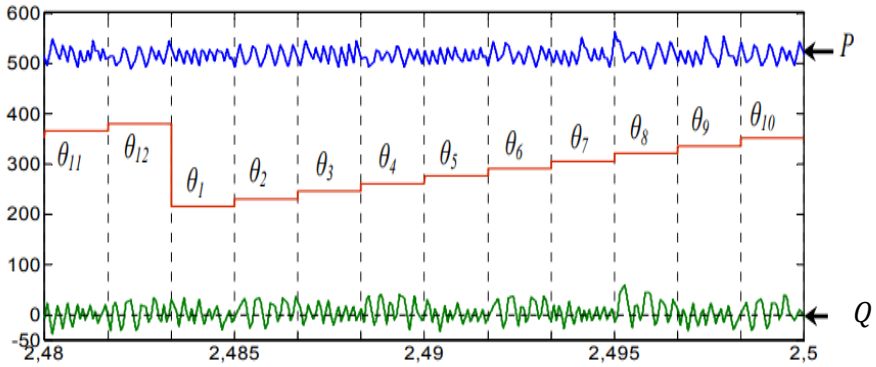

Figure III.10 Active power, reactive power, and sector.

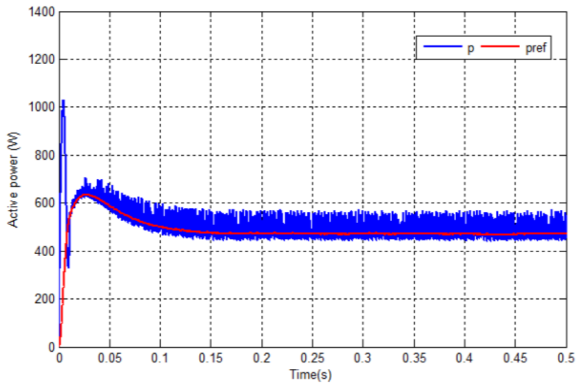

(a)

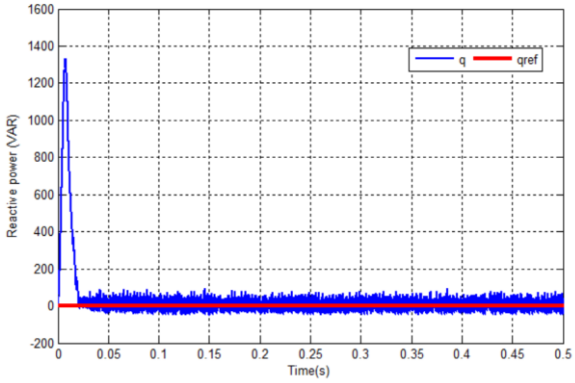

(b)

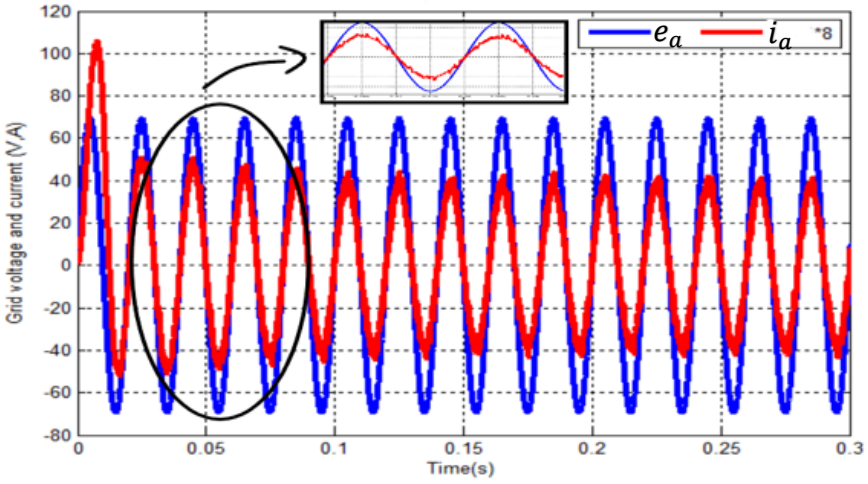

(c)

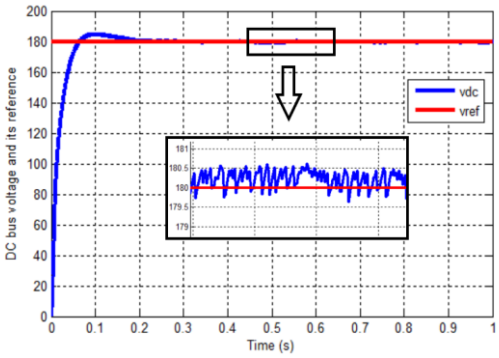

(d)

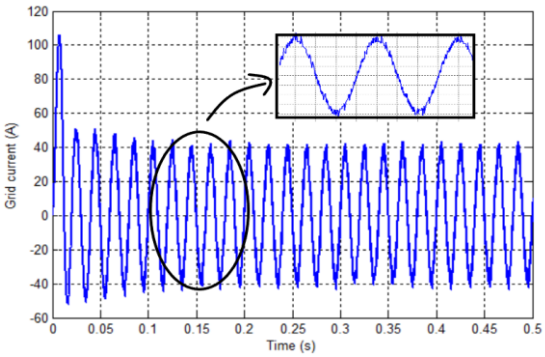

(e)

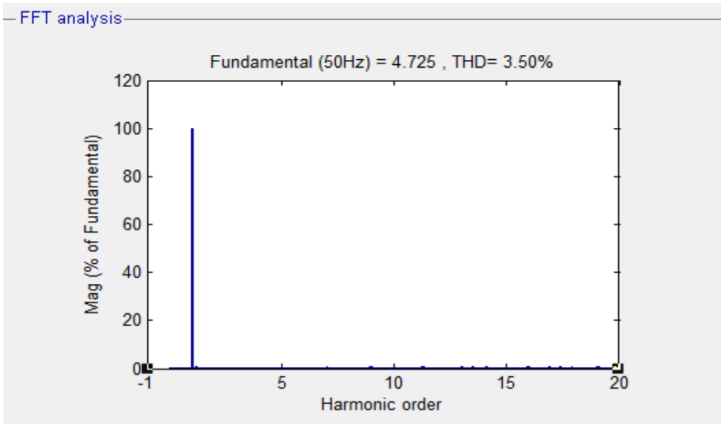

(f)

Figure III.11 Performance of the DPC-controlled PWM Rectifier with new table for V_{dc}^{*}=180 : **(a)** The active power P and its reference, **(b)** The reactive power Q and its reference,**(c)** Grid voltage and current, **(d)** The DC bus voltage and its reference**, (e)** Grid current, **(f)** FFT analysis for current THD**.**

- Here, in this test a step of the reference DC voltage is applied at t = 0.3s from 180 V to 220 V, so that we can observe the changes that will occur in the current, voltage, and THD. Thus, we obtain the following results :

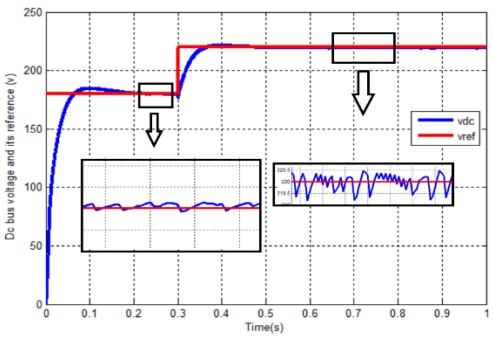

(a)

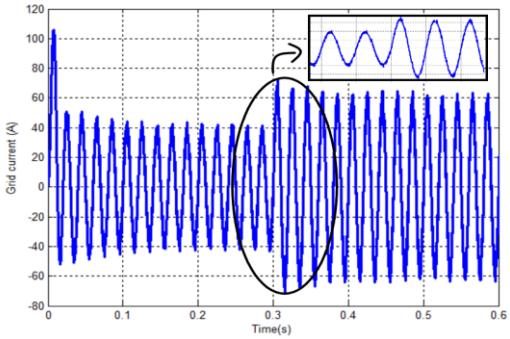

(b)

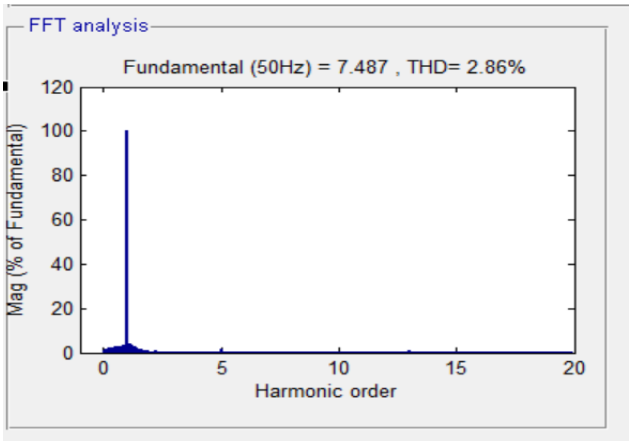

(c)

Figure III.12 Performance of the DPC-controlled PWM Rectifier with predefined new table for a variable reference voltage V_{dc}^{*}: **(a)** The DC bus voltage and its reference, **(b)** Grid current, **(c)** FFT analysis for current THD.

- Here , in this test a step of the load R_L is applied at t = 0.3s from 68.6 Ω to 120 Ω , so as to observe the same changes in the system and obtain the following results :

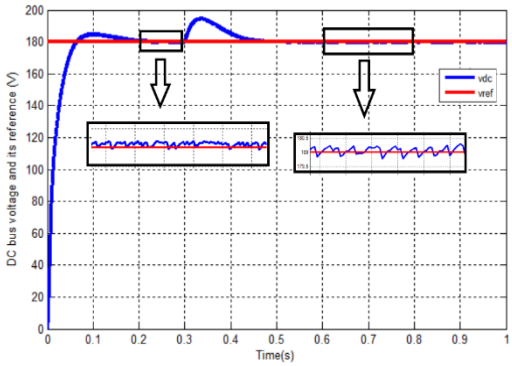

(a)

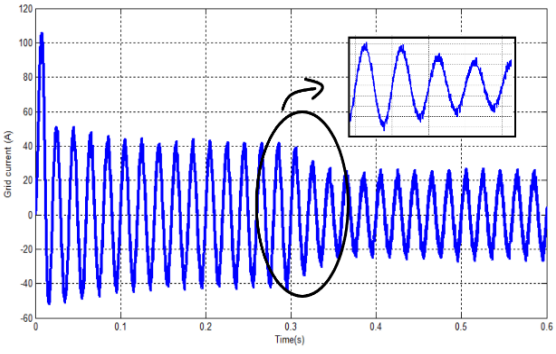

(b)

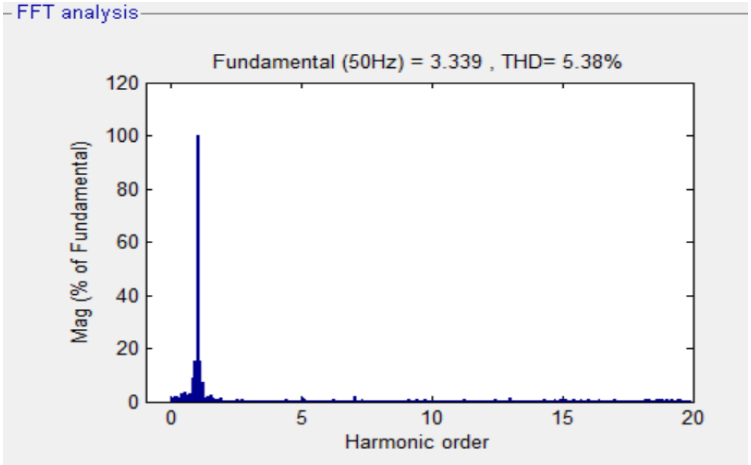

(c)

Figure III.13 Performance of the DPC-controlled PWM Rectifier with new table for a variable load R_L: **(a)** The DC bus voltage and its reference, **(b)** Grid current, **(c)** FFT analysis for current THD.

III.6.2 Interpretation of simulation results

- **The Figure III.10** represents the variation of active power p and reactive power q in each sector. It can be observed that there is an increase in energy consumption, both in terms of active and reactive power, during the even-order sectors.

- **The Figure III.11** represents the simulation results for a constant output reference voltage V_{dc}^{*}, we can clearly observed that :
  - The current harmonic distortion rate is very low (3.50 %).
  - The grid voltage and current are perfectly synchronized.
  - Reactive power is almost constant at 0 VAR, and the active power remains consistently high at 500 watts.
  - The DC bus voltage reaches the reference voltage.

- **The Figure III.12** represents the results for a variable output voltage reference $V_{dc}^{*}$with a constant load (R_L= 68,6 Ω) , we can notice that :
  - The grid current increases with the increase of the reference.
  - The current harmonic distortion rate is (THD=2.86 %).
  - The DC bus voltage reaches the reference value (after 0.1 s).

- **The Figure III.13** represents the results for the case of a variable load R_L , while the reference voltage remains constant (V_{dc} = 180v) , we notice that :
  - The grid current value shows an inverse relationship with the variable load.
  - The current harmonic distortion rate is (THD =5.38 %).
  - The DC bus voltage reaches the reference.

III.7. Advantages and Disadvantages of DPC Control

- **The advantages**
  - No separate (PWM) block.
  - Very high dynamic response.
  - No use of nested loops, coordinate transformations, modulators, or decoupling between current components.
  - Simple algorithm.
  - Decoupled control of active and reactive power.
  - Instantaneous variable with all harmonic components estimated (Improving power factor and efficiency).

- **The disadvantages**
  - Very high sampling frequency, which requires the use of a very fast microprocessor.
  - Variable switching frequency, with the inductance value needing to be sufficiently high to smooth the current waveform.
  - Power and voltage estimation should be avoided during switching.

III.8. Conclusion

This chapter has described a direct power control of three-phase PWM Rectifier (DPC) based on switching table. The main goal of the control system is to maintain the dc-bus voltage at the required level and satisfy the Unity Power Factor (UPF) operation of the three-phase PWM rectifier. The converter switching states of the new switching table are chosen by analysing the instantaneous active and reactive power correction. The best rectifier vector allowing smooth control of active and reactive power during each sector is selected. The proposed DPC was

simulated and implemented using conventional PI controller for dc-bus voltage regulation. The presented results indicate that the new DPC is much better than the classical one in steady and transient states. Input currents waveforms are more sinusoidal, near unit power factor and decoupled active and reactive power control are successfully achieved using the proposed switching table.

CHAPITRE IV Direct Power Control of three-phase PWM Rectifier based on Fuzzy and ANFIS controller.

IV.1 Intoduction

Different control methods have been proposed for the regulation of the three-phase PWM Rectifiers. A Voltage Oriented Control (VOC) is used in the last few decades, this control strategy can indirectly regulate the input powers by regulating the input current vector in the d-q coordinates **[Mal 03]** Another prominent control technique of three phase PWM Rectifiers is Direct Power Control (DPC). This control strategy allows a decoupled instantaneous powers control, strong robustness to parameter variations and fast dynamic response **[Jam 17]**. DPC is same as to Direct Torque Control (DTC) strategy of induction motors **[Gad 09]**. Therefore, the DPC does not need the transformation of coordinate, separate PWM block and internal current regulation. Hence, for the improvement of the system performances, significant studies which improve the conventional DPC technique have been conducted. Among these research works, we find the decoupled control of instantaneous powers with a single cost function using model predictive control method **[Kwa 15]**, sliding mode control technique **[Dje 14]**, and others . Furthermore, other control algorithms based on artificial intelligent techniques have been developed recently, such as Fuzzy Logic (FL) approach **[Ben 17]**, and Artificial Neural Networks (ANN) method **[Shu 14]**.

On the other hand, the combination of the ANN approach and the FL technique has received during those days a great interest. So, it's using in a lot of area and exactly in control of power electronic converters, in order to achieved good advantages. The ANFIS is one of the most technique combining two intelligent methods to obtain a high performance of the control system. In the present study, an improvement DPC technique based on ANFIS for three phase PWM rectifiers is proposed. This control technique combines ANN approach and FL theory for dc link voltage control and decoupled regulation of instantaneous powers with a UPF condition.

- In this chapter, we propose an approach to enhance the Direct Power Control (DPC) of the three-phase PWM rectifier by suggesting these two methods.
    - Fuzzy DC voltage control for a DPC- PWM Rectifier.
    - DC voltage control for a DPC- PWM Rectifier based on ANFIS.

IV.2 Fuzzy DC voltage control for a DPC- PWM Rectifier

IV.2.1 Basic Components in Fuzzy control

A fuzzy logic controller (FLC) is based on a collection of control rules governed by the compositional rule of inference, as shown in Figure IV.1. A fuzzy system achieves a nonlinear mapping between a vectorial input and a scalar output **[Bos 14]**. The Fuzzy Logic Controller (FLC) is more used when the precision required is moderate and the plant is to be devoid of complex mathematical analysis. Other advantages are :

- It does not require highly precise Inputs.
- It needs very fewer data comparatively, which is mainly rules and membership functions.
- It is more efficient and can perform better even in non-linear models.

The three main components of a Fuzzy Logic Controller are:

1. Fuzzification.
2. Fuzzy Rule base and interfacing engine.
3. Defuzzification.

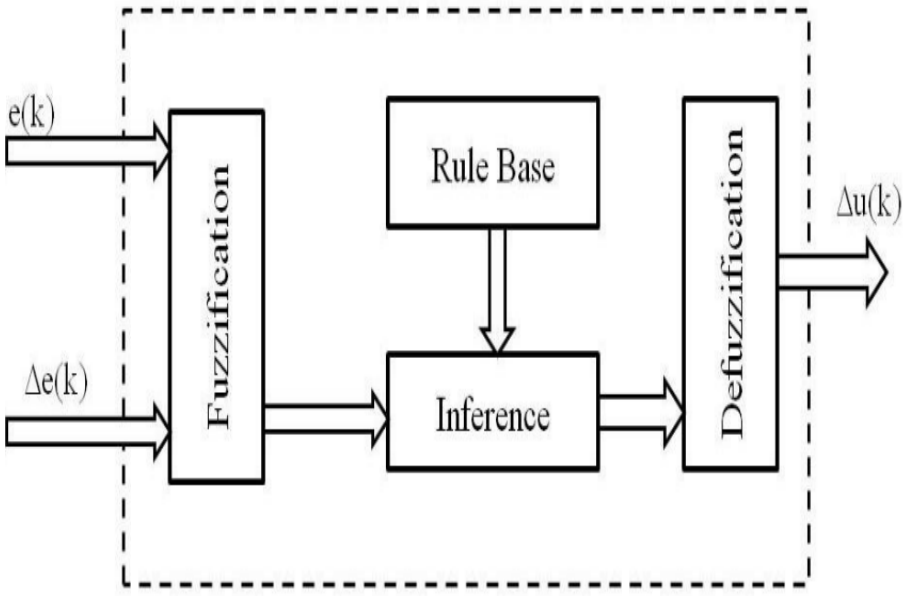

Figure IV.1 Internal structure of a fuzzy system.

IV.2.1.1 Fuzzification

The fuzzification module converts the crisp values of the control inputs into fuzzy values, so that they are compatible with the fuzzy set representation in the rule base. The choice of fuzzification strategy is dependent on the inference engine, i.e. whether it is composition based or individual-rule-firing based **[Cri 02]**.

IV.2.1.2 Fuzzy Rule Base and inference

Fuzzy rule base is set of rules consist proposition after IF called antecedents, while the proposition after THEN is called the consequent **[Zai 16]**. In the Fuzzy Rule Inference, the values of the input and output linguistic variables are connected by multiple rules that need to consider the static and dynamic behavior of the system being regulated, as well as the desired control objectives, particularly the stability and the proper damping of the control circuit. The tuning strategy largely depends on the adopted inferences. It is not possible to provide precise rules, as experience plays an important role in this aspect. The rules will be expressed, for example, as follows:

If x_1 is A_1 AND x_2 is A_2, THEN y is B.

If x_1 is A_1 OR x_2 is A_2, THEN y is B.

Where x_1, x_2, and y are the characteristic physical quantities of the system, A_1, A_2, and B are the linguistic terms, and "OR" and "AND" are the operators used to link the input functions.

IV.2.1.2.1 Inference mechanism

Considered as the "brain" of the controller, the inference mechanism links the membership degrees of the input membership functions to the output membership functions. The degree of membership of the output function can be calculated using various methods **[Buh 94]**:

- The min-max inference method.
- The max-product inference method.
- The sum-product inference method.

These methods determine the degree to which each rule contributes to the output and are used to aggregate the fuzzy outputs into a crisp output value or control action.

IV.2.1.3 Defuzzification

The defuzzification process involves transforming the fuzzy output set resulting from the aggregation of rules into a deterministic and precise control value to be applied to the process. The following defuzzification methods are of practical importance **[Dim 96]**:

- Defuzzification by calculating the center of gravity (centroid).
- Defuzzification by calculating the maximum value.
- Defuzzification by calculating the weighted average of the crisp values.

The center of gravity method is the most commonly used defuzzification method in fuzzy control because it intuitively provides the most representative value of the fuzzy set resulting from the rule aggregation. Note that normalization and denormalization blocks are added respectively at the input and output of the fuzzy controller to make it portable and adaptable even with different parameters. **[Buh 94] [Pas 98]**.

IV.2.2 The Fuzzy Inference Systems

The Fuzzy Inference System is a process that enables mapping from a given set of inputs to an output space by the use of fuzzy logic. The FIS comprises:

a) membership function.

b) fuzzy logic operator.

c) if-then rule.

A Membership Function (MF) is a curve that defines mapping of each point in the input space to a membership value between 0 and 1, called the degree of membership. There are several types of membership functions, triangular, trapezoidal, Gaussian, sigmoidal, asymmetrical polynomial, etc… **[Bac 15],** of which the sigmoidal function is the most commonly used function and is used in the present work. There are two types of fuzzy inference systems:

- Mamdani Fuzzy Inference Systems.
- Sugeno Fuzzy Inference Systems.

IV.2.2.1 Mamdani Fuzzy Inference Systems

Mamdani fuzzy inference was first introduced as a method to create a control system by synthesizing a set of linguistic control rules obtained from experienced human operators **[Mam 75]**. In a Mamdani system, the output of each rule is a fuzzy set.

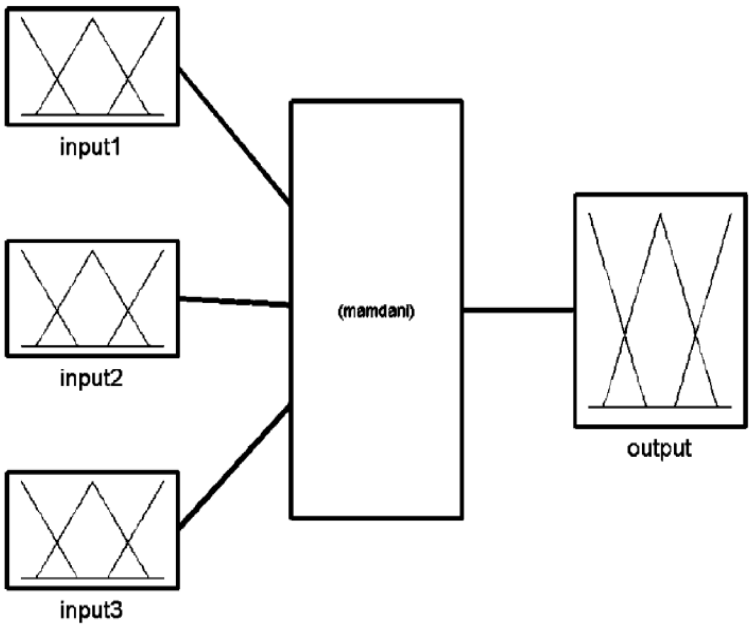

Figure IV.2 Fuzzy inference systems using Mamdani-type.

Since Mamdani systems have more intuitive and easier to understand rule bases, they are well-suited to expert system applications where the rules are created from human expert knowledge, such as medical diagnostics. The mamdani system uses the minimum as the conjunction operator and implication to represent the fuzzy graph associated with each rule and the maximum operator for aggregation in rule *i*:

$if\ x_1 is\ A_1\ and \dots and\ x_n\ is\ A_n then\ y\ is\ B^i$

B^i is a Fuzzy sets, in general, form a partition of the output universe.

IV.2.2.2 Sugeno Fuzzy Inference Systems

Sugeno fuzzy inference, also referred to as Takagi-Sugeno-Kang fuzzy inference, uses singleton output membership functions that are either constant or a linear function of the input values.

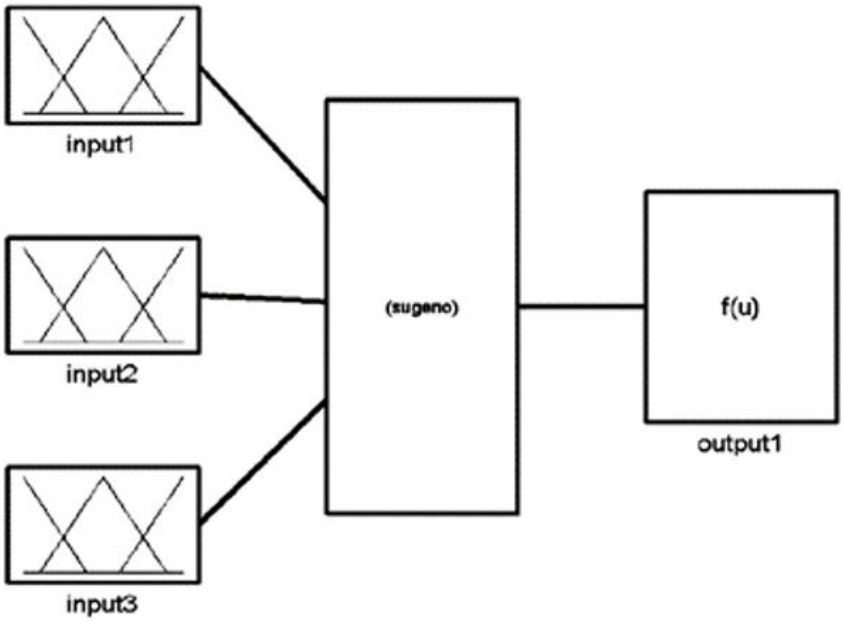

Figure IV.3 Fuzzy inference systems using Sugeno-type.

The defuzzification process for a Sugeno system is more computationally efficient compared to that of a Mamdani system, since it uses a weighted average or weighted sum of a few data points rather than compute a centroid of a two-dimensional area **[Sug 85]**.

This model has the particularity of not having a fuzzy conclusion but rather a function of the inputs .The rule R_i for an input vector *x* of dimension *n* is:

$if\ x_1\ is\ X_1^i\ and \dots and\ x_n\ is\ X_1^n\ then\ y\ is\ G_i(x)$

If $G_i(x)$ is a first-order linear rule, it will be formed as follow :

$$G_i(x) = \sum_{j=1}^{n} a_j^i\ x_j + b^i \qquad \text{(IV.1)}$$

IV.2.3 Design of the proposed Fuzzy control of the DC bus voltage for DPC

Since several years, the Fuzzy Logic Controller has been of great topical. Indeed, this technique allows obtaining a very effective control law without having to do extensive modelling **[Kri 14]**. Figure IV.4 shows the configuration of DPC equipped with this fuzzy control and the Figure IV.5 shows the block diagram of the Fuzzy Logic Controller used to control the dc bus voltage of a three-phase PWM Rectifier.

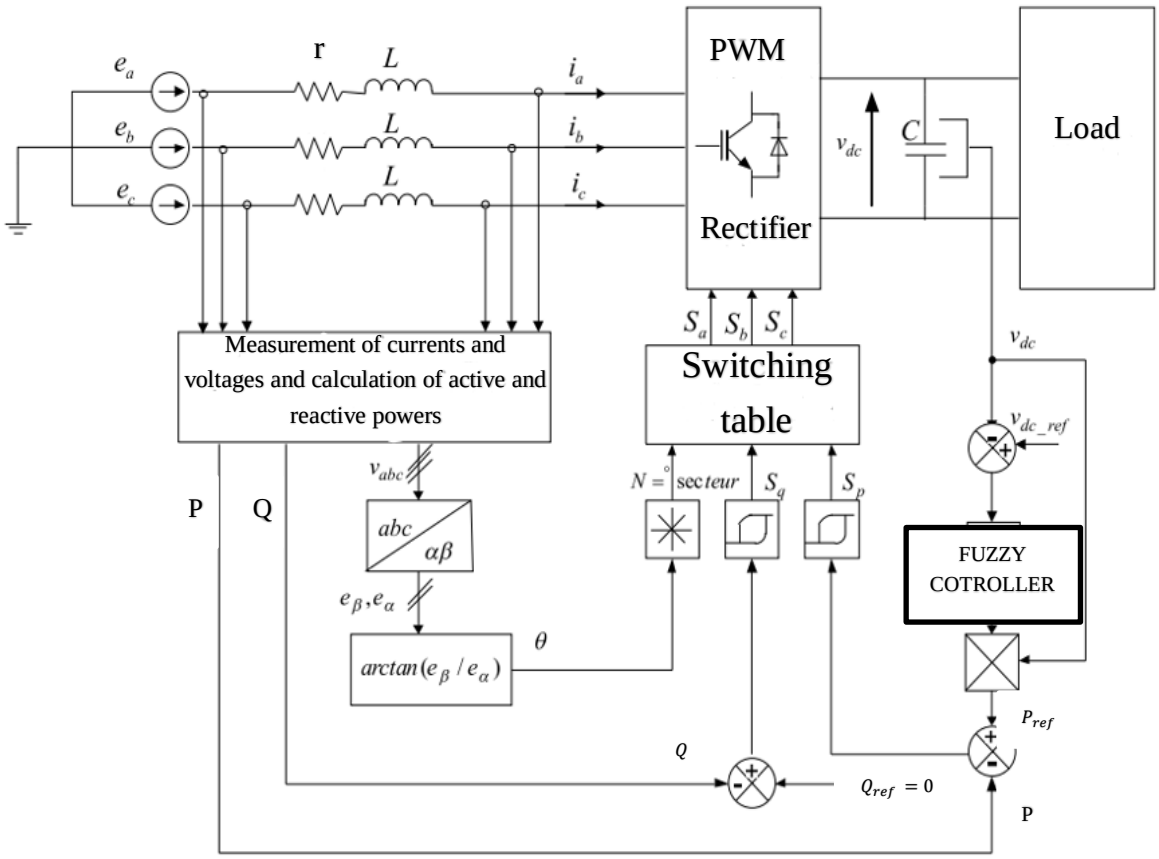

Figure IV.4 The configuration of DPC equipped with fuzzy control.

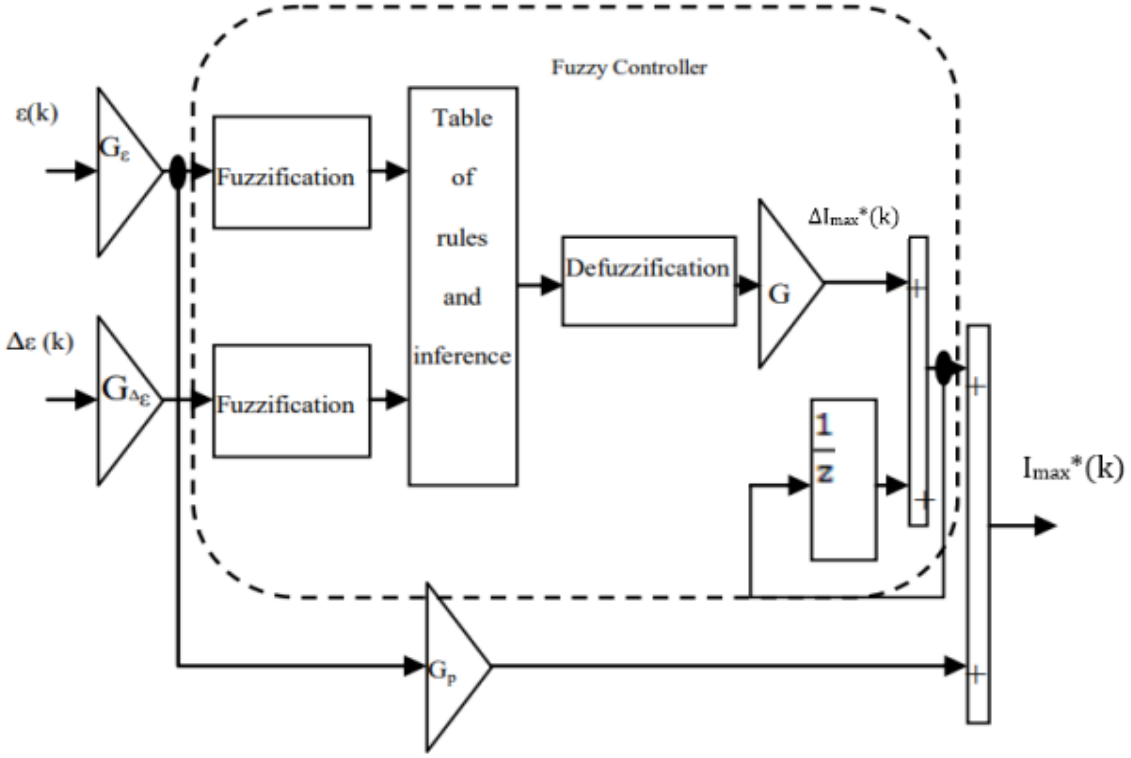

Figure IV.5 Schematic diagram of fuzzy controller.

This fuzzy control has been designed using the method of fuzzy implication of Mamdani, founded on the min-max decision. It comprises three main blocks, wish are, fuzzification, decision block and defuzzification **[Kri 14]**. In the system of the Figure IV.5, the fuzzy controller inputs are the error ε and its derivative $\Delta\varepsilon$. They are defined as follows:

$$\begin{cases} \varepsilon(k) = V_{dc}{}^{*}(k) - V_{dc}(k) \\ \Delta\varepsilon\,(k) = \varepsilon(k) - \varepsilon\,(k-1) \end{cases} \quad \text{(IV.2)}$$

The final output of the system is calculated as:

$$P_{ref}(k) = G.\Delta P_{ref}(k) + P_{ref}(k) \quad \text{(IV.3)}$$

The output of the fuzzy controller is multiplied by the measured value of the DC bus voltage in order to obtain the reference of the active power. The membership functions of the input and output variables are illustrated in Figure IV.6. The seven fuzzy sets chosen to accomplish the fuzzification and defuzzification are: NB (Negative Big), NM (Negative Medium), NS (Negative Small), ZE (Zero), PS (Positive Small), PM (Positive Medium) and PB (Positive Big).

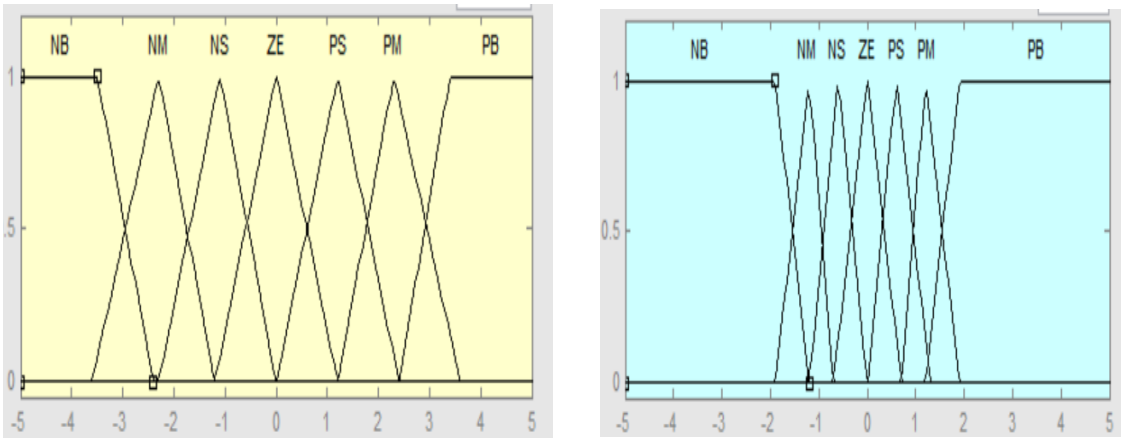

(a) **(b)**

Figure IV.6 Membership functions of inputs/outputs variable: **(a)** The input variables ε(k) and Δε(k), **(b)** The input variables ε(k) and Δε(k) .

Fuzzy rules are gathered in an inference matrix shown in Table IV.I

		ε(k)						
		NB	***NM***	***NS***	***ZE***	***PS***	***PM***	***PB***
Δε(k)	***NB***	*NB*	*NB*	*NB*	*NB*	*NM*	*NS*	*ZE*
	NM	*NB*	*NB*	*NB*	*NM*	*NS*	*ZE*	*PS*
	NS	*NB*	*NB*	*NM*	*NS*	*ZE*	*PS*	*PM*
	ZE	*NB*	*NM*	*NS*	*ZE*	*PS*	*PM*	*PB*
	PS	*NM*	*NS*	*ZE*	*PS*	*PM*	*PB*	*PB*
	PM	*NS*	*ZE*	*PS*	*PM*	*PB*	*PB*	*PB*
	PB	*ZE*	*PS*	*PM*	*PB*	*PB*	*PB*	*PB*

Table IV.1 Inference rules.

IV.3 Simulation of Fuzzy DC voltage control for a DPC- PWM Rectifier

IV.3.1 Simulation Results

The simulations have been carried out using the same electrical parameters of power circuit and control data used in DPC control simulation:

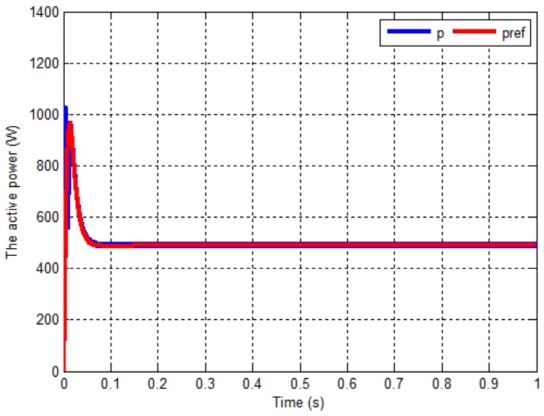
p
pref
The active power (W)
Time (s)

(a)

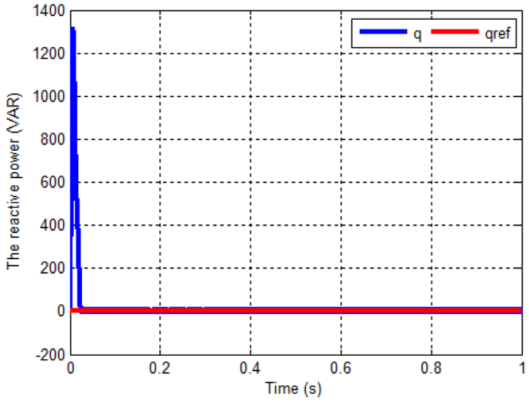
q
qref
The reactive power (VAR)
Time (s)

(b)

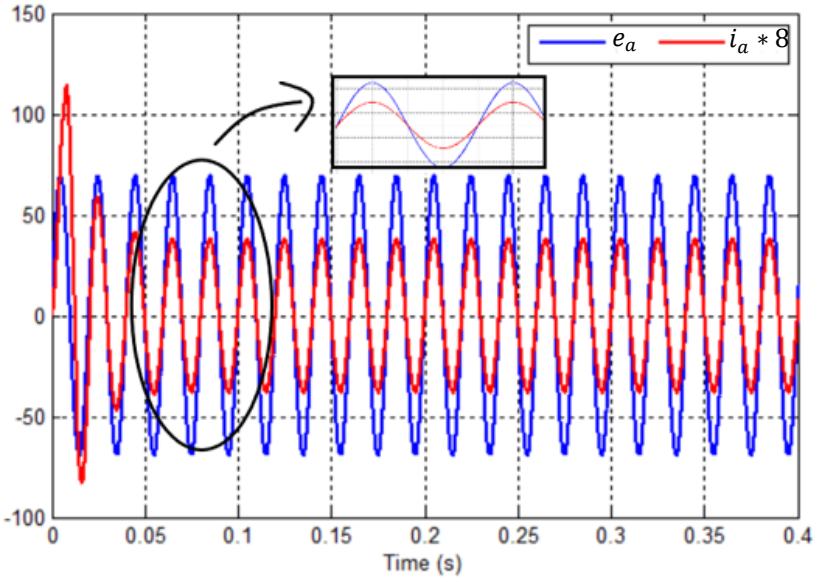
e_a
$i_a * 8$
Time (s)

(c)

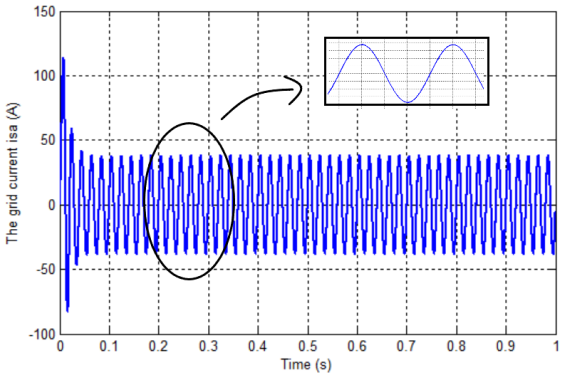

(d)

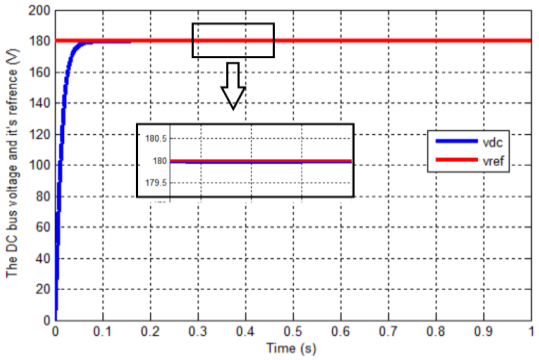

(e)

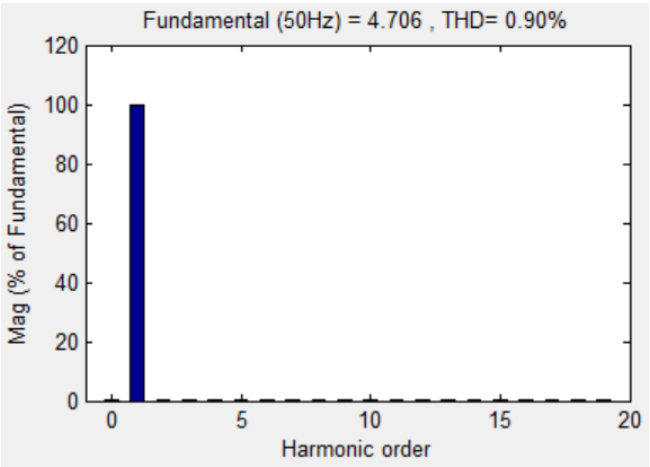

(f)

Figure IV.7 Performance of the fuzzy DC voltage control for a DPC- PWM Rectifier

V_{dc}^{*}=180 : **(a)** The active power P and its reference, **(b)** The reactive power Q and its reference,**(c)** Grid voltage and current, **(d)** Grid current**, (e)** The DC bus voltage and its reference, **(f)** FFT analysis for current THD **.**

- Here, in this test a step of the reference DC voltage is applied at t = 0.3s from 180 V to 220 V, so that we can observe the changes that will occur in the current, voltage, and THD. Thus, we obtain the following results :

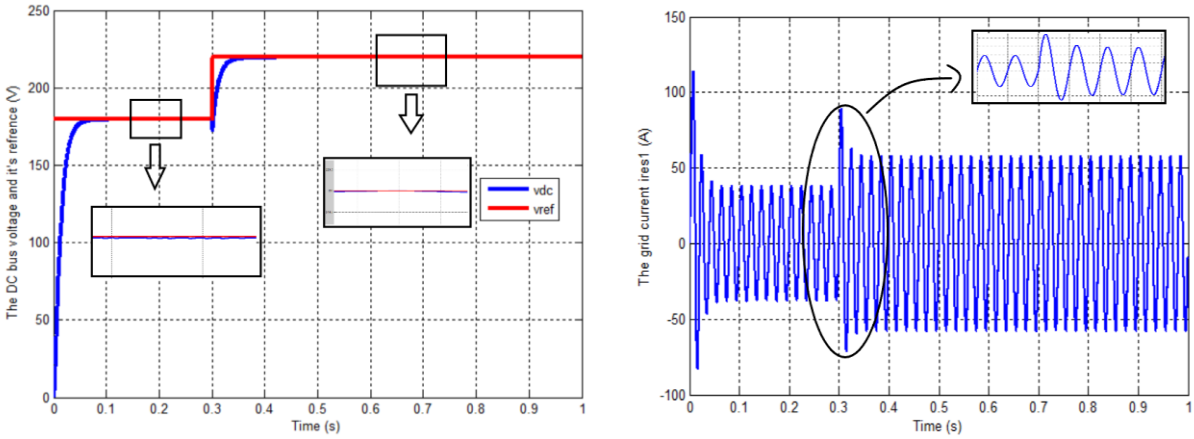

(a) **(b)**

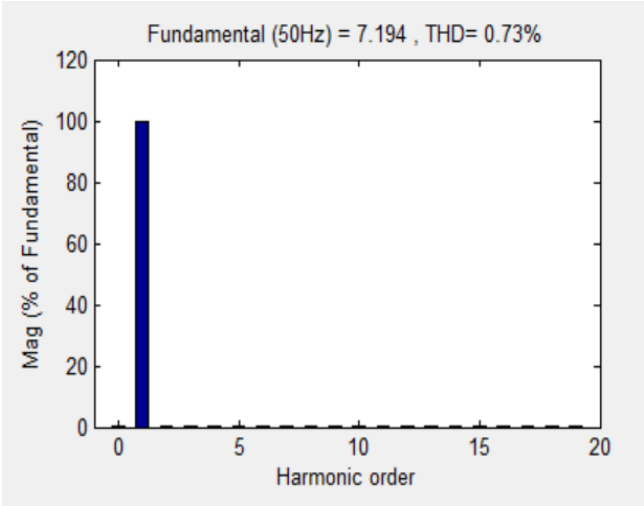

(c)

Figure IV.8 Performance of the fuzzy DC voltage control for a DPC- PWM Rectifier for a variable reference voltage V_{dc}^{*}: **(a)** The DC bus voltage and its reference, **(b)** Grid current, **(c)** FFT analysis for current THD.

- Here, in this test a step of the load R_L is applied at t = 0.3s from 68.6 Ω to 120 Ω , so as to observe the same changes in the system and obtain the following results:

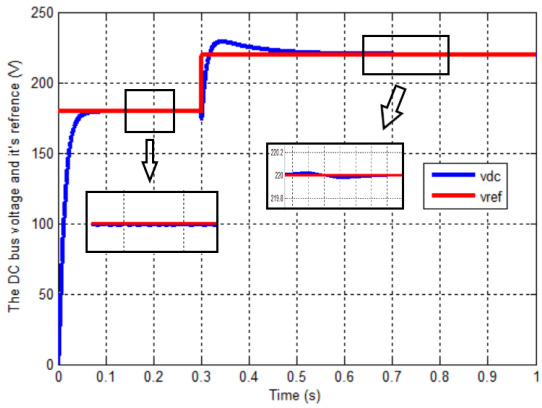

(a)

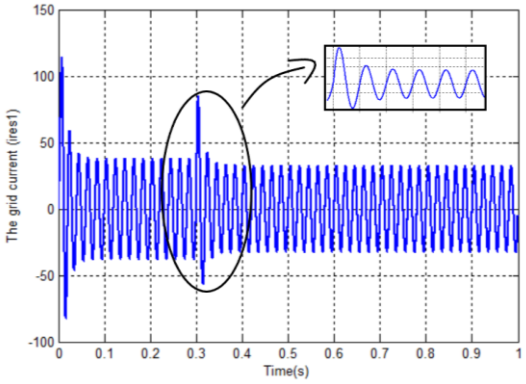

(b)

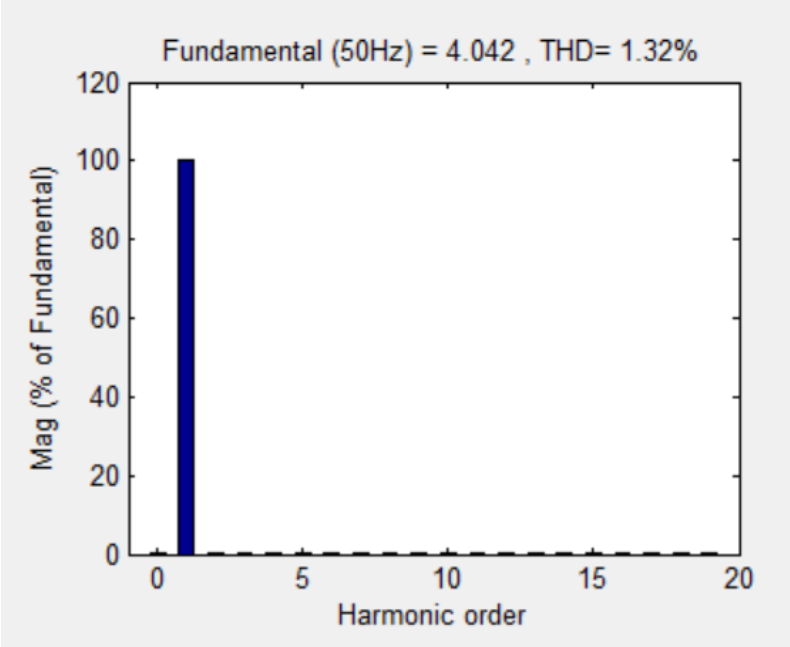

(c)

Figure IV.9 Performance of the fuzzy DC voltage control for a DPC- PWM Rectifier for a variable load R_L: **(a)** The DC bus voltage and its reference, **(b)** Grid current, **(c)** FFT analysis for current THD.

IV.3.2 Interpretation of simulation results

- **The Figure IV.7** represents the simulation results for a constant output reference voltage V_{dc}*, we can clearly observed that :
  - The current harmonic distortion rate is very low (0.90 %).

- The grid voltage and current are perfectly synchronized .
- Reactive power is almost constant at 0 VAR, and the active power remains consistently high at 500 watts.
- The DC bus voltage reaches the reference voltage.

- **The Figure IV.8** represents the results for a variable output voltage reference V_{dc}^{*} with a constant load (R_L = 68,6 Ω), we can notice that :
  - The grid current increases with the increase of the reference.
  - The current harmonic distortion rate is (THD=0.73 %).
  - The DC bus voltage reaches the reference value (after 0.1 s).

- **The Figure IV.9** represents the results for the case of a variable load R_L, while the reference voltage remains constant (V_{dc} = 180v), we notice that :
  - The grid current value shows an inverse relationship with the variable load.
  - The current harmonic distortion rate is (THD =1.32 %).
  - The DC bus voltage reaches the reference.

IV.4 Neural-Fuzzy Network

Neural network structures can deal with imprecise data and ill-defined activities. However, the subjective phenomena such as reasoning and perceptions are often regarded beyond the domain of conventional neural network theory. It is interesting to note that fuzzy logic is another powerful tool for modeling uncertainties associated with human cognition, thinking and perception **[Cha 09]**. Neural-fuzzy network system combines the advantages of neural network and fuzzy logic system. Neural network provides connectionist structure and learning abilities to the fuzzy logic systems, and the fuzzy logic systems provide neural networks with a structural framework with high-level fuzzy IF-THEN rule of thinking and reasoning. The neural network approach fuses well with fuzzy logic that's what led some research endeavors to given birth to the field of "Fuzzy Neural Networks" or "Fuzzy Neural Systems". That is what made it gained popularity in the control of nonlinear systems **[Are 10]**.

IV.5 Principle of ANFIS

The adaptive NF inference system (ANFIS) is one of the proposed methods to combine Fuzzy logic and artificial neural networks. Jang proposed ANFIS that represented the Takagi-Sugeno Kang model. This model will be used throughout for controller design and evaluation. ANFIS uses back propagation learning to determine premise parameters and least mean squares estimation to determine the consequent parameters. This is referred to as hybrid learning. In the first or forward pass, the input patterns are propagated, and the optimal consequent parameters are estimated by an iterative least mean square procedure, while the premise parameters are assumed to be fixed, In the second or backward pass the patterns are propagated again, and in this approach, back propagation is used to modify the premise parameters by the gradient descent algorithm, while the consequent parameters remain fixed. This procedure is then iterated until the error criterion is satisfied. ANFIS model is a universal approximator, which has the non-linear modeling and forecasting function **[Cha 09],** the Table IV.2 summarizes the different steps of the algorithm.

-	Forward (once)	Backward (once)
Premise parameters	Fixed	Gradient descent
consequent parameters	Least mean square	Fixed

Table IV.2 The hybrid method used in ANFIS.

IV.6 DC voltage control for a DPC- PWM Rectifier based on ANFIS

In recent years, Neuro-Fuzzy Controlles (NFCs) which are successfully applied to many industrial applications, are based on the execution of the functions of fuzzy controller (FC) by Artificial Neural Network (ANN) constructively **[Jan 97] [Dan 05]**. NFCs have non-linear structure and do not require the mathematical model of the system to be controlled. Therefore, the NFCs are used widespread in the systems that are uncertain, non-linear and have parameter changes **[Liu 03].** The configuration of the studied system with the proposed control description is presented in Figure IV.10. The ANFIS is applied to control the dc link voltage, whose inputs are the error of dc link voltage ($\varepsilon = v_{dcref} - v_{dc}$), and the error change $\Delta\varepsilon$, where its output is the active power current component

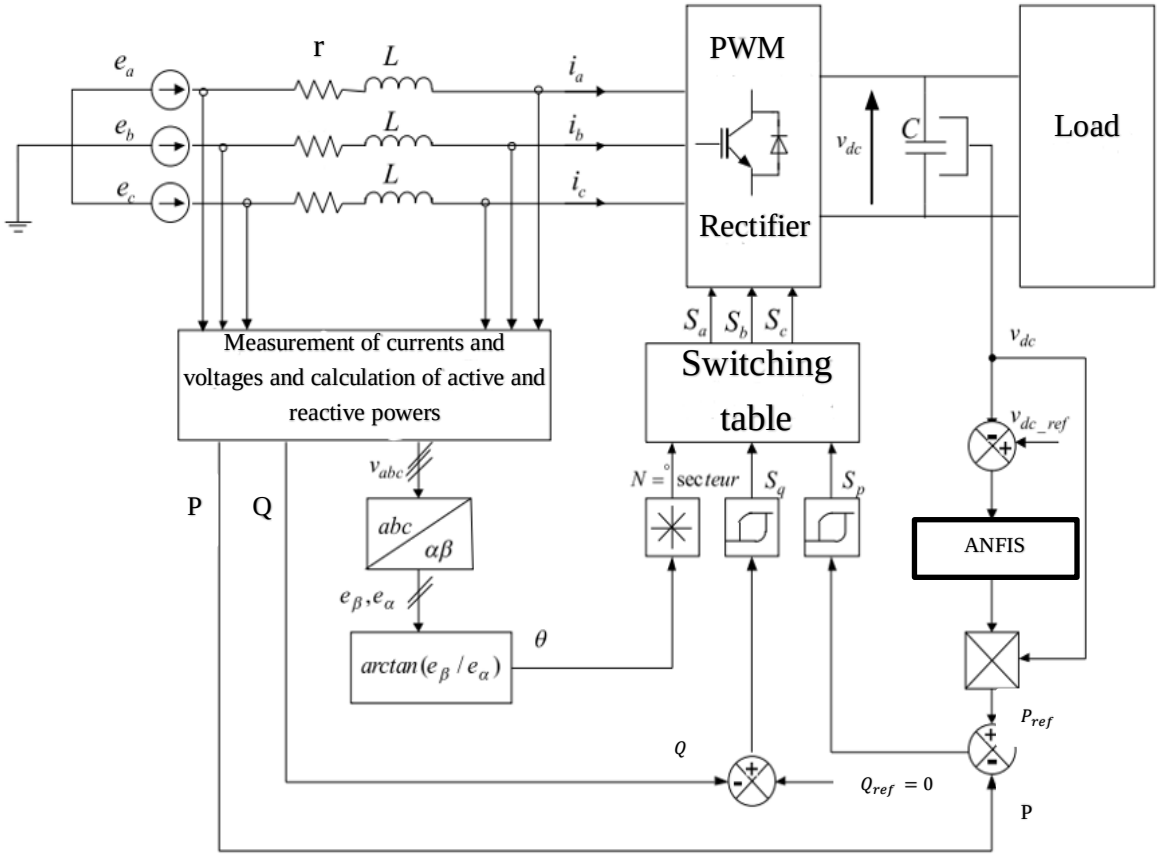

Figure IV.10 The configuration of DPC equipped with ANFIS.

The ANFIS structure based on a Takagi-Sugeno inference system is presented in Figure IV.11

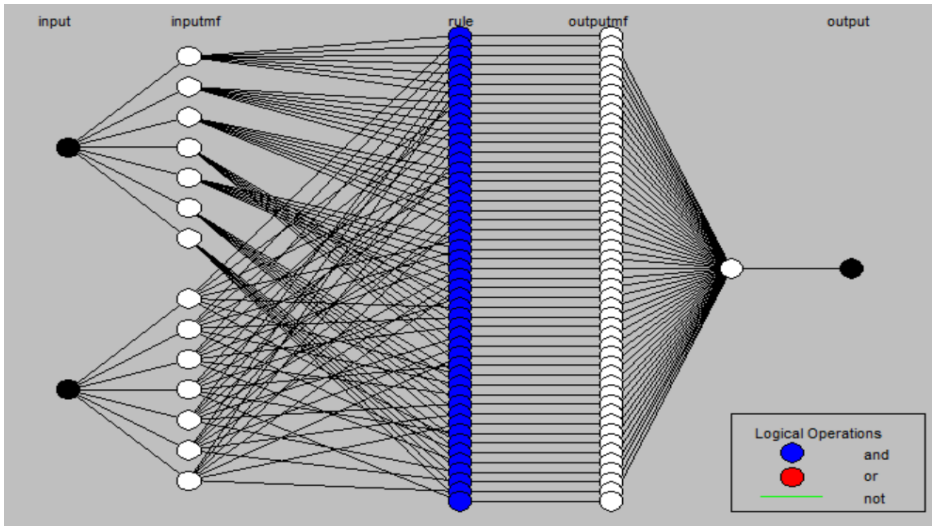

Figure IV.11 ANFIS structure in MATLAB/SIMULINK.

It contains five layers, in which the adaptive nodes are located at the first and fourth layers. The description of each layer is presented next.

IV.6.1 Design of the proposed ANFIS based DC-link voltage control

During the last years, genetic algorithm, artificial neural networks and fuzzy logic techniques have been intensively employed in many areas, include control applications such as, process control and power converters regulation. These artificial intelligence techniques are not limited by mathematical assumptions utilized in control theories and does not need an exact knowledge about the studied system. Indeed, the combination of ANN and FL methods are very important thanks to its advantages such as, control of non-linear system and noise rejection **[Jam 18]**. In this work, an ANFIS control technique is proposed to control the DC-link voltage of under different operating conditions. The ANFIS uses the fuzzy reasoning in handling uncertainties and the neural networks learning capability. Besides, the ANFIS control approach has many advantages such as, adaptive and excellent tracking capabilities with fast convergence. Figure IV.12 shows the block diagram of the proposed ANFIS structure based on a Takagi-Sugeno inference system. It contains five layers, to reflect different adaptive capabilities, we use both circle and square nodes in an adaptive network, in which the adaptive nodes are located at the first and fourth layers **[Jam 18]**.

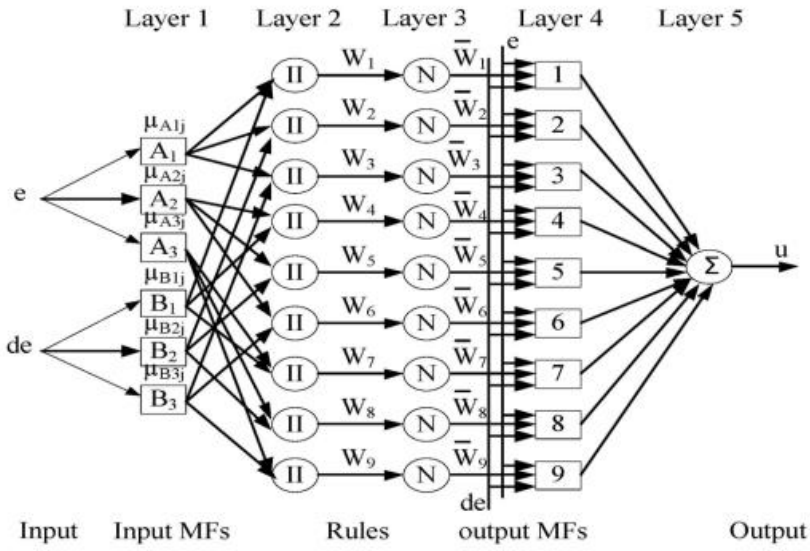

Figure IV.12 ANFIS based DC-link voltage control structure.

The developed ANFIS consists of five layers, two inputs, seven membership functions (MFs) per input, 49 rules and one output. Indeed, one of the input is the error between the reference of DC-

link voltage and its sensed value and the other input is the error change (IV.2), whereas its output is the active power current component (IV.3), which is multiplied by V_{dc} to get the active power reference P_{dc}. The detail description of each layer is given below **[Jam 18] [Cha 09]**:

Layer 1: This layer is also known as the fuzzification layer where each node is represented by a square. Here, seven membership functions are assigned to each input.

$$\begin{cases} O_{1,i} = \mu_{Aij}(x_1), & i = 1,2 \\ O_{1,i} = \mu_{Bij}(x_2), & i = 1,2 \end{cases} \quad \text{(IV.4)}$$

The corresponding equation to each gaussian membership function are expressed as:

$$\mu_{Aij}(x_i) = \mu_{Bij}(x_i) = \exp\left[-\frac{(x_i - c_{ij})^2}{2\sigma_{ij}}\right] \quad \text{(IV.5)}$$

Where x_1=ε, x_2 = Δε ; x_i is equal to x_1 and x_2 ; {A_j and B_j } are the linguistic label. {c_{ij}, σ_{ij}} is the parameter set referred to as premise parameters.

Layer 2: In this layer, each node is a circle labeled as **Π**, it multiplies the input signals and transmit it to the layer 3 according to the following expression:

$$O_{2,k} = \omega_k = \mu_{Aij}(x_1).\mu_{Bij}(x_2) \quad \text{(IV.6)}$$

Where the subscript k is equal 1,2,...,49 and the subscript j (input) is equal to 1,...,2. Thus, the output of each node is referred to the firing strength.

Layer 3: Each node in this layer is a circular node called N. In this layer, the cells calculate the ratio between the truth values of each rule and the sum of all truth values given by each rule. They estimate the "normalized" firing weight of each rule.

$$O_{3,k} = \overline{\omega_k} = \frac{\omega_k}{\omega_1 + \omega_1 + \cdots + \omega_{49}} \quad \text{(IV.7)}$$

Layer 4: In this layer, each node is a point of connection with the node function as given in the following equation:

$$O_{4,k} = \overline{\omega_k} f_k = \overline{\omega_k}(p_i x_i + q_i x_i + r_i) \quad \text{(IV.8)}$$

With p_i, q_i r_i and represent the consequent parameters, and $\overline{\omega_k}$ is the output of the third layer.

Layer 5: is the output layer, its determination is done by the summation of all incoming signals according to the expression (IV.9):

$$y = \sum_{k=1}^{49} \overline{\omega_k} f_k \quad \text{(IV.9)}$$

Generalizing the network to a system with n inputs poses no particular issues. The number of nodes in Layer 1 is always equal to the total number of defined linguistic terms. The number of nodes in Layers 2, 3, and 4 is always equal to the number of fuzzy rules.

IV.6.2 Learning Algorithm of ANFIS

The subsequent to the development of ANFIS approach, a number of methods have been proposed for learning the parameters and for obtaining an optimal number of MFs. ANFIS's network organizes two parts like fuzzy systems. The first part is the antecedent part and the second part is the consequent part which they are connected to each other by rules in network form. These two parts can be adapted by different optimization methods, one of which is the hybrid learning procedure combining the least mean square and gradient descent. In a conventional fuzzy inference system, the number of rules is determined by expert who is familiar with the target system to be modelled. In our simulation, however, no expert is available and the number of MFs assigned to each input variable is chosen empirically-that is, by plotting the data sets and examining them visually **[Zan 11]**.

IV.6.2.1 The process of determining premise parameters and consequent parameters

The ANFIS system operates in a loop, which first determines the connections responsible for the error and their contribution to it. Based on this information, we can modify the weights that need adjustment.

The error used is of quadratic type, calculated as the square of the difference between the desired output and the obtained output.

$$J(t) = \frac{1}{2}(\varepsilon(k))^2 = \frac{1}{2}(y_d - y_p\,(k))^2 \quad \text{(IV.10)}$$

Where y_d is the desired output, y_p (t) is the actual system output and ε (k) is the error between y_d and y_p (t).

The idea is to modify the weights of the network's inputs based on the error. This allows the system to decrease the weights of neurons that have contributed the most to the error and increase the weights of other neurons.

Initially, it should be noted that the network's output could be expressed in the following form for two input and two linguistic label:

$$y = \frac{\omega_1}{\omega_1 + \omega_2} f_1 + \frac{\omega_2}{\omega_1 + \omega_2} f_2$$

$$y = \overline{\omega_1} f_1 + \overline{\omega_2} f_2 = \overline{\omega_1}(p_1 x_1 + q_1 x_2 + r_1) + \overline{\omega_2}(p_2 x_2 + q_2 x_2 + r_2) \quad \text{(IV.11)}$$

$$y = (\overline{\omega_1} x_1) p_1 + (\overline{\omega_1} x_2) q_1 + (\overline{\omega_1}) r_1 + (\overline{\omega_2} x_1) p_2 + (\overline{\omega_2} x_2) q_2 + (\overline{\omega_2}) r_2$$

The equation (IV.11) demonstrates that, by fixing the premise parameters, the output y is linear with respect to the consequent parameters. We can then use the least squares estimation to determine the optimal consequent parameters $\{p, q, r\}$. During the learning phase, the inputs and actual outputs are known. Therefore, we propagate the inputs up to Layer 4 (with the premise parameters fixed) and then apply the least squares estimation **[Mer 17]**. For the determination of the nonlinear premise parameters of fuzzy rules with Gaussian membership functions, which is defined in the equation (IV.12), the error gradient backpropagation algorithm is used. The learning process is supervised, where each input is associated with a desired output. The backpropagation algorithm is an iterative gradient-based algorithm designed to minimize a quadratic error criterion between the obtained output and the desired output. This minimization is achieved through an appropriate configuration of parameters.

$$\mu_{Aij}(x_i) = exp\left[-0.5\,(v_{ij}.(x_i - c_{ij}))\right] \qquad avec \quad v_{ij} = \frac{1}{\sigma_{ij}} \quad \text{(IV.12)}$$

Where c, represents the central value and v is the inverse of the spread or width of the Gaussian membership function. Considering the set of premise parameters characterized by the vector θ, and input-output data set pairs are (xk, yk). Our objective is to find the values of the vector $\theta = [c\ v]^T$ such that the output of the fuzzy system closely approximates the desired output y_d.

The backpropagation algorithm is given by:

$$\theta(k+1) = \theta(k) - \eta \frac{\partial J}{\partial \theta} \quad \text{(IV.13)}$$

$$J(t) = \frac{1}{2}(\varepsilon(k))^2 = \frac{1}{2}(y_d - y_p\,(k))^2 \quad \text{(IV.14)}$$

$$\frac{\partial J}{\partial \theta} = \left[\frac{\partial J}{\partial c} \quad \frac{\partial J}{\partial v}\right]^t \quad \text{(IV.15)}$$

With η being the learning rate **[Sai 08]**.

IV.7 Simulation of DC voltage control for a DPC- PWM Rectifier based on ANFIS

IV.7.1 Simulation Results

The simulations have been carried out using the same electrical parameters of power circuit and control data used in DPC control simulation:

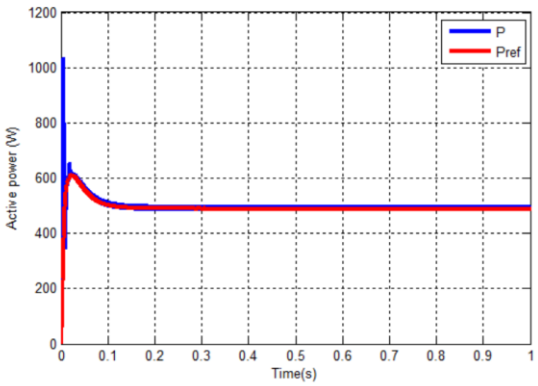

(a)

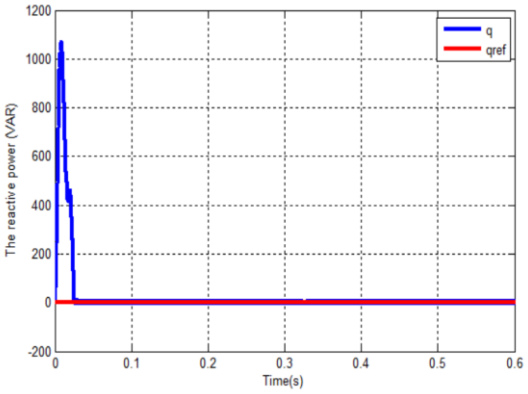

(b)

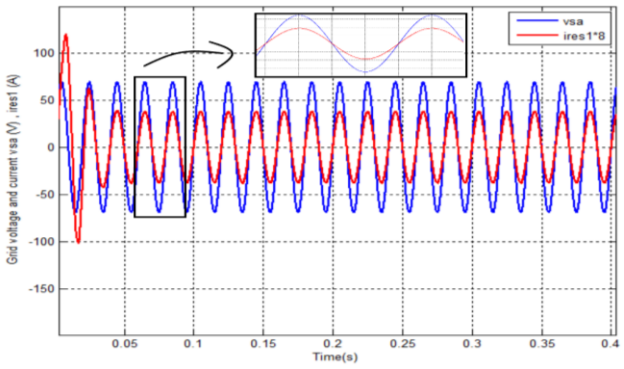

(c)

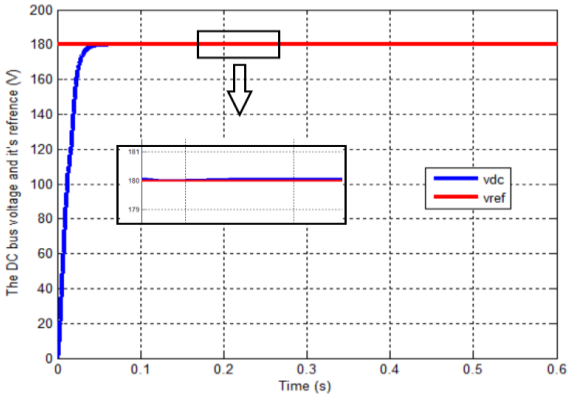

(d)

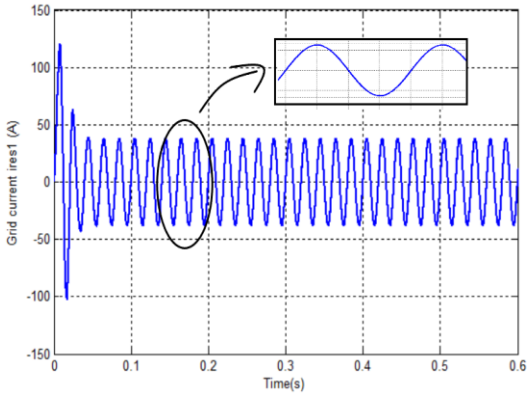

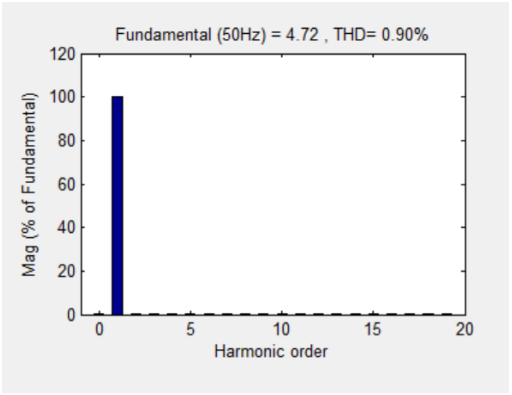

(e) **(f)**

Figure IV.13 Performance of the ANFIS DC voltage control for a DPC- PWM Rectifier V_{dc}^{*}=180: **(a)** The active power P and its reference, **(b)** The reactive power Q and its reference,**(c)** Grid voltage and current, **(d)** The DC bus voltage and it's reference**, (e)** Grid current, **(f)** FFT analysis for current THD **.**

- Here, in this test a step of the reference DC voltage is applied at t = 0.3s from 180 V to 220 V, so that we can observe the changes that will occur in the current, voltage, and THD. Thus, we obtain the following results :

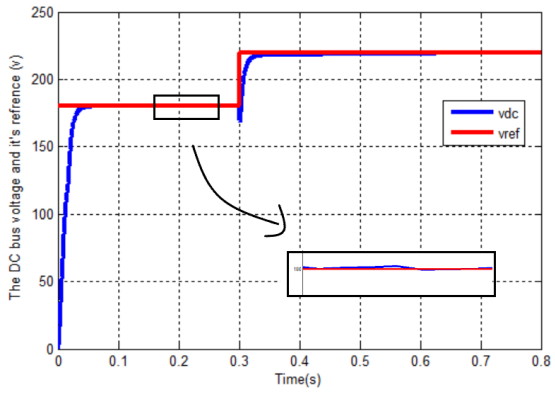

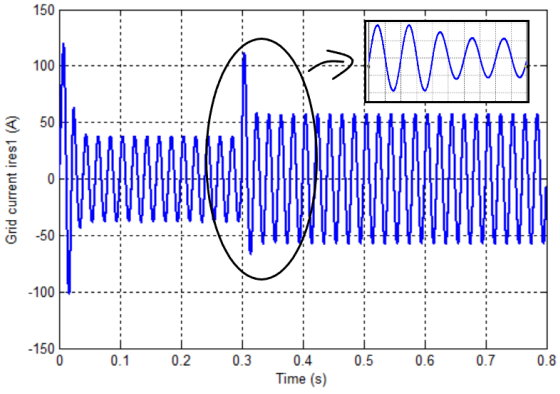

(a) **(b)**

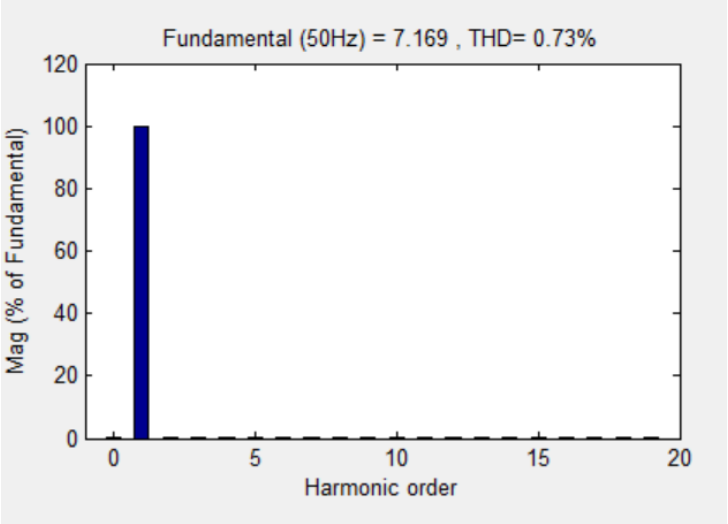

(c)

Figure IV.14 Performance of the ANFIS DC voltage control for a DPC- PWM Rectifier for a variable reference voltage V_{dc}^{*}: **(a)** The DC bus voltage and its reference, **(b)** Grid current, **(c)** FFT analysis for current THD.

❖ Here, in this test a step of the load R_L is applied at t = 0.3s from 68.6 Ω to 120 Ω , so as to observe the same changes in the system and obtain the following results:

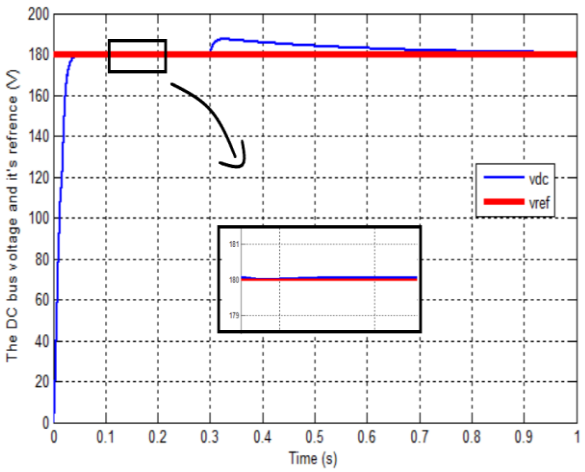

(a)

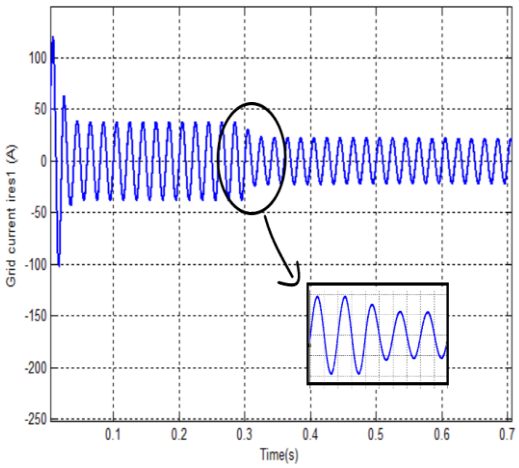

(b)

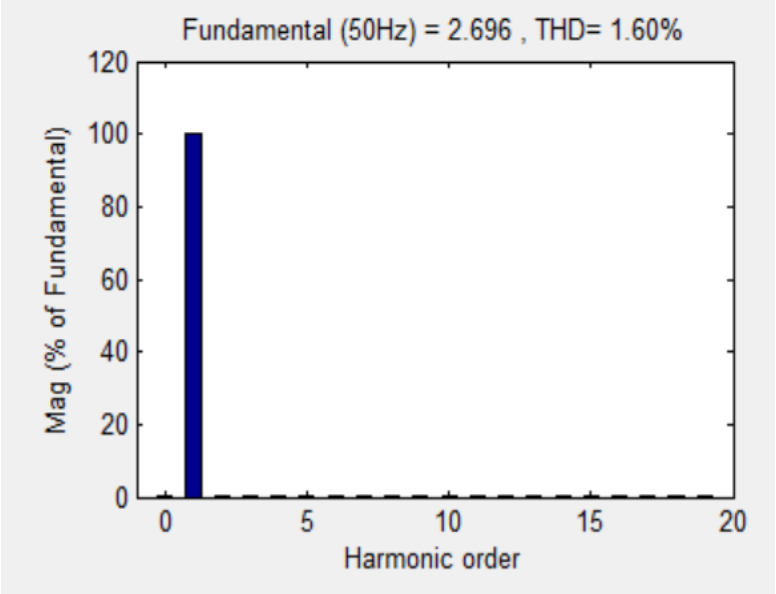

(c)

Figure IV.15 Performance of the ANFIS fuzzy DC voltage control for a DPC- PWM Rectifier for a variable load R_L: **(a)** The DC bus voltage and its reference, **(b)** Grid current, **(c)** FFT analysis for current THD.

IV.7.2 Interpretation of simulation results

- **The Figure IV.13** represents the simulation results for a constant output reference voltage V_d^*, we can clearly observed that :
  - The current harmonic distortion rate is very low (0.90 %).
  - The grid voltage and current are perfectly synchronized.
  - Reactive power is almost constant at 0 VAR, and the active power remains consistently high at 500 watts.
  - The DC bus voltage reaches the reference voltage.

- **The Figure IV.14** represents the results for a variable output voltage reference V_{dc}^*, with a constant load (R_L = 68,6 Ω), we can notice that :
  - The grid current increases with the increase of the reference.
  - The current harmonic distortion rate is (THD=0.73 %).
  - The DC bus voltage reaches the reference value (after 0.1s).

- **The Figure IV.15** represents the results for the case of a variable load R_L , while the reference voltage remains constant (V_{dc}= 180v), we notice that :
  - The grid current value shows an inverse relationship with the variable load.
  - The current harmonic distortion rate is (THD =1.60 %).
  - The DC bus voltage reaches the reference (after 0.4 s).

IV.8 Comparative study of the previous control techniques results

The objective of this study is to demonstrate the contribution of each three Direct Power Control methods presented throughout this work. The two factors considered in evaluating the performance of these controls are:

- The DC bus voltage regulation.
- The Total Harmonic Distortion (THD) of grid currents.
- The reactive power control.

- **Performance**: In terms of performance, DPC-FUZZY and DPC-ANFIS demonstrate superior results compared to DPC-PI as shown in Figure IV.16. They exhibit faster response times and better dynamic behavior, leading to improved control of the system.
- **Response Time:** DPC-ANFIS shows the fastest response time among the three methods, with the DC bus voltage reaching the reference value in less than 0.1s. DPC-FUZZY also performs well, achieving the reference value in less than 0.3s. On the other hand, DPC-PI takes more than 0.4s to reach the reference value.

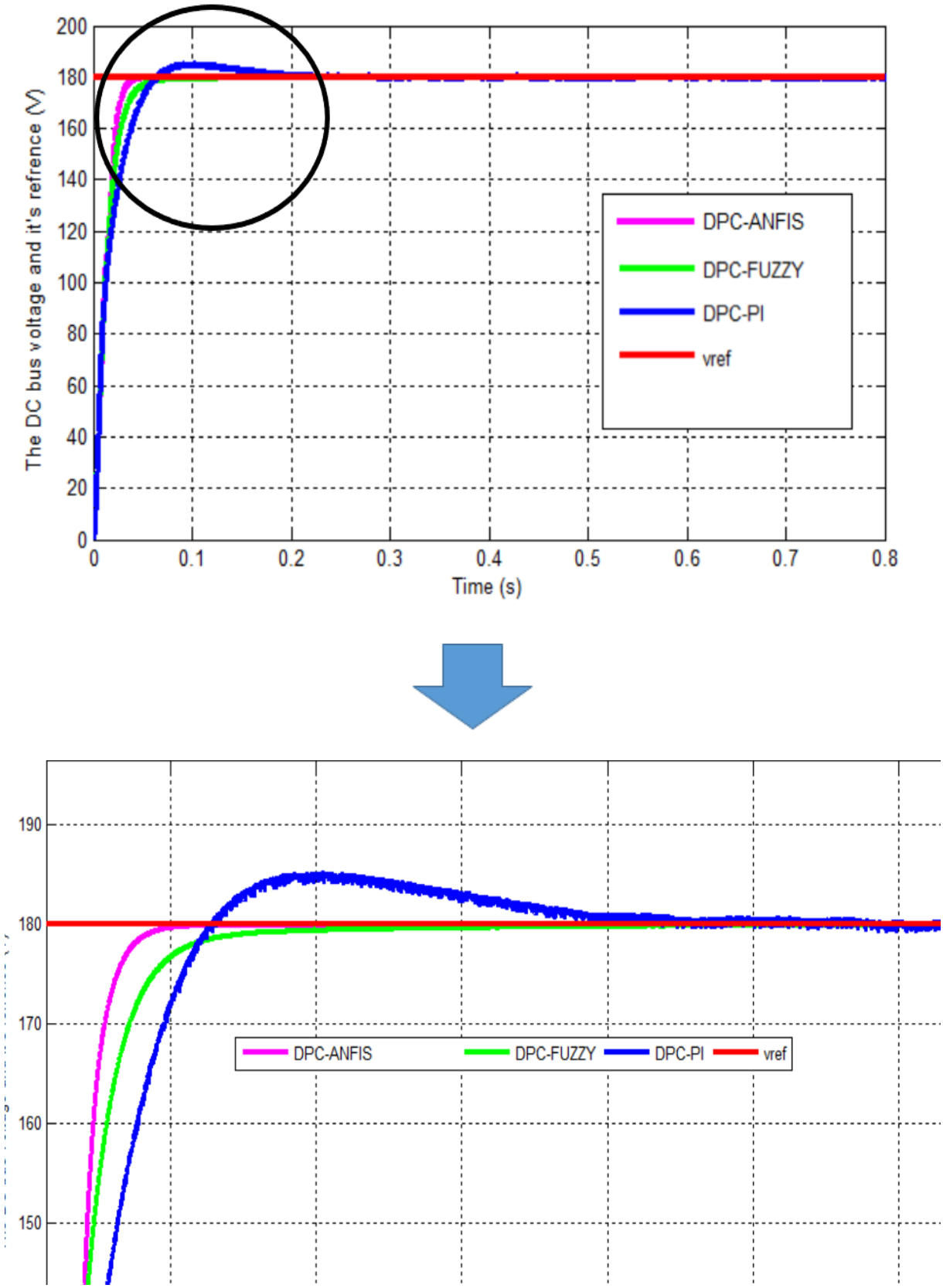

Figure IV.16 Regulation of the DC bus voltage in the three methods.

- **THD Reduction:** In Table IV.3, all three methods effectively reduce Total Harmonic Distortion (THD) values below 4%, which is considered acceptable. However, DPC-FUZZY and DPC-ANFIS exhibit better results in terms of THD reduction compared to DPC-PI.

Method de control / THD	DPC-PI	DPC-FUZZY	DPC-ANFIS
	3.50 %	**0.90 %**	**0.90 %**

Table IV.3 THD Values Comparison for the Three Control Methods.

- **Control Complexity**: DPC-PI has a relatively simpler control structure compared to DPC-FUZZY and DPC-ANFIS, which involve fuzzy logic and adaptive neuro-fuzzy inference systems, respectively. This simplicity may be advantageous in terms of implementation and computational requirements.
- **Adaptability:** DPC-FUZZY and DPC-ANFIS offer higher adaptability and flexibility in handling different operating conditions and system parameters. They can adapt their control strategies based on the system's dynamic behavior, resulting in improved performance.

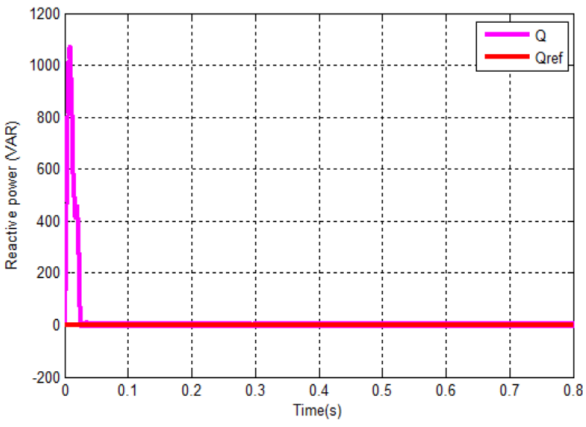

(a)

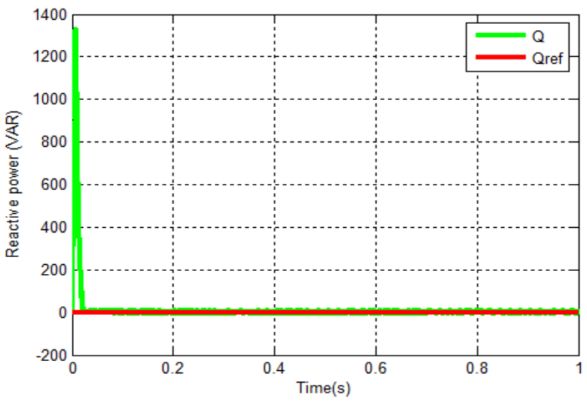

(b)

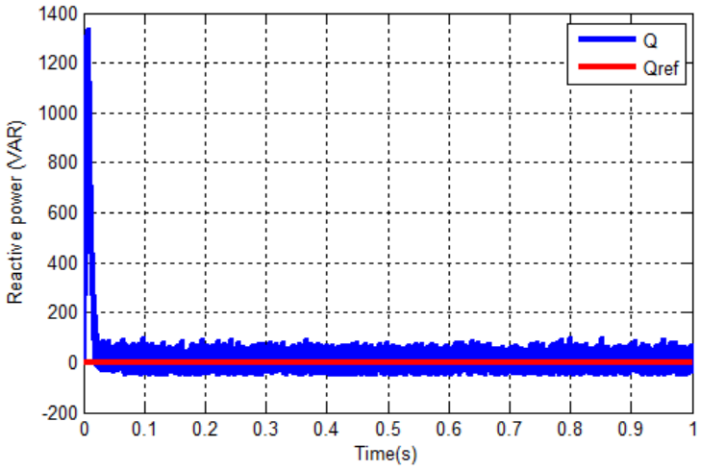

(c)

Figure IV.17 The reactive power response in the three methods: **(a)** DPC-ANFIS method, **(b)** DPC-FUZZY method, **(c)** DPC-PI method.

When comparing DPC-PI, DPC-Fuzzy, and DPC-ANFIS, all three control strategies offer different levels of reactive power control. DPC-Fuzzy and DPC-ANFIS outperform DPC-PI in minimizing reactive power losses, with DPC-ANFIS providing the highest level of control and efficiency. The adoption of fuzzy logic and ANFIS controllers allows for adaptive and intelligent control, resulting in reduced reactive power and improved performance of the PWM rectifier system.

Overall, DPC-FUZZY and DPC-ANFIS demonstrate better performance in terms of response time, THD reduction, and adaptability compared to the classical DPC-PI method. These advanced control techniques offer enhanced control capabilities and are well suited for applications that require precise and efficient power regulation.

IV.9 Conclusion

In this chapter, we proposed an approach to enhance the Direct Power Control (DPC) of the three-phase PWM rectifier by suggesting this two methods: Fuzzy DC voltage control for a DPC-PWM Rectifier and DC voltage control for a DPC- PWM rectifier based on ANFIS. After conducting the proposed methods and their simulation on MATLAB/SIMULINK and obtaining the results, we investigated and compared three different control methods for the power electronics system. The Direct Power Control (DPC) method with classical Proportional-Integral (PI) controller, DPC with Fuzzy Controller, and DPC based on Adaptive Neuro-Fuzzy Inference

System (ANFIS), were studied and their performances were evaluated. The results showed that all three control methods achieved acceptable Total Harmonic Distortion (THD) values below 4%, indicating their effectiveness in reducing harmonic pollution in the system. However, in terms of performance, it was observed that both DPC-Fuzzy and DPC-ANFIS outperformed DPC-PI. These methods exhibited faster response times and demonstrated better regulation of the DC bus voltage, reaching the reference value in less than 0.3 seconds and 0.1 seconds, respectively. Overall, the findings highlight the advantages of utilizing advanced control techniques, such as Fuzzy Control and ANFIS, in enhancing the performance and dynamic behavior of the power electronics system. These methods offer improved regulation, reduced cost of installation, and greater potential for achieving optimal system performance. Further research and experimentation can be conducted to explore the applicability and scalability of these control methods in various power electronics applications.

General conclusion

The research presented in this memory focuses on exploring modern solutions based on power electronics to address the issue of harmonic pollution in the electrical grid, specifically in the distribution system. The primary solution investigated is the PWM Rectifier, which has the capability to independently mitigate reactive energy consumption and provides a bidirectional power flow, low harmonic distortion, and adjustable DC voltage. In this work, we addressed the operational principles and control strategies of an AC/DC converter integrated with a controlled balanced electrical network, employing various control techniques such as hysteresis current control, Direct Power Control (DPC) with a classical switching table, DPC with a new switching table, and DC voltage control for a DPC- PWM Rectifier based on Fuzzy Logic and ANFIS.

In the first part of this work, a bibliographic study was carried out concerning harmonic disturbances affecting network voltage and degrading the quality of electrical energy. Different traditional and modern means of harmonic reduction were discussed. In the light of this study, we have been able to observe that research on PWM Rectifiers is widespread throughout the world not only for the absorption of sinusoidal currents but also for eliminating different types of disturbances that can affect the network.

For this, we have devoted the second part of our theoretical study to the operating principle and modeling of the PWM Rectifier, for their control techniques, hysteresis current control technique have been used. We concluded that hysteresis control is simple and easy, ensuring unity power factor and low harmonic distortion, but it also has drawbacks such as variable switching frequency dependent on the bandwidth.

The third part of this work is dedicated to the modeling and simulation of Direct Power Control (DPC) technique, as well as a synthesis of continuous bus voltage PI regulators. In addition to its simplicity, offers better control of instantaneous active and reactive powers. This control strategy is widely used for many converters as it directly selects optimal switch states to control instantaneous active powers without requiring current loops or PI regulators. The configuration and principle of DPC using the classical and new switching table have been explained in detail. The simulation results have been analyzed, and the performance of this control is evaluated based on these results.

General conclusion

In the last part, an improvement scheme based on Fuzzy Logic and ANFIS (Adaptive Neuro-Fuzzy Inference System) for the DC-link voltage control approach in Direct Power Control (with new switching table) of a PWM Rectifier system is presented. The error of the DC link voltage ($\varepsilon = V_{dc\_ref} - V_{dc}$) and the rate of change of the error Δe are used as inputs for both control techniques. The output of these techniques is the active power current component.

A brief comparative study between the developed ANFIS-based controller and the Fuzzy logic controller has been introduced to show the different effect of each one of this controller on the PWM Rectifier system.

As future prospects for this work, we can mention:

- A new configuration of DPC, without hysteresis comparators and with using ANFIS controller to represent the switching table of DPC.
- Using a different type of load, such as an electric machine, to demonstrate the four-quadrant operation capability of the PWM Rectifier.

Annex.

As shown in the table below, the reactive power signs of the three vectors switch between positive and negative. For active power, the sign changes of four vectors are positive and the sign changes of two or three vectors are negative:

- **Sector 01**

According to Figure III.8 and III.9 for each combination of output signals S_p and S_q, the selected voltage vectors for the first sector are expressed in the following table :

$\Delta P_1>0$	$\Delta P_1<0$	$\Delta q_1>0$	$\Delta P_1<0$	$\Delta P_1 =0$
V_3, V_4, V_5, V_0	V_1, V_6	V_1, V_2, V_3	V_4, V_5, V_6	V_0/V_7

The two-level hysteresis controllers for instantaneous reactive power can be written as follows:

If $\Delta_P > 0$ then $S_p = 1$ and $\Delta_P < 0$ then $S_p = 0$

If $\Delta_Q > 0$ then $S_q = 1$ and $\Delta_Q < 0$ then $S_q = 0$

S_{p1} \ S_{q1}	1	0
1	v_3	v_4, v_5
0	v_1	v_6

- **Sector 02**

$\Delta P_2>0$	$\Delta P_2<0$	$\Delta q_2>0$	$\Delta P_2<0$	$\Delta P_2 =0$
V_3, V_4, V_5, V_0	V_1, V_2	V_2, V_3, V_4	V_1, V_5, V_6	V_0/V_7

The selected voltage vectors for sector 02 are expressed in the following table:

S_{p2} \ S_{q2}	1	0
1	v_3, v_4	v_5
0	v_2	v_1

- **Sector 03**

$\Delta P_3>0$	$\Delta P_3<0$	$\Delta q_3>0$	$\Delta P_3<0$	$\Delta P_3=0$
V_4, V_5, V_6, V_0	V_1, V_2	V_2, V_3, V_4	V_1, V_5, V_6	V_0/V_7

The selected voltage vectors for sector 03 are expressed in the following table:

S_{p_3} \ S_{q_3}	1	0
1	v_4	v_5, v_6
0	v_2	v_1

- **Sector 04**

$\Delta P_4>0$	$\Delta P_4<0$	$\Delta q_4>0$	$\Delta P_4<0$	$\Delta P_4=0$
V_4, V_5, V_6, V_0	V_2, V_3	V_3, V_4, V_5	V_1, V_2, V_6	V_0/V_7

The selected voltage vectors for sector 04 are expressed in the following table:

S_{p_4} \ S_{q_4}	1	0
1	v_4, v_5	v_6
0	v_3	v_2

- **Sector 05**

$\Delta P_5>0$	$\Delta P_5<0$	$\Delta q_5>0$	$\Delta P_5<0$	$\Delta P_5=0$
V_1, V_5, V_6, V_0	V_2, V_3	V_3, V_4, V_5	V_1, V_2, V_6	V_0/V_7

The selected voltage vectors for sector 05 are expressed in the following table:

S_{p_5} \ S_{q_5}	1	0
1	v_5	v_1, v_6
0	v_3	v_2

- **Sector 06**

$\Delta P_6>0$	$\Delta P_6<0$	$\Delta q_6>0$	$\Delta P_6<0$	$\Delta P_6 =0$
V_1, V_5, V_6, V_0	V_3, V_4	V_4, V_5, V_6	V_1, V_2, V_3	V_0/V_7

The selected voltage vectors for sector 06 are expressed in the following table:

S_{p_6} \ S_{q_6}	1	0
1	v_5, v_6	v_1
0	v_4	v_3

- **Sector 07**

$\Delta P_7>0$	$\Delta P_7<0$	$\Delta q_7>0$	$\Delta P_7<0$	$\Delta P_7 =0$
V_1, V_2, V_6, V_0	V_3, V_4	V_4, V_5, V_6	V_1, V_2, V_3	V_0/V_7

The selected voltage vectors for sector 07 are expressed in the following table:

S_{p_7} \ S_{q_7}	1	0
1	v_6	v_2, v_1
0	v_4	v_3

- **Sector 08**

$\Delta P_8>0$	$\Delta P_8<0$	$\Delta q_8>0$	$\Delta P_8<0$	$\Delta P_8 =0$
V_1, V_2, V_6, V_0	V_5, V_4	V_1, V_5, V_6	V_4, V_2, V_3	V_0/V_7

The selected voltage vectors for sector 08 are expressed in the following table:

S_{p8} \ S_{q8}	1	0
1	v_1, v_6	v_2
0	v_5	v_4

- **Sector 09**

$\Delta P_9>0$	$\Delta P_9<0$	$\Delta q_9>0$	$\Delta P_9<0$	$\Delta P_9 =0$
V_1, V_2, V_3, V_0	V_5, V_4	V_1, V_5, V_6	V_4, V_2, V_3	V_0/V_7

The selected voltage vectors for sector 09 are expressed in the following table:

S_{p9} \ S_{q9}	1	0
1	v_1	v_2, v_3
0	v_5	v_4

- **Sector 10**

$\Delta P_{10}>0$	$\Delta P_{10}<0$	$\Delta q_{10}>0$	$\Delta P_{10}<0$	$\Delta P_{10} =0$
V_1, V_2, V_3, V_0	V_5, V_4	V_1, V_5, V_6	V_4, V_2, V_3	V_0/V_7

The selected voltage vectors for sector 10 are expressed in the following table:

$S_{p_{10}}$ \ $S_{q_{10}}$	1	0
1	v_1, v_2	v_3
0	v_6	v_5

- **Sector 11**

$\Delta P_{11}>0$	$\Delta P_{11}<0$	$\Delta q_{11}>0$	$\Delta P_{11}<0$	$\Delta P_{11}=0$
V_2, V_3, V_4, V_0	V_5, V_6	V_1, V_2, V_6	V_3, V_4, V_5	V_0/V_7

The selected voltage vectors for sector 11 are expressed in the following table:

$S_{p_{11}}$ \ $S_{q_{11}}$	1	0
1	v_2	v_3, v_4
0	v_6	v_5

- **Sector 12**

$\Delta P_{12}>0$	$\Delta P_{12}<0$	$\Delta q_{12}>0$	$\Delta P_{12}<0$	$\Delta P_{12}=0$
V_2, V_3, V_4, V_0	V_1, V_6	V_1, V_2, V_3	V_4, V_5, V_6	V_0/V_7

The selected voltage vectors for sector 12 are expressed in the following table:

$S_{p_{12}}$ \ $S_{q_{12}}$	1	0
1	v_2, v_3	v_4
0	v_1	v_6

Bibliographic References

[Arr 03] J. Arrillaga, "Power System Harmonics, 2nd ed", Chichester, U.K.Wiley, 2003.

[Are 10] F. G. Areed, A. Y. Haikal, R. H. Mohammed, "Adaptive neuro-fuzzy control of an induction motor", Elsevier, Vol. 1, No. 1, pp.71-78, 2010.

[Bou 07] A. Boukadoum, "contrubution à l'analyse et la Réduction de la pollution harmonique dans le réseau électrique ", master's memory, university of Annaba, Algeria, 2007.

[Ben 13] S. Bengana, "Stratégie de contrôle de puissance d'un redresseur PWM Triphasé", master's thesis, université kasdi merbah, Ouargla, Algeria, 2013.

[Bei 91] Husam. M. Beides, G. T. Heydt, "Dynamic State Estimation of Power System Harmonics Using Kalman Filter Methodology ", IEEE,Transactions on Power Delivery, Vol. 6, No. 4, October 1991.

[Bou 10] A. Bouafia, "Techniques de commande prédictive et floue pour les systèmes d'électronique de puissance : application aux redresseurs à MLI", PhD thesis, ferhat abbas university of sétif, Algeria, 2010.

[Ben 98] L. Benchaita, "Etude, par simulation numérique et expérimentation, d'un filtre actif parallèle à structure courant avec une nouvelle méthode de contrôle - commande", PhD thesis, Université Henri Poincaré, Nancy 1, 1998.

[Bie 20] Y. Bie, et all,"PWM rectifier impedance modelling and analysis", China Electric Power Research Institute (CEPRI), Beijing, China, 2021.

[Blo 11] A. Blorfan, P. Wira, D. Flieller, G. Sturtzer, J. Mercklé, "A Three-Phase Hybrid Active Power Filter with Photovoltaic Generation and Hysteresis Current Control", 37th Annual Conference of the IEEE Industrial Electronics Society (IECON 2011), Melbourne, Australia, 2011.

[Bou 08] A. Bouafia, J-P. Gaubert, F. Krim , " Analysis and design of new switching table for direct power control of three-phase PWM rectifier ",13th International Power Electronics and Motion Control Conference. pp.703-709 . Sep30th .2008.

[Ben 14] K. Ben Salem, K. Yahia, "Modélisation et Simulation D'un Convertisseur Statique AC/DC Commandée", master's memory, the University of El-Oued, Algeria, 2014.

[Bel 17] B. Lakhdar, "Commande directe de puissance basée sur le flux virtuel d'un convertisseur AC/DC triphasé sans capteur de Tension", Magister memory, Military Polytechnic School, 2017.

[Ben 17] A. Bennassar, M. Jamma, M. Akherraz, C. Fahassa, M. Barara, and M. Oproescu "Self-tuning fuzzy PI dc-bus voltage controller and fuzzy switching sequences selection for direct power

control of PWM AC/DC converter," in 9th International Conference on Electronics, Computers and Artificial Intelligence. pp.1–6. 2017.

[Cic 02] M. Cichowlas, M. P. Kazmierkowski, "Comparison of: Current' Control Techniques. For PWM Rectifiers", PhD thesis, Warsaww University, Poland, 2002.

[Cha 08] A. Chaoui, F. Krim, J.-P. Gaubert, and L. Rambault, "DPC controlled three-phase active filter for power quality improvement", Int. J. Electr. Power Energy Syst., vol. 30, no. 8, pp. 476–485, Oct. 2008.

[Cha 09] Y. Chai, L. Jia, Z. Zhang, "Mamdani Model based Adaptive Neural Fuzzy Inference System and its Application", International Journal of Computer, Electrical and Information Engineering, Vol. 3, No. 3,pp. 663-670, 2009.

[Dug 02] R. C. Dugan, M. F. McGranaghan, S. Santoso, H. W. Beaty, "Electrical Power Systems Quality, Second Edition", McGraw-Hill, 2002.

[Dwi 17] A. Dwivedi, A.N. Tiwari, "Analysis of three-phase PWM rectifiers using hysteresis current control techniques",Int. J. Power Electronics, Vol. 8, No. 4,pp. 349-377, 2017.

[Dja 20] S. Djabali, M. Ait Hamou Ali, "Control and Power Quality Improvement of Three-Phase PWM-Rectifier", master's memory, University M'Hamed bougara, Algeria, 2020.

[Den 17] H. Denoun, A. Fekik, M. Zaouia, N. Benyahia, N. Benamrouche, A. Badji and S. Vaidyanathan, " Improvement of the Performances of the Direct Power Control Using Space Vector Modulation of Three Phases PWM-Rectifier ", International Journal of Control Theory and Applications Vol. 10, No. 30, pp. 133-145, 2017.

[Dja 21] S. Djabali, M. Ait. Hamou. Ali, A. Ammar : " Voltage Sensorless Direct Power Control for PWM Rectifier Under Distorted Network Using Improved Virtual Flux Estimator ", algerian journal of signals and systems (AJSS), Vol. 6, Issue 1, pp. 32-40, March .2021.

[Dje 14] A. Djerioui, K. Aliouane, and F. Bouchafaa, "Sliding mode direct power control strategy of a power quality based on a sliding mode observer", Int. J. Electr. Power Energy Syst ,vol.56, pp.325–331. 2014.

[Dan 05] B. Dandil, M. Gokbulut, "Adaptive control of induction motors using neuro-fuzzy controllers", *Journal* of the Faculty of Engineering and Architecture of Gazi University .vol 20, pp.145–153.2005.

[Een 11] ENERDIS CHAUVIN ARNOUX GROUP, "Compensation d'énergie réactive Condensateurs et armoires de rephasage", pp .314, 2011.

[Fek 18] M. Fekik Arezki, "Commande Directe De Puissance D'un Redresseur à MLI Par DSP ", PhD Thesis, Mouloud Mammeri University of Tizi-Ouzou, Algeria, 2018.

[Fek 16] A. Fekik, H. Denoun, N. Benamrouche, N. Benyahia , A. Badji , M. Zaouia, "Comparative Analysis of Direct Power Control and Direct power control with space vector modulation of PWM rectifier", 4th IEEE International Conference on Control Engineering & Information Technology (CEIT-2016) Tunisia, Hammamet- December, 16-18, 2016 .

[Fek 19] A. Fekik, H. Denoun, M. Zaouia, M. Hamida, S .Vaidyanathan, " A new switching table based neural network for direct power control of three-phase PWM-rectifier " , International Journal of Modelling, Identification and Control,vol.33, pp. 358-368 , May .2019.

[**God 13**] Godbole. P, "Effect of harmonics on active power flow and apparent power in the power system", IOSR Journal of Electronics and Communication Engineering, PP: 39-43, 2013.

[Gado 09] S. M. Gadoue, D. Giaouris, J. W. Finch, "Artificial intelligence-based speed control of DTC induction motor drives A comparative study", Electr. Power Syst. Res ,vol .79, no.1,pp.210–219 , 2009.

[Ham 16] Z. Hameed et all, "Harmonics in Electrical Power Systems and how to remove them by using filters in ETAP", Faculty of Engineering and Technology Superior University, Pakistan, February 2016.

[Jang 97] J.S.R Jang, C.T Sun, E.Mizutani, "Neuro-fuzzy and soft computing", Prentice Hall, USA . book.1997.

[Jam 18] M. Jamma, D. Joshi, M. Akherraz, A. Bennassar, "Direct Power Neuro-Fuzzy Controller Scheme of Three-Phase PWM Rectifiers for Power Quality Improvement", International Conference on Computational Intelligence and Data Science (ICCIDS), pp. 595-605, 2018.

[Jam 17] M. Jamma, M. Barara, M. Akherraz, A. Bennassar, "Comparative Study of PI and Backstepping with Integral Action Controllers Based on Direct Power Control for Three-Phase PWM Rectifier", Int. J. Electr. Eng. Inform , vol.9 , no.2 , pp . 234–243, 2017.

[Jam 18] M. Jamma, M. Akherraz' M. Barara, "ANFIS Based DC-Link Voltage Control of PWM Rectifier-Inverter System with Enhanced Dynamic Performance", University of Lyon, France, 2018.

[Kas 19] A. Kasmiouri, " Étude par simulation de la commande MLI d'un redresseur de courant", master's memory, Mohamed Khider University of Biskra, Alegria, 2019.

[Kaz 98] M. P. Kazmierkowski, L. Malesani, "Current Control Techniques for Three-Phase Voltage-Source PWM Converters", IEEE Transactions on industry applications, Vol. 45, No. 5, pp. 691-703, 1998.

[Kwa 15] S. Kwak and J.-C. Park, "Model-Predictive Direct Power Control With Vector Preselection Technique for Highly Efficient Active Rectifiers", IEEE Trans. Ind. Inform ,vol.11, no.1, pp. 44–52. 2015.

[Lis 01] M. Liserre, "Innovative control techniques of power converters for industrial automation", PhD thesis, Politecnico Di Bari, Italie, 2001.

[Liu 03] F. Liua, S. Meia , Q. Lua , Y. Nib ,F. Wub , A. Yokoyamac, "The nonlinear internal control of STATCOM: theory and application ", Electrical Power and Energy Systems , vol 25 ,pp. 421–430.2003.

[**Maz 18**] A. Abu Mazhar, N. Ijaz, M. Ejaz Hassan, M. Mehdy, "Reduction of Harmonic Distortion in Power System During Fault Occurrence", Journal of Energy Technologies and Policy, Vol.8, No.5, 2018.

[Mas 22] B. Masood, N. Ammari, " Commande par Logique Floue d'un Redresseur de Tension à MLI", master's memory, Mohamed Boudiaf University of M'sila, Algeria, 2022.

[Mal 01] M. Malinowski, M. P. Kazmierkowski, S. Hansen, f. Blaabjerg, and G. D. Maeques, "Virtual flux based direct power control of three phase PWM rectifiers", IEEE Trans. on Industry Applications, vol. 37, no. 4, pp. 1019-1027. 2001.

[Mar 14] P. R. Martinez-Rodriguez, G. Escobar, A. A. Valdez-Fernandez, M. Hernandez-Gomez, and J. M. Sosa, "Direct Power Control of a Three-Phase Rectifier Based on Positive Sequence Detection," IEEE Trans. Ind. Electron., vol. 61, no. 8, pp. 4084–4092, Aug. 2014.

[Mal 04] M. Malinowski, M. Jasinski, and M. P. Kazmierkowski, "Simple Direct Power Control of Three-Phase PW M Rectifier Using Space-Vector Modulation (DPC-SVM)", IEEE Trans. Ind. Electron., vol. 51, no. 2, pp. 447–454, Apr. 2004.

[Mal 03] M. Malinowski, M. P. Kazmierkowski, and A. M. Trzynadlowski, "A comparative study of control techniques for PWM rectifiers in AC adjustable speed drives", IEEE Trans. Power Electron ,vol.18, no.6, pp. 1390–1396 , 2003.

[Mam 75] E.H.Mamdani, S. Assilian, "An experiment in linguistic synthesis with a fuzzy logic controller", International Journal of Man-Machine Studies, vol 7, No 1, pp.1-13, 1975.

[Mer 17] A. Merikhi, M. A. Benchohra, "Etude d'un drone, analyse de commande par la méthode Neuro-Floue, simulation par MATLAB/Simulink", master's memory, University of Blida, Algeria, 2017.

[Nou 98]T. Noguchi, H. Tomiki, S. Kondo, and I. Takahashi: "Direct power control of PWM converter without power-source voltage sensors", IEEE Trans. on Industry Applications,vol. 34, no. 3, pp. 473-479. 1998.

[Ohn 91] T. Ohnishi, "Three phase PWM converter/inverter by means of instantaneous active and reactive power control " in Proc. IEEE Int. Conf. Ind. Electron., Control Instrum. (IECON), vol. 1, pp. 819–824. 1991.

[Oue 08] S. Ouerdia, "Commande floue et neuro-floue du niveau de liquide d'un réservoir", master's memory, Mouloud Mammeri University of Tizi Ouzou,2008.

[Pin 15] R. Pinyol, "Harmonics: Causes, Effects and Minimization", SALICRU White Papers, August 2015.

[Ros 06] F. De. La. Rosa, "Harmonics and Power Systems", Taylor & Francis Group, USA, 2006.

[Rab 19] R. Rabehi, "Investigation to Harmonics Identification in Power System Based on Advanced Signal Processing Techniques", PhD thesis, Achour Zain University of Djelfa, Algeria, 2019.

[Sad 17] S. Radhwane, "Commande directe du couple (DTC-SVM) d'une MASDE associée à deux onduleurs multiniveaux en cascade avec un redresseur à MLI piloté par DPC", PhD Thesis, University of Sidi-bel-Abbes, 2017.

[Tak 86] T. Takahashi, T. Noguchi, " A new quick-response and high-efficiency control strategy of induction motor ", IEEE Trans. on Industry Applications, vol. I5-22, no.5, pp. 820-827, Sep-Oct. 1986.

[Uli 10] A. Ulinuha, M.A.S. Masoum, S. Islam, "Hybrid genetic-fuzzy algorithm for volt/var/total harmonic distortion control of distribution systems with high penetration of non-linear loads", Published in IET Generation, Transmission & Distribution, Vol. 5, Iss. 4, pp. 425–439, 2011.

[Rah 17] A. Rahoui, " techniques avancées pour la commande et l'observation d'un redresseur MLI", PhD Thesis, Mouloud Mammeri University of Tizi-Ouzou, Algeria, 2017.

[Shu 14] Shuhui. Li, M. Fairbank, C. Johnson, D. C. Wunsch, E. Alonso, and J. L. Proao, "Artificial Neural Networks for Control of a Grid Connected Rectifier/Inverter Under Disturbance, Dynamic and Power Converter Switching Conditions," IEEE Trans. Neural Netw. Learn. Syst, vol.25, no. 4, pp.738–750.2014.

[Sug 85] M. Sugeno, "An introductory survey of Fuzzy Control" Information Sciences vol.36, pp.59-83, 1985.

[Vis 11] F. Visser, "Design and implementation of a bi-directional 3 phase converter for a 30kW range extender application", Master thesis, TUDelft University, Netherlands, 2011.

[Vik 97] V. Kaura, V. Blasko, "Operation of a phase locked loop systeme under discorted utility conditions", IEEE Transactions on industry applications, Vol. 33, No. 1, pp. 58-63, 1997.

[Vaz 08] S. Vazquez, J. A. Sanchez, J. M. Carrasco, J. I. Leon, and E. Galvan, “A Model-Based Direct Power Control for Three-Phase Power Converters,” IEEE Trans. Ind. Electron., vol. 55, no. 4, pp. 1647–1657, Apr. 2008.

[Zob 18] Ahmed F. Zobaa, S. Aleem, Murat. E. Balci, " Power System Harmonics: Analysis, Effects and Mitigation Solutions for Power quality improvement ", 2018.

[Zan 11] A. Z. Zangeneh, M. Mansouri, M. Teshnehlab, A. K. Sedigh, "Training ANFIS System with DE Algorithm", Fourth International Workshop on Advanced Computational Intelligence Wuhan, China, 2011.